

AN EXPERIMENTAL INVESTIGATION OF NATURAL  
CONVECTION IN MERCURY AT LOW GRASHOF NUMBERS

by

BONG HYON CHANG 4871

B.E., Yonsei University, 1968

---

A MASTER'S THESIS

submitted in partial fulfillment of the

requirements for the degree


MASTER OF SCIENCE

Department of Chemical Engineering

KANSAS STATE UNIVERSITY  
Manhattan, Kansas

1970

Approved by:

  
Major Professor

LD  
2668  
T4  
1970  
C468  
C.2

# TABLE OF CONTENTS

<u>Title</u>	<u>Page</u>
LIST OF FIGURES . . . . .	1v
LIST OF TABLES . . . . .	vi
INTRODUCTION . . . . .	1
REVIEW OF LITERATURE . . . . .	3
THEORETICAL ANALYSIS . . . . .	20
Similarity Transformation Method . . . . .	24
Integral Method . . . . .	30
Perturbation Technique . . . . .	35
Recent Theoretical Work . . . . .	42
APPARATUS . . . . .	51
PROCEDURE . . . . .	58
DATA ANALYSIS . . . . .	62
DISCUSSION OF RESULTS . . . . .	66
Overall Dimensionless Temperature Profile . . . . .	66
Dependence of Dimensionless Temperature Profiles On the Distance Up the Plate; At Constant Heat flux . . . . .	71
Dependence of Dimensionless Temperature Profiles On the Power Level; At Fixed Position Up the Plate . . . . .	85
Dependence of Dimensionless Temperature Profiles on Nusselt number; At Constant $Gr_x^*$ . . . . .	91
Local Nusselt Number versus $Gr_x^*$ . . . . .	97
CONCLUSIONS . . . . .	101
NOMENCLATURE . . . . .	104

# **ILLEGIBLE DOCUMENT**

**THE FOLLOWING  
DOCUMENT(S) IS OF  
POOR LEGIBILITY IN  
THE ORIGINAL**

**THIS IS THE BEST  
COPY AVAILABLE**

**THIS BOOK  
CONTAINS  
NUMEROUS PAGES  
WITH DIAGRAMS  
THAT ARE CROOKED  
COMPARED TO THE  
REST OF THE  
INFORMATION ON  
THE PAGE.**

**THIS IS AS  
RECEIVED FROM  
CUSTOMER.**



**THIS BOOK WAS  
BOUND WITH TWO  
PAGES NUMBERED  
109. THESE PAGES  
ARE THE SAME.**

**THIS IS AS  
RECEIVED FROM  
CUSTOMER.**

BIBLIOGRAPHY . . . . .	108
ACKNOWLEDGEMENTS . . . . .	121
APPENDICES . . . . .	122
Appendix A      Computer Program . . . . .	122
Appendix B      Sample Calculations . . . . .	124
Appendix C      Copper-Constantan Thermocouple Calibration . . . . .	132

## LIST OF FIGURES

<u>Title</u>	<u>Page</u>
1. Dimensionless Temperature Distribution for various Prandtl Number . . . . .	28
2. Dimensionless Velocity Distributions for Various Prandtl Number . . . . .	29
3. Variation of $Gr_x^{1/5}/Nu_x$ with Prandtl Number . . . . .	31
4. Comparison of Temperature Profiles for $Pr = 0.03$ When $Gr_L^* = 10^7$ . . . . .	43
5. Comparison of Temperature Profiles for $Pr = 0.03$ When $Gr_L^* = 10^9$ . . . . .	44
6. Comparison of Velocity Profiles for $Pr = 0.03$ When $Gr_L^* = 10^7$ . . . . .	45
7. Comparison of Velocity Profiles for $Pr = 0.03$ When $Gr_L^* = 10^9$ . . . . .	46
8. Vertical Plate and Thermocouple Probe . . . . .	52
9. Probe Positioning Mechanism . . . . .	54
10. Copper-Constantan Micro Miniature Thermocouple . . . . .	55
11. Typical X-Y plotter Outputs . . . . .	63
12. Overall Temperature Distributions - Present Work . . . . .	67
13. Overall Temperature Distributions - Julian's Work. . . . .	70
14. Dimensionless Temperature Profiles at $87 \text{ Btu/hr-ft}^2$ . . . . .	73
15. Dimensionless Temperature Profiles at $87 \text{ Btu/hr-ft}^2$ . . . . .	74
16. Dimensionless Temperature Profiles at $121 \text{ Btu/hr-ft}^2$ . . . . .	75
17. Dimensionless Temperature Profiles at $121 \text{ Btu/hr-ft}^2$ . . . . .	76
18. Dimensionless Temperature Profiles at $354 \text{ Btu/hr-ft}^2$ . . . . .	77

19.	Dimensionless Temperature Profiles at 354 Btu/hr-ft <sup>2</sup> . . . . .	78
20.	Dimensionless Temperature Profiles at 512 Btu/hr-ft <sup>2</sup> . . . . .	79
21.	Dimensionless Temperature Profiles at 512 Btu/hr-ft <sup>2</sup> . . . . .	80
22.	Dimensionless Temperature Profiles at 735 Btu/hr-ft <sup>2</sup> . . . . .	81
23.	Dimensionless Temperature Profiles at 735 Btu/hr-ft <sup>2</sup> . . . . .	82
24.	Dimensionless Temperature Profiles at 1168 Btu/hr-ft <sup>2</sup> . . . . .	83
25.	Dimensionless Temperature Profiles at x = 1/16 inch . . . . .	86
26.	Dimensionless Temperature Profiles at x = 1/8 inch . . . . .	87
27.	Dimensionless Temperature Profiles at x = 1/4 inch . . . . .	88
28.	Dimensionless Temperature Profiles at x = 1 inch .	89
29.	Dimensionless Temperature Profiles at . . . . . x = 5/4 inch	90
30.	Dimensionless Temperature Profiles at Gr <sub>x</sub> <sup>*</sup> = 0.6 x 10 <sup>4</sup> . . . . .	92
31.	Dimensionless Temperature Profiles at Gr <sub>x</sub> <sup>*</sup> = 0.9 x 10 <sup>5</sup> . . . . .	93
32.	Dimensionless Temperature Profiles at Gr <sub>x</sub> <sup>*</sup> = 0.2 x 10 <sup>6</sup> . . . . .	94
33.	Dimensionless Temperature Profiles at Gr <sub>x</sub> <sup>*</sup> = 0.5 x 10 <sup>7</sup> . . . . .	95
34.	Dimensionless Temperature Profiles at Gr <sub>x</sub> <sup>*</sup> = 0.2 x 10 <sup>8</sup> . . . . .	96
35.	Nusselt Number - Grashof Number Correlations . . .	98

## LIST OF TABLES

<u>Title</u>	<u>Page</u>
1. Values of $\bar{\theta}_0'(0)$ and $\bar{\theta}_1'(0)/\bar{\theta}_0'(0)$ . . . . .	49
2. Comparison of experimental results with those of Julian . . . . .	71

## INTRODUCTION

Physically, free or natural convection flow arises from a difference in density in the fluid. Visualize a heated surface exposed to colder air in a room. Since the density of air near the heated surface is less than that of mainbody of the air, buoyant forces cause an upward flow of air near the surface. If the surface were colder than the air, because of greater density near the surface, the air would flow downward. In either case heat is conducted through the air layers and is carried away by bulk motion or convection. Although both conduction and convection are involved, the process is called "natural" or "free" convection.

In recent years, there has been a growing interest in the use of low-melting metals as heat transfer media. Liquid metals have had limited applications in the field of heat transfer, but the developments in handling and metering liquid metals and their suitability for high temperature, high-heat-flux applications have led to a considerable amount of theoretical and experimental investigation in this field. Liquid metals have been used extensively to cool valves in aircraft engines. Power generation using mercury instead of water as the working fluid in boilers has been carried out commercially since 1922. The present interest in liquid metals in the field of heat transfer stems from their use in atomic reactors. The use of nuclear reactors in spacecraft or satellite systems has been

suggested and the cooling of such reactors would be in general achieved using liquid metals. The natural convection effects may be quite significant and, in fact, there may be an advantage in eliminating the pumping system and using natural convection for heat transfer.

Theoretically, the natural convection phenomenon has been of interest in that it represents a system of coupled differential equations. This coupling results from the fluid flow being caused by the temperature gradient in the thin boundary layer surrounding the heated object. These equations and their solutions have been subject of numerous papers. However, experimental verifications of the analytical work have not been as numerous.

This work experimentally investigates the laminar, steady, two dimensional, free convection heat transfer from a vertical flat plate with a uniform heat flux, immersed in mercury at rest. The work is especially directed toward the condition of low Grashof numbers ( $Gr_x^*$ ) where appreciable deviation from the boundary layer theory are predicted by the perturbation analysis. There have been no experimental investigations for fluids at small Grashof numbers.

## REVIEW OF LITERATURE

This review is concerned with research in the field of natural convection heat transfer, the results of which have been published until early 1970. Recent literature has been especially well surveyed.

In 1881, L. Lorenz [83]\* presented, in his pioneer paper, a theoretical analysis for natural convection from a vertical, isothermal, flat plate in air at rest. He assumed that the fluid flow was parallel to the plate, and that the fluid temperature at any point depended only on the distance from the plate. Although inadequate assumptions were used, his results were in agreement with the then-existing experimental results. In 1928, Nusselt and Jurges [96] improved Lorenz's work by taking into account his improper assumptions, and measured the temperature field in air at 100° C.

In 1904, L. Prandtl [103] simplified the Navier-Stokes equations by dividing the flow into two regions; a thin boundary layer along the solid surface where viscous effects were important and the velocity gradient normal to the wall was large, and a bulk flow region where viscous effects could be neglected. The first exact\*\* solution of the boundary layer equations for the case of an isothermal vertical flat plate was developed by

---

\* The number corresponds to the reference in the Bibliography.

\*\* A solution which is obtained using a similarity transformation is conventionally called "exact", even though the solutions are obtained numerically via the digital computer.



E. Pohlhausen. In 1930, he applied a similarity transformation method he had used in 1921 [101] for the boundary layer on a semi-infinite flat plate parallel to a uniform flow. He showed how the resulting partial differential equations could be transformed into ordinary differential equations with a single independent variable, i.e., a similarity variable. Pohlhausen obtained a numerical solution of these ordinary differential equations for a Prandtl number of 0.733 and compared the results with experimental values of the temperature and velocity gradients in air which were measured by Schmidt and Beckmann [120] in 1930.

An experimental correlation derived in 1934 by H. Lorenz [84] based on measurements on a vertical hot plate in oil was given by Schlichting [118]. In 1935 and 1936, Weise [152] and Saunders [108], obtained extensive data for short vertical plates, which were later correlated by McAdams [91].

In 1939, Saunders [107] also presented approximate solutions for air and compared his results with those of Pohlhausen [120] and Squire [53]. Saunders obtained some experimental data for mercury and water and appears to have been the first to study free convection in a liquid metal. However, the plate he used was attached to a surface of fireclay containing a heater coil, and it was a portion of the wall surface. Therefore, it had no leading and trailing edges.

In 1946, H. Schuh [122] extended Pohlhausen's calculations to high Prandtl numbers of 10, 100, and 1000, and Sugawara and Michiyoshi [138] obtained numerical solutions for comparatively

small Prandtl numbers of 0.03, 0.09, and 0.5.

In 1953, Ostrach [98], starting from the complete steady state equations for variable properties, determined the conditions under which E. Pohlhausen's equations adequately describe the physical process. These equations were then solved numerically for various Prandtl numbers: 0.01, 0.72, 0.733, 1, 2, 10, 100 and 1000. Ostrach compared his solutions with the experimental data in air by Schmidt and Beckmann [120], and pointed out that, in general, the agreement was good for small values of the similarity variable and less satisfactory for larger values of the similarity variable.

All the approaches mentioned so far were concerned with isothermal vertical plates or planes. The present work, however, is concerned with a uniformly heated, vertical plate. In 1956, Sparrow and Gregg [131] analyzed laminar free convection from a uniformly heated (constant heat flux), vertical, flat plate by determining a similarity transformation which would reduce the boundary-layer equations to ordinary differential equations. These equations were solved numerically for Prandtl numbers of 0.1, 1, 10 and 100, and Dotson's experimental data [23] for air were used to verify the theory. In 1964, Chang, et al. [15] extended Sparrow and Gregg's solution to small Prandtl numbers of 0.01 and 0.03 for liquid metals.

In 1955, Sparrow [129] used the approximate Von Karman-Pohlhausen integral method to solve the boundary layer equations for natural convection from a vertical plate with a

nonuniform wall heat flux and wall temperature for Prandtl numbers of 0.01 to 1000. Results for the case of constant heat flux were in good agreement with those obtained using the similarity transformation [131].

In 1956, Finston [38] showed that according to the boundary layer theory the problem of free convection past a vertical plate had an exact solution for a surface temperature which is proportional to a power of the distance from the leading edge of the plate. Foote [39], in 1958, extended Finston's method and obtained the solution by asymptotic expansions, and Niuman and Pohlhausen [94] numerically evaluated Finston's equations for a Prandtl number of 0.733.

Sparrow [128], in his 1956 Ph.D. Thesis, included the temperature dependence of physical properties when he solved boundary layer equations for an isothermal, vertical, flat plate. He developed a reference temperature for perfect gases and liquid metals (mercury) so that the results from the constant property analysis could be used to approximate the values of temperature-dependent physical properties. Sparrow and Gregg [133], in 1958, extended the analysis to treat the variable fluid-property problem in free convection. Tanaev [142], in 1956, studied the effect of variable viscosity on laminar free convection of a gas. Gebhart [45], in 1962, indicated that viscosity dependence could result in an inflexion point for gases at low temperature or for higher Prandtl number fluids whose viscosities are large.

In 1959, Fujii [41] applied a modified integral method for laminar free convection from a vertical flat plate and supplemented Squire's approximation [54]. He also treated non-isothermal surface problems. In addition, he analyzed turbulent free convection from a vertical surface [40]. Bobco [6], in 1959, also used the integral technique to obtain an approximate solution in closed form to the problem of nonuniform wall heat flux.

In 1960, Yang [156] established the necessary and sufficient conditions required for the existence of similarity solutions to the problem of steady and unsteady free convection on vertical plates with various surface temperature distributions.

Then in 1961, he presented an improved integral procedure for compressible fluids in laminar natural convection near a flat vertical plate [153].

In 1962, Gebhart [42] investigated the effect of viscous dissipation in the natural convection boundary layer close to a vertical flat plate, and concluded that the effect is small for all Prandtl numbers where the only buoyant force constitutes body force. Acrivos [2] showed how an approximate but accurate expression could be obtained for the rate of heat and mass transfer in laminar boundary-layer flows by piecing together certain asymptotic solutions. Acrivos pointed out that free convection is mathematically similar to forced convection if the velocity is replaced by a characteristic velocity.

Scherberg [114], in 1962, investigated the effect of leading

edge configuration, and found that it did not affect the velocity and temperature profiles at sufficient upstream distances except shifting the relative starting point of boundary layer.

Scherberg [112], in 1965, extended his previous work by matching the solutions at the leading edge with the known solution immediately above this region. Arbitrary surface temperature variations along a vertical flat plate were treated in 1964 by Scherberg [113] using an integral technique.

In 1958, Schechter and Isbin [111] presented theoretical and experimental analyses of natural convection heat transfer in water at  $4^{\circ}\text{C}$  where water has its maximum density. Similarity equations for an isothermal plate were solved on an analog computer. The results indicated that fluid motion should occur in both the upward and downward directions simultaneously. These results were verified experimentally on a one-foot square, vertical, aluminum, isothermal plate immersed in a large container of water. Goren [56], in 1966, solved this same problem (without any knowledge of Schechter and Isbins' work) and concluded that the convection currents would be reduced. Vanier and Tien [147] extended Goren's work in 1967. They showed that heat transfer coefficients investigated by Goren were too low by 15 per cent and were restricted to plate temperatures of less than  $8^{\circ}\text{C}$ . They found more accurate solutions which are applicable to plate temperatures of up to  $35^{\circ}\text{C}$ .

Most of the analytical solutions of laminar free convection presented up to 1964 were based on Prandtl's boundary

layer assumptions which apply for large Grashof numbers. In 1964, Yang and Jerger [158], presented for the first time a perturbation analysis which they expected to be more accurate for moderate Grashof numbers. Their analytical method was similar to that applied by Kuo [76] to forced convection flow over a horizontal plate. However, the free convection problem is more complicated due to the coupled motion and energy equations. Numerical solutions were presented for Prandtl numbers of 0.72 and 10.

In 1965, Suriano, Yang, and Donlon [139] developed a perturbation method for extremely small Grashof numbers (less than one). In 1968, Suriano and Yang [140] extended the previous work [139] for small and moderate Grashof numbers (Rayleigh number from 1 up to 300) with Prandtl numbers of 0.72 and 10. They concluded that effects of viscous dissipation were negligible, and that the effects of Grashof number (or Rayleigh number) on the free convection phenomena may be broken down into three regions with different characteristics. For Rayleigh numbers up to unity, heat is transferred by pure conduction and slow flow field varies about linearly with Grashof numbers. In the Rayleigh number region from one to about fifty, convection effects start to be increasingly more important, while conduction still persists, especially in the immediate neighborhood of the plate. For Rayleigh numbers above fifty, a boundary layer type of behavior is developed along the vertical plate. This is accompanied by sharp increase in Nusselt

numbers. Suriano and Yang indicated that as Rayleigh number increases beyond 300, both the flow and energy fields would vary monotonically toward true boundary layer behaviors. The numerical results were compared with the existing experimental correlations [13, 59, 65, 91] and it was claimed that, even though there exist discrepancies between the theoretical and the experimental results, this theoretical work could be considered as reasonable, considering the order of magnitude of discrepancies between the experimental correlations.

The perturbation analysis assumed that streamlines leaving the trailing edge of the plate would essentially be parallel to the plate. Yang [154], in 1964, theoretically studied the momentum and energy fields in this laminar wake region above the plate. He carried out numerical calculations for Prandtl numbers of 0.72 and 10, and found that spreading of the boundary layer was rather gradual and that the assumption of streamlines parallel to the plate was well justified.

In 1966, Chang, Akins, and Bankoff [16] extended Yang and Jergers' [158] perturbation analysis to the case of a uniformly heated plate. They presented numerical solutions for Prandtl numbers of 0.01, 0.03 and 0.1.

In 1969, Julian and Akins [68] carried out experiments on natural convection from a uniformly heated, vertical, flat plate in water and mercury in the range of moderate Grashof number. The results were in good agreement with the similarity and integral solutions to the boundary layer equations. The dimension-



less profiles also showed the trends, with position up the plate, predicted by the first order perturbation analysis [16]. The present work shows the experimental results on natural convection as an extension of Julian and Akins' work, especially at low Grashof numbers where appreciable deviation from the boundary layer solution was predicted.

In 1967, Hayday, Bowlus, and McGraw [60] numerically solved a nonsimilar free convection problem, the nonsimilarity of the flow being generated by step discontinuities in surface temperature. Results were compared with experimental correlation of Schetz and Eichhorn [117] and formed a theoretical basis for their experiments.

In 1967, O'Brien and Shine [97] investigated some effects of an electric field on heat transfer from a vertical plate in free convection. They showed that the local heat transfer from a vertical plate increased significantly in the presence of a large electric field.

Gebhart, Dring, and Polymeropoulos [50], in 1967, studied the transient natural convection from a vertical sheet following a step input (with time) of heat. Gebhart and Dring [49], in 1967, showed the rate of propagation of leading edge effects up the plate. Also in 1967, Polymeropoulos and Gebhart [102], presented the results of an experimental investigation of the behavior of artificial disturbances produced by an oscillating ribbon in the free convection boundary layer over a vertical uniform flux plate. Dring and Gebhart [24], in 1968, theoretic-



cally investigated the nature of instability and disturbance amplification for the basis of Polymeropoulos and Gebhart's experiments [102]. In the same year, Knowles and Gebhart [72], showed that thermal capacity coupling exists between the fluid and the wall which generates the flow. This coupling was shown to have a first order effect for particular Grashof-number Wave-number products. In 1969, Gebhart [47] summarized what was known at that time concerning the incipient instability and transition of laminar flow.

In 1968, Takhar [141] presented a numerical solution for the development of free convection from a semi-infinite flat plate, which was isothermal up to a certain length from the leading edge and was insulated for the rest of its length. He pointed out that at the insulated part above the isothermal part of the plate, the velocity and temperature distributions behave as if the heated part were put in as a line source of heat at the base of the insulated part.

In 1967, Tien [143] applied an integral method to study the laminar natural convection heat transfer from both an isothermal and a non-isothermal plate to a power-law fluid. Tien and Tsue [144], in 1969, presented an approximate solution for the problem of determining the laminar natural convection heat transfer between a vertical, isothermal plate and a fluid whose rheological behavior is characterized by Ellis' model. The results were obtained by integral method and compared with available experimental data.

In 1968, Sparrow and Guinle [135] investigated the deviations from classical boundary layer theory at small Prandtl numbers. They evaluated effects of transverse pressure variations, and streamwise shear stress and conduction phenomena, which are neglected in the conventional boundary layer theory. It was shown that for very low Prandtl numbers, the Grashof number must be quite large in order that the classical boundary layer results are applicable. It was also pointed that the local heat transfer exceeds that of classical boundary layer theory.

In the same year, Cygan and Richardson [22] used a transcendental approximation to the velocity and temperature profiles to obtain integral solutions of the natural convection boundary layer at small Prandtl number.

Papaïliou and Lykoudis [100], in 1968, performed an experiment to show the effect of a magnetic field on a laminar natural convection of electrically conducting fluid. The case examined in this experiment was that of a vertical hot plate of uniform temperature with mercury as conducting fluid, in the presence of a transverse magnetic field. The existence of similarity solutions theoretically investigated by Lykoudis [85] and independently by Gupta [58] in 1962 was fully established by the experiment.

Experimental results investigated in 1968 concerning turbulent natural convection from a vertical flat plate were in general agreement with each other even though there were some discrepancies in a number of the details. Cheesewright [18]

performed an experiment and comparison was made with predictions of Eckert and Jackson [28]. It was in good agreement. Another experimental study carried out by Warner and Arpaci [151] showed that their results were in good agreement with analytical correlation of Bayley [7], and that the use of power law temperature profiles is undesirable for the case of turbulent natural convection. The absence of a laminar sublayer was noted in another study carried out by Lock and Trotter [82]. Kato, Nishiwaki, and Hirata [70] predicted the turbulent velocity and temperature profiles using eddy diffusivities similar to those found in forced convection. New criterion was proposed for transition. In 1969, Vliet and Liu [150] conducted an experimental investigation on turbulent natural convection from a constant heat flux, vertical plate in water. Their results showed that natural transition occurs in the range of Rayleigh number from  $10^{12}$  to  $10^{14}$ .

In 1969, Nishikawa and Ito [95] theoretically studied the laminar free convection from an isothermal plate to fluids, water and carbon dioxide, at supercritical pressures, taking into account temperature dependence of all the physical properties.

Yung and Oetting [159], in 1969, presented the results of experimental work on the free convection heat transfer from a heated flat plate in air moving from the vertical position through three inclined positions to the horizontal position. Vliet [149], in 1969, presented experimental local heat transfer data for natural convection on constant-heat flux, inclined

surface in water and air. The data extended to Rayleigh number of  $10^{16}$ , covered angles from the vertical to 30 degrees with the horizontal, and included the laminar, transition, and turbulent regimes.

MacGregor and Emery [88], in 1969, theoretically and experimentally investigated the effect of Prandtl number, Grashof number, Rayleigh number, aspect ratio, and variable properties on the free convection through vertical plane. They divided flow regime into five divisions and presented corresponding Rayleigh numbers. Results were compared with other experimental correlations [25, 35, 77].

Sparrow and Husar [136], in 1969, conducted experimental investigation on the free convection from a flat vertical surface, the leading edge of which is not horizontal. They pointed out that the three dimensionality of the problem due to non-horizontal leading edge could be reduced to quasi-two dimensional, because of very small spanwise velocities and as the result of an order of magnitude estimate.

Kuiken [74], in 1969, developed a method, using a singular perturbation technique of the type described in the book of Van Dyke [146]. The method is free of the objectionable features of the integral method and similarity transformation, but it maintains the advantages of each, i.e., accuracy from similarity transformation and explicit Prandtl number from the integral method. He solved the first and the second perturbation solutions using matching principle to the inner flow (boundary

layer flow) and outer flow (inviscid flow). Kuiken [75], in 1969, theoretically studied free convection past a vertical plate for a general class of nonlinear wall temperature distributions. He developed a method which makes it possible to find two series solutions. One is for small distance up the plate and the other is for large distance, and both are applicable to the same wall temperature distribution. An overall valid solution was obtained through graphical joining of two solutions.

Again in 1969, Merkin [92], investigated the effect of buoyancy forces on the boundary layer flow over a semi-infinite vertical flat plate in a uniform free stream. When this buoyancy force acts in the direction of the free stream, he indicated that two series solutions can be obtained, one which holds near the leading edge and the other which holds far downstream. When the direction of buoyancy force is opposite to that of free stream, a series, valid near the leading edge was obtained and it was extended by a numerical method to the point where the boundary layer was shown to separate.

Here some experimental techniques on natural convection for measurement of flow and energy fields are summarized. Conventionally, local temperature profiles have been easily measured by a single movable and/or several fixed thermocouples. Many difficulties have been involved in measuring flow field. Visual techniques have been generally used for measuring the velocity profiles and sometimes for temperature profiles.

The dimensions of the boundary layer and also the temperature

profiles were first observed visually about a horizontal tube using a Schlieren photograph by E. Schmidt [119] in 1932. A more advanced device, the interferometer, was developed by Mach and Zehnder [110] and was used by Kennard [71] and later by Eckert and Soehngnen [29, 30] to study isotherms in air about a vertical plate in laminar and turbulent free convection. Goldstein and Eckert [55] and Schetz [116] used the Mach-Zehnder interferometer to observe steady and transient free convection. Schetz and Eichhorn [117] used both Schlieren and Mach-Zehnder interferometer to study the temperature and flow fields adjacent to a vertical plate subjected to a spatially discontinuous surface temperature. Simon and Eckert [125] used the interferometer to observe laminar free convection in carbon dioxide near its critical point and Hill [64] used it to study natural convection from a nonisothermal vertical plate in air and water.

Eichhorn [32], in 1962, devised a new method for measuring small flow velocities by using photographic techniques to measure the trajectories of small dust particles carried with the flow. Eckert, Hartnett, and Irvine [27] studied experimentally three-dimensional process of transition to turbulence in air by the introduction of thin threads into the heated free convection layer.

Gebhart and his co-workers used a Mach-Zehnder interferometer to measure the transient natural convection response [50], to investigate the leading edge effect in transient natural convection [49], and to observe the approximate location of neutral curve

after artificial disturbances were initially given [102].

O'Brien and Shine [97] observed the distortion of the boundary layer in the vicinity of an electric field by use of an interferometer.

Cheesewright [18], in 1968, developed new experimental measuring technique. He used fine wire, platinum resistance thermometer to measure the temperature and the thermometer was also used as a hot wire anemometer. Electrical current through the wire and wire temperature were used to calculate the Nusselt number. The corresponding Reynolds number for flow past the wire was determined from a calibration graph, thus permitting the flow velocity to be calculated.

Vliet and Liu [150], in 1969, used a combined time-streak marker hydrogen bubble method to observe the flow pattern in the x-y plane (normal to the test surface) as well as in the x-z plane (parallel to the test surface). A film type B-1A 16-mm movie camera was used to record the hydrogen-bubble motions as observed through a mirror box.

Sparrow and Husar [136], in 1969, applied the flow visualization technique to investigate the effect of non-horizontal leading edge. The flow was made visible by local changes of color of the fluid itself, the color change resulting from the change in pH. Thymol blue was used as pH indicator, which is blue in basic solution and yellow orange in acidic solution. Initially the solution was made acidic and yellow, and when small d.c. voltage was impressed between the test surface

(negative electrode) and copper billet (positive electrode), there was a proton transfer reaction at the test surface. As a result, there was a change in pH of the fluid, with a corresponding change in color from yellow to blue. This process did not give rise to density difference within the fluid, so no extraneous buoyancy forces were induced.

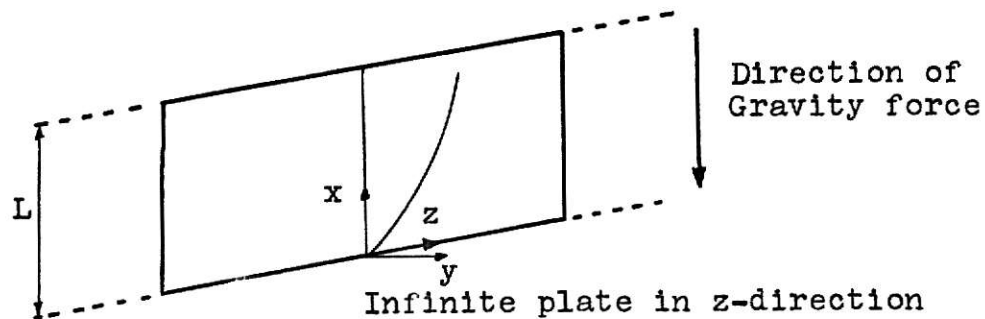


## THEORETICAL ANALYSIS

The problem of laminar natural convection heat transfer from a uniformly heated (constant heat flux), vertical plate will be analyzed to give the theoretical basis to this experimental work. Consider a vertical flat plate of zero thickness, infinite width, and finite height immersed in a large amount of fluid initially at rest. Heat transfer will occur from the thin plate to the fluid due to conduction and convection (radiation will be neglected). Electrical energy is passed through the plate to generate the uniform heat flux.

A nonuniform temperature field is established near the plate, which causes the fluid adjacent to the plate to be set in motion because of density differences resulting from temperature-dependence of fluid density. Assuming no slip at a solid-fluid interface, the fluid next to the plate (as well as the fluid far away from the plate) will not be in motion.

A rectangular Cartesian coordinate system is adopted as shown below.



The origin is located at the leading edge of the plate and plate itself is defined by  $0 \leq x \leq L$  and  $y = 0$ . The direction of gravitational field is chosen to be parallel and opposite to the X-coordinate. The complete and exact equations of continuity, momentum, and energy are [8]:

Continuity:

$$\frac{\partial \rho}{\partial t} + \nabla \cdot \rho \bar{V} = 0 \quad (1)$$

Motion:

$$\rho \left( \frac{D\bar{V}}{Dt} \right) = -\nabla \cdot \bar{\tau} - \nabla p + \rho \bar{g} \quad (2)$$

Energy

$$C_V \left( \frac{DT}{Dt} \right) = -\nabla \cdot \bar{q} - T \left( \frac{\partial p}{\partial T} \right)_V (\nabla \cdot \bar{V}) - \bar{\tau} : \nabla \bar{V} \quad (3)$$

Assuming steady state, a Newtonian fluid, constant thermal conductivity, incompressible fluid, no viscous dissipation, and two-dimensional flow, equations (1) through (3) reduce to :

Continuity:

$$\frac{\partial u}{\partial x} + \frac{\partial v}{\partial y} = 0 \quad (4)$$

Motion:

$$\rho \left( u \frac{\partial u}{\partial x} + v \frac{\partial u}{\partial y} \right) = \mu \left( \frac{\partial^2 u}{\partial x^2} + \frac{\partial^2 u}{\partial y^2} \right) - \frac{\partial p}{\partial x} - \rho g_x \quad (5)$$

$$\rho \left( u \frac{\partial v}{\partial x} + v \frac{\partial v}{\partial y} \right) = \mu \left( \frac{\partial^2 v}{\partial x^2} + \frac{\partial^2 v}{\partial y^2} \right) - \frac{\partial p}{\partial y} \quad (6)$$

Energy:

$$u \frac{\partial T}{\partial x} + v \frac{\partial T}{\partial y} = \alpha \left( \frac{\partial^2 T}{\partial x^2} + \frac{\partial^2 T}{\partial y^2} \right) \quad (7)$$

In free convection, the body force is important, because it gives rise to buoyancy which generates fluid motion. Physical properties except density are assumed to be independent of temperature and will be evaluated at a reference temperature. The density is assumed to be variable only in  $\rho g_x$  which brings about buoyancy to generate free convection. This term will be expanded in a Taylor series in temperature about the reference temperature  $T_R$ :

$$\rho g_x = \rho g_x \Big|_{T_R} + \left( \frac{\partial \rho}{\partial T} \right)_{T_R} (T - T_R) g_x + \left( \frac{\partial^2 \rho}{\partial T^2} \right)_{T_R} \frac{(T - T_R)^2}{2!} g_x + \dots \quad (8)$$

Taking the first two terms and introducing the coefficient of volume expansion, reduces equation (8) to:

$$\rho g_x = \rho g_x \Big|_{T_R} - \rho \beta \Big|_{T_R} g_x (T - T_R) \quad (9)$$

The components of pressure gradient in a static fluid far from the plate are:

$$\frac{\partial p}{\partial x} = - \rho g_x \quad (10)$$

$$\frac{\partial p}{\partial y} = 0 \quad (11)$$

Assuming the incremental increase in pressure due to fluid motion near the plate to be negligible, equations (10) and (11) for stationary fluid can be used for moving fluid in laminar natural convection. Substitution of equations (9) through (11) into the equation of motion yields:

$$u \frac{\partial u}{\partial x} + v \frac{\partial u}{\partial y} = \nu \left( \frac{\partial^2 u}{\partial x^2} + \frac{\partial^2 u}{\partial y^2} \right) + \beta g_x (T - T_R) \quad (12)$$

$$u \frac{\partial v}{\partial x} + v \frac{\partial v}{\partial y} = \nu \left( \frac{\partial^2 v}{\partial x^2} + \frac{\partial^2 v}{\partial y^2} \right) \quad (13)$$

The boundary conditions for equations (4), (7), (12) and (13) are:

$$u = 0 \quad (\text{no slip at the plate}), \text{ at } y = 0 \text{ and } 0 \leq x \leq L$$

$$v = 0 \quad (\text{no suction or injection}), \text{ at } y = 0 \text{ and } 0 \leq x \leq L$$

$$\begin{aligned}
q &= q_0 \quad (\text{constant heat flux}), \text{ at } y = 0 \text{ and } 0 \leq x \leq L \\
u &\rightarrow 0 \quad (\text{no bulk motion}), \text{ at } y \rightarrow \infty \text{ and all } x \\
v &\rightarrow 0 \quad (\text{no bulk motion}), \text{ at } y \rightarrow \infty \text{ and all } x \\
T &\rightarrow T_\infty \quad (\text{constant bulk temperature}), \text{ at } y \rightarrow \infty \text{ and all } x
\end{aligned}
\tag{14}$$

Prandtl [103] used an order of magnitude argument to simplify the Navier-Stokes equations in boundary layer. Applying the general boundary-layer assumptions to equations (4), (7), (12) and (13) yields:

$$\frac{\partial u}{\partial x} + \frac{\partial v}{\partial y} = 0 \tag{15}$$

$$u \frac{\partial u}{\partial x} + v \frac{\partial u}{\partial y} = \nu \frac{\partial^2 u}{\partial y^2} + \beta g_x (T - T_R) \tag{16}$$

$$u \frac{\partial T}{\partial x} + v \frac{\partial T}{\partial y} = \alpha \frac{\partial^2 T}{\partial y^2} \tag{17}$$

Note that conduction in the x-direction has been neglected and that these equations are valid for large Grashof numbers. The boundary layer equations (15), (16), and (17) will be solved by two methods, similarity transformation and integral method.

#### SIMILARITY TRANSFORMATION METHOD

The stream functions are defined as:

$$\frac{\partial \psi}{\partial y} = u \tag{18}$$

$$\frac{\partial \psi}{\partial x} = -v \quad (19)$$

Substitution of the stream functions defined above into the boundary layer equations (15), (16) and (17) gives:

$$\frac{\partial^2 \psi}{\partial y \partial x} - \frac{\partial^2 \psi}{\partial x \partial y} = 0 \quad (20)$$

$$\frac{\partial \psi}{\partial y} \frac{\partial^2 \psi}{\partial y \partial x} - \frac{\partial \psi}{\partial x} \frac{\partial^2 \psi}{\partial y^2} = \nu \frac{\partial^3 \psi}{\partial y^3} + \beta g(T - T_R) \quad (21)$$

$$\frac{\partial \psi}{\partial y} \frac{\partial T}{\partial x} - \frac{\partial \psi}{\partial x} \frac{\partial T}{\partial y} = \alpha \frac{\partial^2 T}{\partial y^2} \quad (22)$$

It is apparent that continuity equation is satisfied.

Sparrow and Gregg [131] transformed the partial differential equations (21) and (22) to ordinary differential equations by introducing following similarity variables:

$$\eta = \left( \frac{Gr_x^*}{5} \right)^{1/5} \frac{y}{x} \quad (23)$$

$$F(\eta) = \left( \frac{Gr_x^*}{5} \right)^{-1/5} \frac{\psi}{5\nu} \quad (24)$$

$$\theta(\eta) = \left( \frac{Gr_x^*}{5} \right)^{1/5} \frac{k}{qx} (T - T_\infty) \quad (25)$$

where  $Gr_x^*$  is modified Grashof number which is defined as:

$$Gr_x^* = g\beta x^4 q / k\nu^2$$

By substituting the similarity variables into the definition of stream functions and integrating with respect to  $y$  and  $x$ , respectively, expressions for the velocity components  $u$  and  $v$  can be found. Expression for temperature can be obtained by rearranging equation (25). They are:

$$u = \frac{5\nu}{x} \left(\frac{Gr_x^*}{5}\right)^{2/5} F'(\eta) \quad (26)$$

$$v = \frac{\nu}{x} \left(\frac{Gr_x^*}{5}\right)^{1/5} [\eta F'(\eta) - 4F(\eta)] \quad (27)$$

$$T = \left(\frac{Gr_x^*}{5}\right)^{-1/5} \frac{q x}{k} \theta(\eta) + T_\infty \quad (28)$$

After substitution of the similarity variables and considerable manipulations are made, equations (21) and (22) reduce to:

$$F + 4FF'' - 3(F')^2 + \theta = 0 \quad (29)$$

$$\theta'' + Pr(4\theta'F - \theta F') = 0 \quad (30)$$

subject to

$$F(0) = F'(0) = 0$$

$$\theta'(0) = -1 \quad (31)$$

$$F'(\infty) = \theta(\infty) = 0$$

Sparrow and Gregg [131] solved equations (29), (30) and (31) numerically on a digital computer. Other necessary boundary conditions,  $\theta(0)$  and  $F''(0)$ , to solve equations have to be guessed until a solution satisfies all the known boundary conditions. The only parameter to this solution is the Prandtl number. They obtained results for Prandtl numbers of 0.1, 1, 10 and 100. Chang, et al. [15] extended the solutions to Prandtl numbers of 0.01 and 0.03. Figure 1 presents dimensionless temperature profiles versus  $\eta$  for various values of Prandtl number. The dimensionless temperature profile was determined from  $\frac{\theta(\eta)}{\theta(0)}$ , as can be seen from equation (28). The velocity profile can be obtained from equation (26) and the computed values of  $F'(\eta)$ . They are:

$$\eta = \frac{y}{x} \left( \frac{Gr_x^*}{5} \right)^{1/5}$$

$$\frac{\theta(\eta)}{\theta(0)} = \frac{T - T_\infty}{T_w - T_\infty} \quad (32)$$

$$F'(\eta) = \frac{\left( \frac{x}{5y} \right)}{\left( \frac{Gr_x^*}{5} \right)^{2/5}} u$$

$F'(\eta)$  is plotted versus  $\eta$  for various Prandtl numbers in Figure 2.

Next we look at Sparrow and Gregg's [131] presentation of the heat transfer results. The surface temperature profile developed on the uniformly heated plate can be evaluated from equation (28) by setting  $\eta = 0$ :



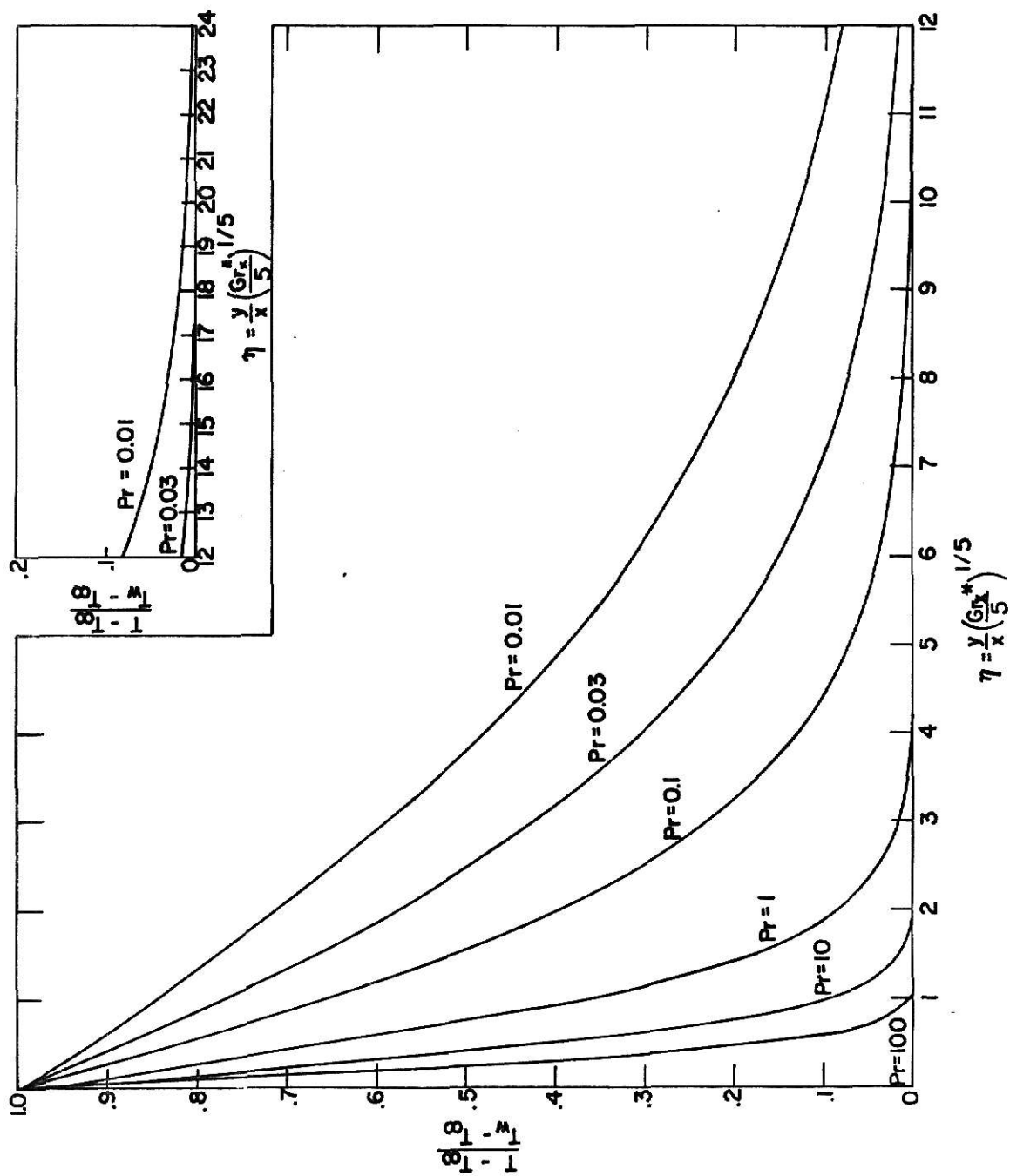


Figure 1. Dimensionless temperature distributions for various Prandtl number .

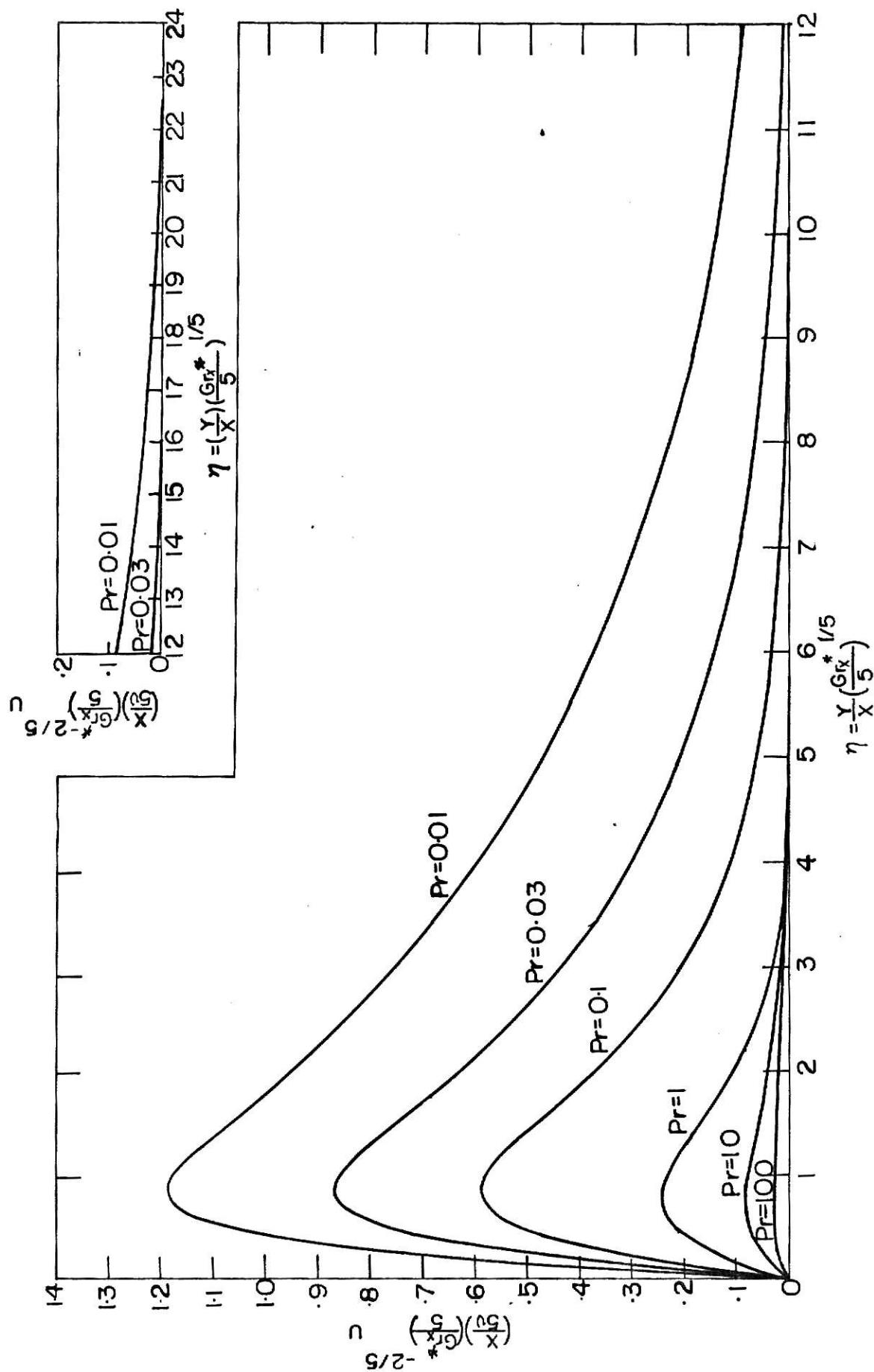


Figure 2. Dimensionless Velocity Distributions for Various Prandtl Numbers.

$$T_w - T_\infty = \left(\frac{Gr_x^*}{5}\right)^{-1/5} \left(\frac{q \cdot x}{k}\right) \theta(0) \quad (33)$$

Rearrangement of equation (33) gives:

$$\frac{T_w - T_\infty}{\left(\frac{q \cdot x}{k}\right)} Gr_x^{*1/5} = 5^{1/5} \theta(0) \quad (34)$$

Introduction of local Nusselt number which is defined as

$$Nu_x = \frac{h_x \cdot x}{k} = \frac{q \cdot x}{k(T_w - T_\infty)} \quad (35)$$

reduces equation (34) to :

$$\frac{Gr_x^{*1/5}}{Nu_x} = 5^{1/5} \theta(0) \quad (36)$$

Since the values of  $\theta(0)$  change with Prandtl numbers equation (36) can be plotted versus Prandtl number. Figure 3 presents this relation, and can be used to give approximate values of  $\theta(0)$  for other Prandtl numbers to solve the boundary layer equations.

### INTEGRAL METHOD

This method was developed by Von Karman and Pohlhausen. The similarity solution can only be carried out with the aid of

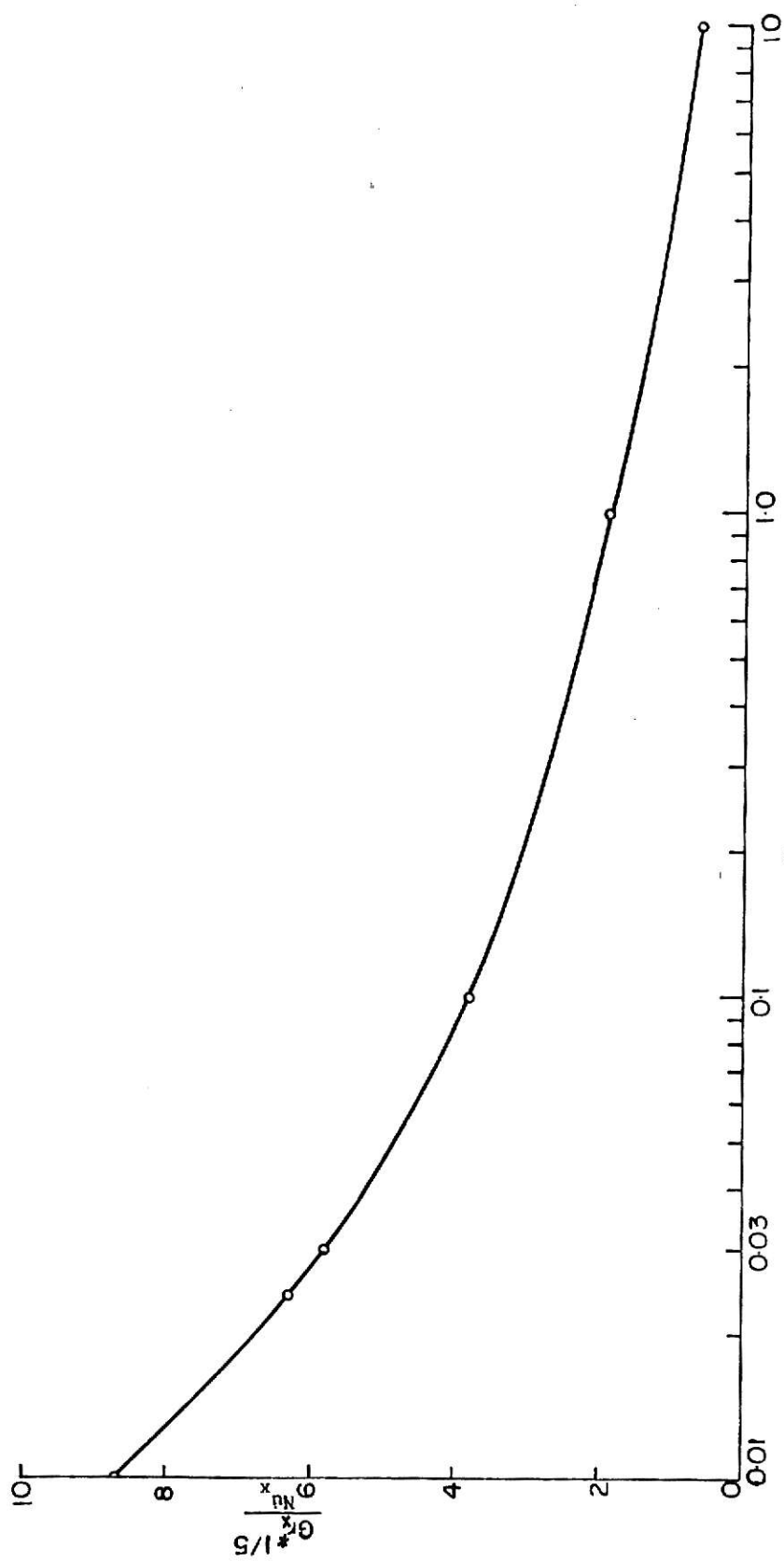


Figure 3. Variation of  $Gr_x^{*1/5}/Nu_x$  with Prandtl number.

an electronic computer, because a complete calculation is so cumbersome and time-consuming. It is desirable to possess at least approximate methods of solution, to be applied in cases when an "exact" solution of the boundary layer equations cannot be obtained with a reasonable amount of work. Such approximate methods can be devised if we do not insist on satisfying the differential equations for every fluid particle. Instead, the boundary layer equation is satisfied in a stratum near the wall by satisfying the boundary conditions, together with certain compatibility conditions. In the remaining region of fluid in the boundary layer, only a mean over the differential equation is satisfied; the mean being taken over the whole thickness of the boundary layer. Such a mean value is obtained from the momentum equation, which is, in turn, derived from the equation of motion by integration over the boundary layer thickness.

Integration of continuity equation, (15), gives the expression for the normal velocity component,  $v$ , and substitution to the expression in the equations of the motion and energy, (16) and (17), gives:

$$u \frac{\partial u}{\partial x} - \left[ \int_0^y \frac{\partial u}{\partial x} dy \right] \frac{\partial u}{\partial y} = \nu \frac{\partial^2 u}{\partial y^2} + \beta g(T - T_R) \quad (37)$$

$$u \frac{\partial T}{\partial x} - \left[ \int_0^y \frac{\partial u}{\partial x} dy \right] \frac{\partial T}{\partial y} = \alpha \frac{\partial^2 T}{\partial y^2} \quad (38)$$

Assuming that momentum and thermal boundary layers have the same thickness  $\delta(x)$ , equations (37) and (38) will be integrated over this boundary layer:

$$\begin{aligned} \int_0^\delta u \frac{\partial u}{\partial x} dy - \int_0^\delta \frac{\partial u}{\partial y} \left( \int_0^y \frac{\partial u}{\partial x} dy \right) dy \\ = \nu \int_0^\delta \frac{\partial^2 u}{\partial y^2} dy + g\beta \int_0^\delta (T - T_R) dy \end{aligned} \quad (39)$$

$$\int_0^\delta u \frac{\partial T}{\partial x} dy - \int_0^\delta \frac{\partial T}{\partial y} \left( \int_0^y \frac{\partial u}{\partial x} dy \right) dy = \alpha \int_0^\delta \frac{\partial^2 T}{\partial y^2} dy \quad (40)$$

The associated boundary conditions are:

$$u = v = 0, \quad q = q_0 \quad \text{at } y = 0 \quad \text{and } 0 \leq x \leq L \quad (41)$$

$$u = 0, \quad T = T_\infty, \quad \frac{\partial u}{\partial y} = 0, \quad \frac{\partial T}{\partial y} = 0 \quad \text{at } y = \delta \quad \text{and } 0 \leq x \leq L$$

Evaluation of equations (39) and (40) term by term and then rearrangement of those terms yields:

$$2 \int_0^\delta u \frac{\partial u}{\partial x} dy = g\beta \int_0^\delta (T - T_R) dy - \nu \left( \frac{\partial u}{\partial y} \right)_{y=0} \quad (42)$$

$$\int_0^\delta \left( u \frac{\partial T}{\partial x} + T \frac{\partial u}{\partial x} - T_\infty \frac{\partial u}{\partial x} \right) dy = -\alpha \left( \frac{\partial T}{\partial y} \right)_{y=0} \quad (43)$$

Equations (42) and (43) can be rewritten to agree with Sparrow's [129] starting equation:

$$\frac{d}{dx} \int_0^\delta u^2 dy = g\beta \int_0^\delta (T - T_R) dy - \nu \left( \frac{\partial u}{\partial y} \right)_{y=0} \quad (44)$$

$$\frac{d}{dx} \int_0^\delta u(T - T_\infty) dy = -\alpha \left( \frac{\partial T}{\partial y} \right)_{y=0} \quad (45)$$

Sparrow pointed out that equations (44) and (45) are the conservation equations for an element of the boundary layer.

Sparrow approximated the velocity and temperature profiles by the following equations:

$$T - T_\infty = \frac{q\delta(x)}{2k} \left(1 - \frac{y}{\delta}\right)^2 \quad (46)$$

$$u = \frac{w(x)y}{\delta(x)} \left(1 - \frac{y}{\delta}\right)^2 \quad (47)$$

where  $w(x)$  is a "velocity function" and must be determined along with  $\delta(x)$ . Equations (46) and (47) are substituted into the equations (44) and (45) and then the integration is carried out. The integrations yield a pair first-order, ordinary differential equations, which are then solved for  $w(x)$  and  $\delta(x)$ . The results agreed well with those obtained by use of a similarity transformation.

Both the similarity transformation and the integral method discussed above are based on the boundary layer theory which is applicable to natural convection at large Grashof numbers, i.e., a thin boundary layer. The boundary layer assumptions may not be valid for the fluid with small Prandtl number and with small

Grashof number. Therefore, a method was developed to solve the problem without boundary layer assumption. It is called perturbation technique which may be used for the fluid at small and moderate Grashof numbers.

#### PERTURBATION TECHNIQUE

Before this technique was developed by Yang and Jerger [158] in 1964, all analyses of natural convection had been based on laminar boundary-layer equations which are physically only adequate for large Grashof numbers. More precisely, they represented asymptotic solutions to the complete Navier-Stokes, continuity, and energy equations for Grashof numbers approaching infinity. For cases where the boundary layer approach is not valid, the perturbation method may be applied. They formulated the zeroth-order and the first-order perturbation equations, and solved them numerically for the Prandtl numbers of 0.72 and 10. Then the zeroth-order equations were shown to be the same as general boundary layer equations.

As pointed in the Review of Literature, all the work by Yang and his co-workers has been concerned with the isothermal plate and with two Prandtl numbers (air and water). Chang, Akins, and Bankoff [16] made a theoretical analysis of the case of constant heat-flux, vertical plate in liquid metals. Since the present experimental work was directly related with the latter case, their work will follow.



The governing equations without the boundary layer simplifications and with viscous dissipation neglected are:

$$\frac{\partial u}{\partial x} + \frac{\partial v}{\partial y} = 0 \quad (48)$$

$$\rho(u \frac{\partial u}{\partial x} + v \frac{\partial u}{\partial y}) = \mu(\frac{\partial^2 u}{\partial x^2} + \frac{\partial^2 u}{\partial y^2}) - \frac{\partial p}{\partial x} - \rho g + \rho g \beta (T - T_R) \quad (49)$$

$$\rho(u \frac{\partial v}{\partial x} + v \frac{\partial v}{\partial y}) = \mu(\frac{\partial^2 v}{\partial x^2} + \frac{\partial^2 v}{\partial y^2}) - \frac{\partial p}{\partial y} \quad (50)$$

$$u \frac{\partial T}{\partial x} + v \frac{\partial T}{\partial y} = \alpha (\frac{\partial^2 T}{\partial x^2} + \frac{\partial^2 T}{\partial y^2}) \quad (51)$$

The boundary conditions associated with present problem are:

$$u = v = 0, \quad q = -k \frac{\partial T}{\partial y} \Big|_{y=0}, \quad \text{at } y = 0 \text{ and } 0 \leq x \leq L \quad (52)$$

$$u \rightarrow 0, \quad v \rightarrow 0, \quad T \rightarrow T_\infty, \quad p \rightarrow p_\infty \quad \text{at } y \rightarrow \infty$$

The following dimensionless quantities are introduced with the stream functions defined as equations (18) and (19).

$$\bar{x} = \frac{x}{L}, \quad \bar{y} = \frac{y}{L} \quad (53)$$

$$\bar{\Psi} = \frac{\Psi}{Gr_L^*}, \quad P = \frac{(p - p_\infty)L^2}{\rho\nu^2 Gr_L^{*4/5}}, \quad G = \frac{gL^3}{\nu^2 Gr_L^{*4/5}} \quad (54)$$

$$\Theta = \frac{(T - T_\infty)k}{qL} Gr_L^{*1/5}, \quad Gr_L^* = \frac{g\beta L^4 q}{k\nu^2}$$

$$\bar{u} = \frac{\partial \bar{\Psi}}{\partial \bar{y}} = \frac{uL}{Gr_L^* \nu}, \quad \bar{v} = -\frac{\partial \bar{\Psi}}{\partial \bar{x}} = \frac{vL}{Gr_L^* \nu} \quad (55)$$

$$X = \bar{x}, \quad Y = Gr_L^{*1/5} \bar{y}, \quad \Psi = Gr_L^{*4/5} \bar{\Psi} \quad (56)$$

Then equations (49), (50) and (51) are transformed, respectively, to:

$$\Psi_Y \Psi_{XY} - \Psi_X \Psi_{YY} = -P_X + Gr_L^{*-2/5} \Psi_{XXY} + \Psi_{YYY} - G + \Theta \quad (57)$$

$$Gr_L^{*-2/5} (-\Psi_Y \Psi_{XX} + \Psi_X \Psi_{XY}) = -P_Y - Gr_L^{*-4/5} \Psi_{XXX} - Gr_L^{*-2/5} \Psi_{XXY} \quad (58)$$

$$\Psi_Y \Theta_X - \Psi_X \Theta_Y = Pr^{-1} (Gr_L^{*2/5} \Theta_{XX} + \Theta_{YY}) \quad (59)$$

where the subscripts denote partial differentiation with respect to the variable indicated.

To solve equations (57), (58) and (59) by a perturbation method, it is assumed that the function  $\Psi$ , the pressure  $P$ , and the dimensionless temperature  $\Theta$  can be expanded in small

constant parameter, viz.,

$$\Psi = \Psi^{(0)} + \epsilon \Psi^{(1)} + \epsilon^2 \Psi^{(2)} + \dots \quad (60)$$

$$P = P^{(0)} + \epsilon P^{(1)} + \epsilon^2 P^{(2)} + \dots \quad (61)$$

$$\Theta = \Theta^{(0)} + \epsilon \Theta^{(1)} + \epsilon^2 \Theta^{(2)} + \dots \quad (62)$$

where the value of constant expansion variable is taken as  $Gr_L^{*-1/5}$ , which results from the smooth joining of horizontal velocity components at the interface between the boundary layer and the exterior. When this definition of  $\epsilon$ , together with the expansions of  $\Psi$ ,  $P$ , and  $\Theta$ , is substituted to equations (57), (58), and (59), and the coefficients of like powers of  $\epsilon$  are equated, the following sets of equations result:

The zeroth-order perturbation equations are:

$$\Psi_Y^{(0)} \Psi_{XY}^{(0)} - \Psi_X^{(0)} \Psi_{YY}^{(0)} = -P_X^{(0)} + \Psi_{YYY}^{(0)} - G + \Theta^{(0)} \quad (63)$$

$$-P_Y^{(0)} = 0 \quad (64)$$

$$\Psi_Y^{(0)} \Theta_X^{(0)} - \Psi_X^{(0)} \Theta_Y^{(0)} = \frac{1}{Pr} \Theta_{YY}^{(0)} \quad (65)$$

The first order perturbation equations are:

$$\Psi_Y^{(0)} \Psi_{XY}^{(1)} + \Psi_Y^{(1)} \Psi_{XY}^{(0)} - \Psi_X^{(0)} \Psi_{YY}^{(1)} - \Psi_X^{(1)} \Psi_{YY}^{(0)}$$

$$= -P_X^{(1)} + \Psi_{YY}^{(1)} + \Theta^{(1)} \quad (66)$$

$$- P_Y^{(1)} = 0 \quad (67)$$

$$\begin{aligned} \Psi_Y^{(0)} \Theta_X^{(1)} + \Psi_Y^{(1)} \Theta_X^{(0)} - \Psi_X^{(0)} \Theta_Y^{(1)} - \Psi_X^{(1)} \Theta_Y^{(0)} \\ = \frac{1}{Pr} \Theta_{YY}^{(1)} \end{aligned} \quad (68)$$

by introducing new variables:

$$\eta = Y/(5X)^{1/5} \quad (69)$$

$$\Psi^{(0)} = (5X)^{4/5} F(\eta) \quad (70)$$

$$\Theta^{(0)} = (5X)^{1/5} \theta(\eta) \quad (71)$$

the zeroth order perturbation equation can be reduced to the following pair of ordinary simultaneous differential equations:

$$F''' + 4FF'' - 3(F')^2 + \theta = 0 \quad (72)$$

$$\theta'' + 4PrF\theta' - PrF'\theta = 0 \quad (73)$$

subject to:

$$F(0) = F'(0) = 0$$

$$\theta'(0) = -1$$

$$F'(\infty) = \theta(\infty) = 0$$

where the primes denote differentiation with respect to  $\eta$ . Equations (72) and (73), along with the boundary conditions turn out to be same as the equations (29) and (30) which were obtained by the similarity transformation of the general boundary layer equations.

Chang, et al. [16] obtained following set of first-order variables:

$$\Psi^{(1)} = \frac{20F(\infty)}{\pi} [S f_{00}(\eta) - \sum_{n=0}^{\infty} \frac{X^{n+1/5}}{5n+1} f_n(\eta)] \quad (74)$$

$$\Theta^{(1)} = \frac{20F(\infty)}{\pi} (5X)^{-3/5} [S \Theta_{00}(\eta) - \sum_{n=0}^{\infty} \frac{X^{n+1/5}}{5n+1} \Theta_n(\eta)] \quad (75)$$

where  $f_{00}$ ,  $f_n$ ,  $\Theta_{00}$ , and  $\Theta_n$  are functions of  $\eta$  alone, and

$$S = \sum_{n=0}^{\infty} \frac{3}{(5n+1)(5n+4)} = 0.864806\dots$$

Substitution of equations (74) and (75) into the first-order perturbation equations (66), (67) and (68) gives the following sets of ordinary differential equations:

$$f_{00}''' + 4Ff_{00}'' - 2F'f_{00}' + \theta_{00} = 0 \quad (76)$$

$$\frac{1}{Pr} \theta_{00}'' + 4F\theta_{00}' + 3F'\theta_{00} - \theta f_{00}' = 0$$

$$f_n''' + 4Ff_n'' - (5n + 3)F'f_n' + (5n + 1)F''f_n + \theta_n = 0 \quad (77)$$

$$\frac{1}{Pr} \theta_n'' + 4F\theta_n' - (5n - 2)F'\theta_n - \theta f_n' + (5n + 1)\theta'f_n = 0$$

where  $n = 0, 1, 2, 3, \dots$ , and the primes denote the differentiation with respect to  $\eta$ . These equations are to be solved subject to the following boundary conditions:

$$\begin{aligned} f_{00}(0) = f_{00}'(0) = \theta_{00}'(0) &= 0 \\ f_{00}'(\infty) = 1, \quad \theta_{00}(\infty) &= 0 \end{aligned} \quad (78)$$

and

$$\begin{aligned} f_n(0) = f_n'(0) = \theta_n'(0) &= 0 \\ f_n'(\infty) = 1, \quad \theta_n(\infty) &= 0 \end{aligned} \quad (79)$$

Note that first-order perturbation equations (76) and (77) include constants which are variables in the zeroth-order equations. Therefore the first-order perturbation equations have to be solved with the zeroth-order perturbation equations simultaneously.

Finally, expressions for velocity profile and temperature

profile are:

$$\frac{x/5\nu}{(Gr_L^*)^{2/5}} u = F'(\eta) + \epsilon \frac{20F(\infty)}{\pi(5X)^{4/5}} [Sf'_{00}(\eta) - \sum_{n=0}^{\infty} \frac{x^{n+1/5}}{5n+1} f'_n(\eta)] \quad (80)$$

$$\frac{T-T_{\infty}}{T_w-T_{\infty}} = \frac{\theta(\eta) + \epsilon \frac{20F(\infty)}{\pi(5X)^{4/5}} [S\theta_{00}(\eta) - \sum_{n=0}^{\infty} \frac{x^{n+1/5}}{5n+1} \theta_n(\eta)]}{\theta(0) + \epsilon \frac{20F(\infty)}{\pi(5X)^{4/5}} [S\theta_{00}(0) - \sum_{n=0}^{\infty} \frac{x^{n+1/5}}{5n+1} \theta_n(0)]} \quad (81)$$

When these equations are compared with the zeroth-order velocity and temperature profiles, equation (32), it is noted that both the second term in right hand side in equations (80), and also the second terms of numerator and denominator in right hand side in equation (81), are additional terms to the zeroth order profiles. Equations (80) and (81) are definitely functions of  $x$ , the distance up the plate, while equations (32) are not so. Numerical results are plotted in Figures 4 and 5 for the temperature profile and in the Figures 6 and 7 for the velocity profile with the Prandtl number of 0.03 at Grashof number  $(Gr_L^*)$  of  $10^7$  and  $10^9$ , respectively. These results are from the Reference [16].

#### RECENT THEORETICAL WORK

As mentioned in the previous chapter, Sparrow and Guinle [135], in 1968, studied the effects of transverse pressure

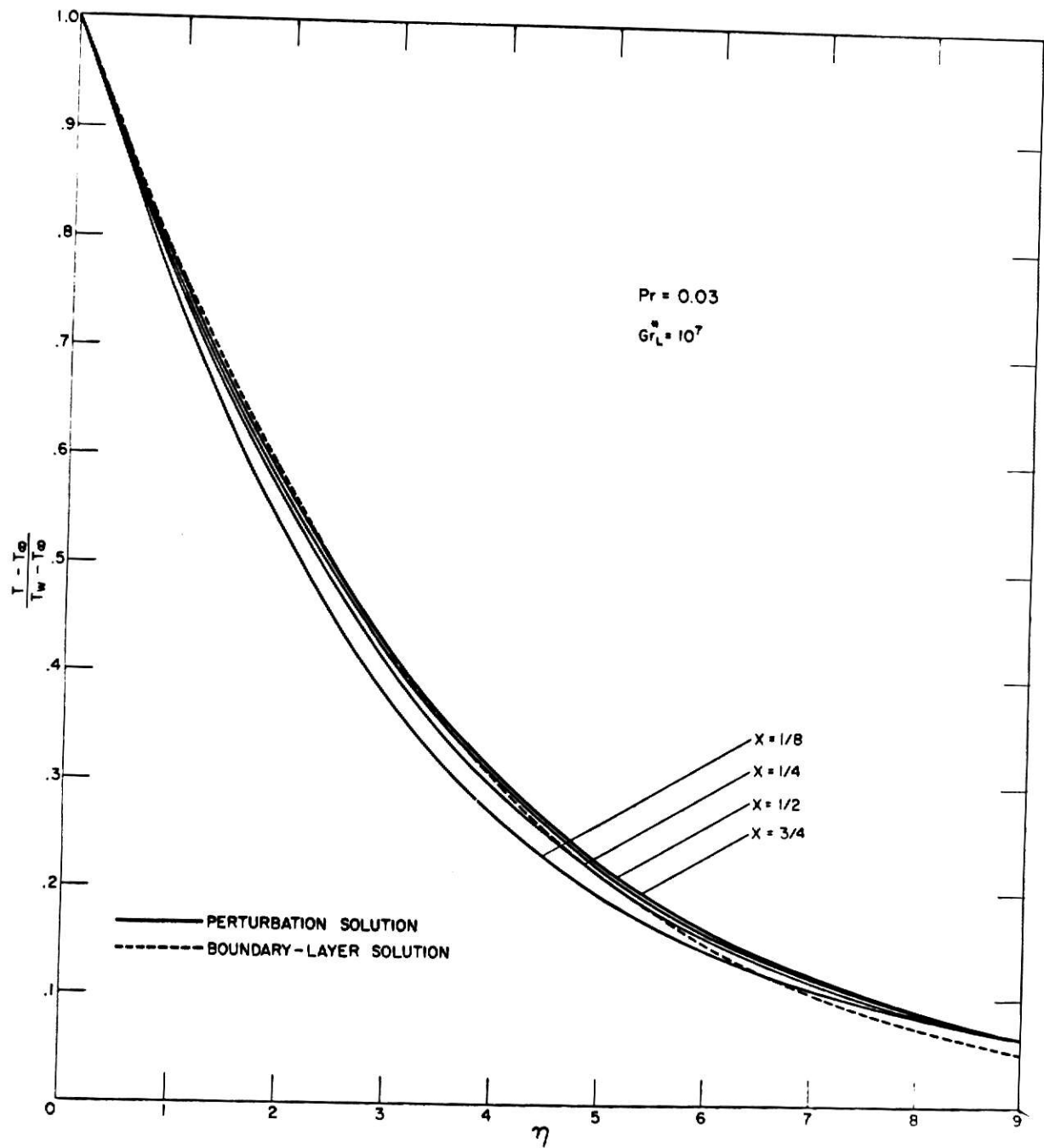


Figure 4. Comparison of Temperature Profiles for  $Pr = 0.03$  When  $Gr_L^* = 10^7$ .



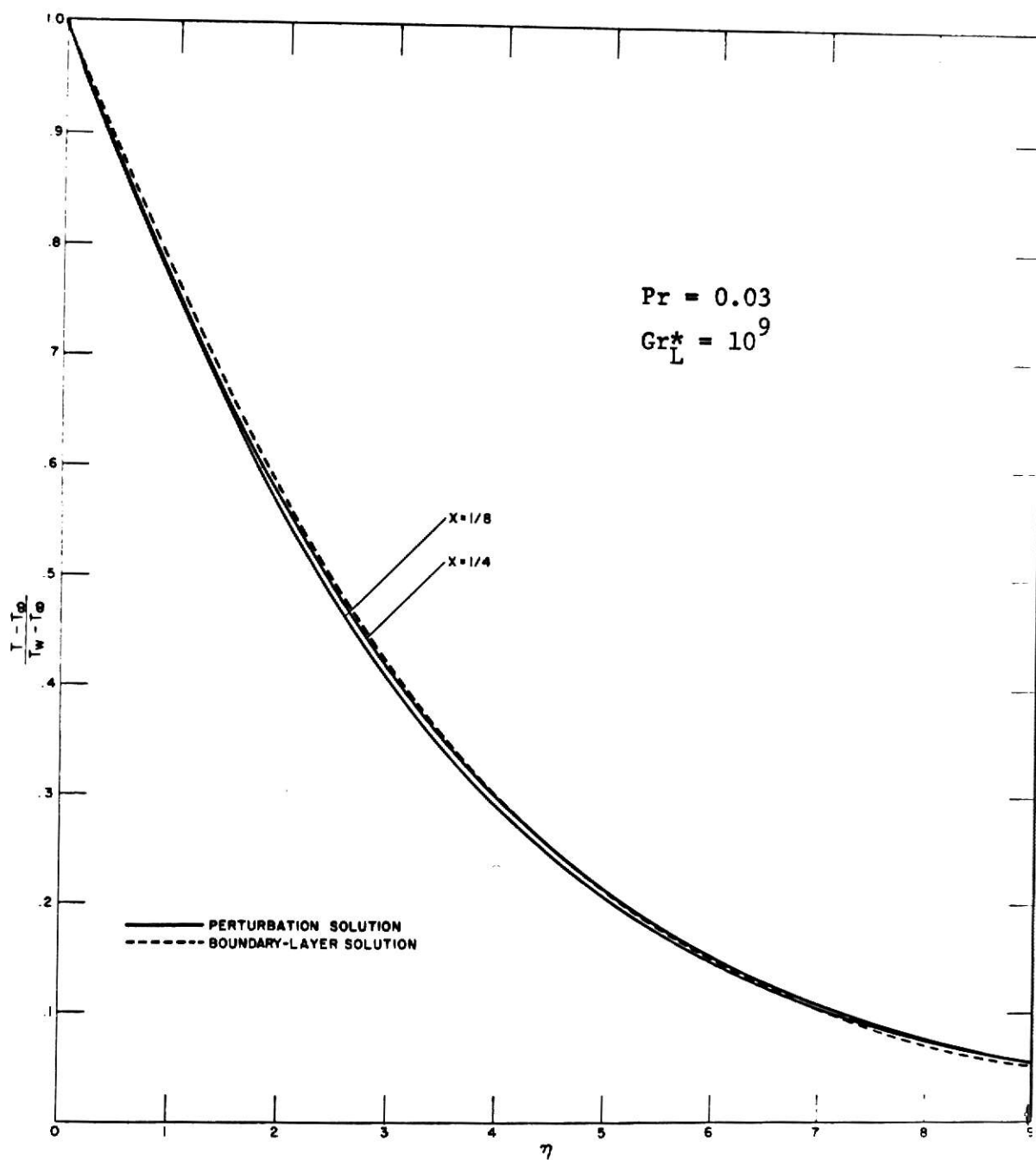


Figure 5. Comparison of Temperature Profiles for  $Pr = 0.03$  When  $Gr_L^* = 10^9$ .

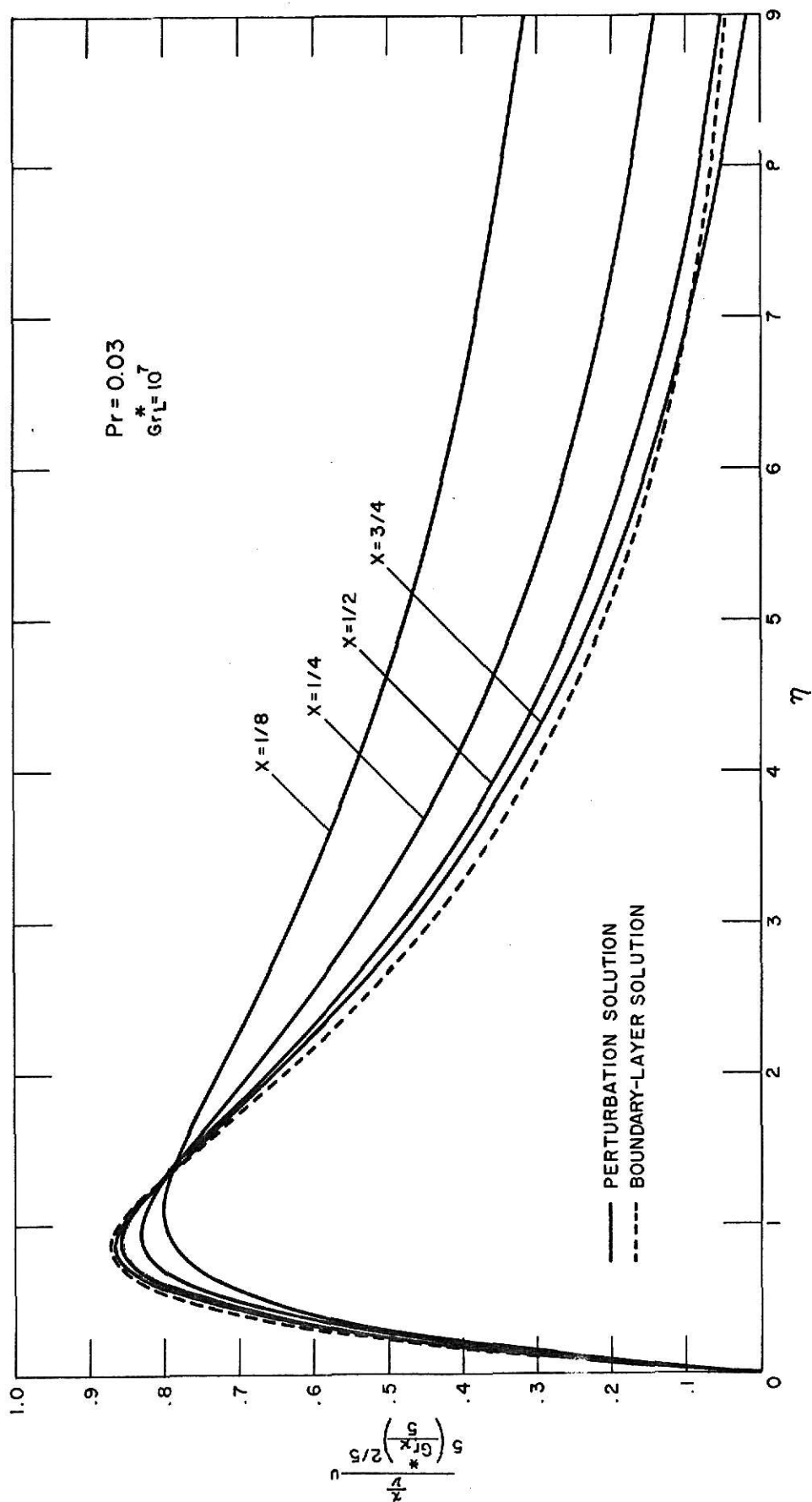


Figure 6. Comparison of Velocity Profiles for  $Pr = 0.03$  When  $Gr_L^* = 10^7$

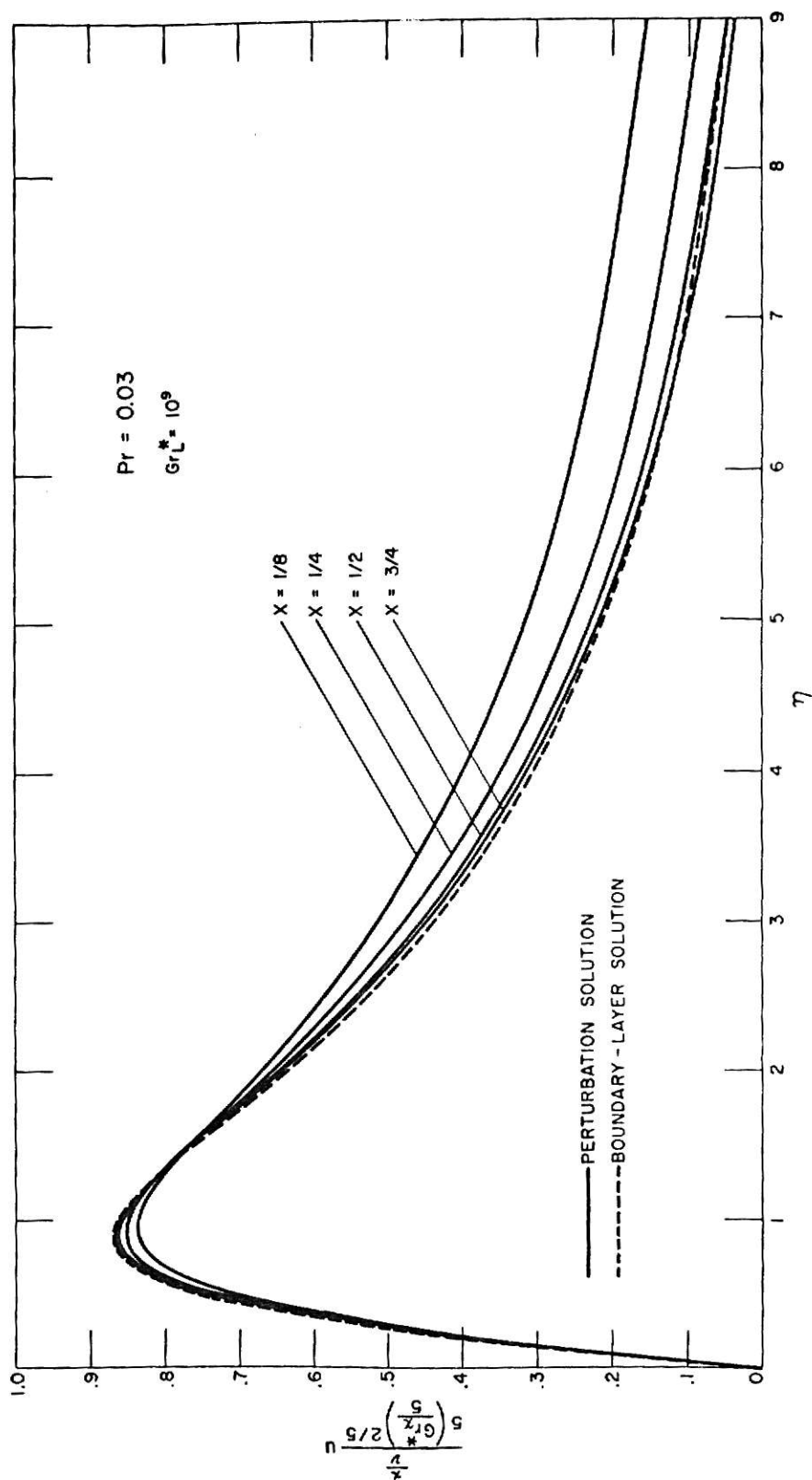


Figure 7. Comparison of Velocity Profiles for  $Pr = 0.03$  When  $Gr_L^* = 10^9$

gradient and streamwise second derivatives on the local heat transfer in laminar free convection from an isothermal vertical plate.

Complete governing equations are given: namely, equations (4), (5), (6) and (7). After the expansion coefficient is introduced, equations (5) and (6) are differentiated with respect to  $y$  and  $x$ , respectively; then subtraction of two resulting equations and deletion of the pressure terms, yields a single, consolidated momentum equation of higher order. The perturbation solution is sought in the form:

$$\psi = 4\nu \left(\frac{Gr_x}{4}\right)^{1/4} [\bar{f}_0(\bar{\eta}) + \varepsilon \bar{f}_1(\bar{\eta}) + \dots] \quad (82)$$

$$\bar{\theta} = (T - T_\infty)/(T_w - T_\infty) = \bar{\theta}_0(\bar{\eta}) + \varepsilon \bar{\theta}_1(\bar{\eta}) + \dots \quad (83)$$

$$\text{where } \bar{\eta} = \frac{y}{x} \left(\frac{Gr_x}{4}\right)^{1/4}, \quad Gr_x = \frac{g(T_w - T_\infty)x^3}{\nu^2}, \text{ and } \varepsilon = Gr_x^{-1/2}$$

Resulting two sets of equations are:

$$\begin{aligned} \bar{f}_0''' + 3\bar{f}_0''\bar{f}_0 - 2(\bar{f}_0')^2 + \bar{\theta}_0 &= 0 \\ \bar{\theta}_0'' + 3Pr\bar{f}_0'\bar{\theta}_0' &= 0 \end{aligned} \quad (84)$$

$$\begin{aligned} \bar{f}_1''' + 3\bar{f}_0''\bar{f}_1' + 2\bar{f}_0'\bar{f}_1'' - 3\bar{f}_0''\bar{f}_1 + \bar{\theta}_1 &= \frac{1}{8} \int_{\bar{\eta}}^{\infty} \bar{F}(\bar{\eta}) d\bar{\eta} \\ \bar{\theta}_1''/Pr + 3\bar{f}_0'\bar{\theta}_1' + 6\bar{f}_0'\bar{\theta}_1' - 3\bar{f}_1'\bar{\theta}_0' &= \frac{1}{8} \bar{G}(\bar{\eta}) \end{aligned} \quad (85)$$

where 
$$\bar{F} = \bar{\eta}^2 [-3\bar{f}_0 \bar{f}_0''' + 7\bar{f}_0' \bar{f}_0'' - 2\bar{\theta}_0'] + \bar{\eta} [6\bar{f}_0''' - 5(\bar{f}_0')^2 + 3\bar{f}_0 \bar{f}_0''] - 27 \bar{f}_0 \bar{f}_0' - 6\bar{f}_0'' \quad (86)$$

and

$$\bar{G} = - \frac{1}{Pr} (5 \bar{\eta} \bar{\theta}_0' + \bar{\eta}^2 \bar{\theta}_0'') \quad (87)$$

for the simultaneous effects of transverse pressure gradient and streamwise second derivatives.

Equations (84) turned out to be the same as those for the boundary layer theory for the isothermal vertical plate. Equation (85) is numerically solved subject to boundary conditions:

$$\bar{f}_1(0) = \bar{f}_1'(0) = \bar{\theta}_1(0) = \bar{f}_1'(\infty) = \bar{\theta}_1(\infty) = 0$$

The quantity of primary interest is the local heat transfer per unit time and area as given by Fourier's law

$$q = -k \left( \frac{\partial T}{\partial y} \right)_{y=0} \quad (88)$$

In terms of the variables of the analysis,  $q$  is expressed as

$$\frac{q}{q^0} = 1 + \frac{1}{Gr_x^{1/2}} \frac{\bar{\theta}_1'(0)}{\bar{\theta}_0'(0)} \quad (89)$$

where

$$q^0 = \frac{k(T_w - T_\infty)}{x} \left( \frac{Gr_x}{4} \right)^{1/4} [-\bar{\theta}_0'(0)]$$

$q^0$  represents the local heat flux corresponding to the classical boundary-layer solution.

Thus, the deviation of  $q/q^0$  from unity is a direct measure of the effects. The magnitude of  $q/q^0$  depends on the ratio  $\bar{\theta}_1'(0)/\bar{\theta}_0'(0)$  and on the Grashof number  $Gr_x$ . Sparrow and Guinle calculated the values of  $\bar{\theta}_1'(0)/\bar{\theta}_0'(0)$  for the three separate effect and the simultaneous effect. Those values for the different Prandtl numbers are presented in Table 1.

Table 1. Values of  $\bar{\theta}_0'(0)$  and  $\bar{\theta}_1'(0)/\bar{\theta}_0'(0)$

Pr	$-\bar{\theta}_0'(0)$	$\bar{\theta}_1'(0)/\bar{\theta}_0'(0)$			
		$\frac{\partial p}{\partial y}$ effect	$\frac{\partial^2 u}{\partial x^2}$	$\frac{\partial^2 T}{\partial x^2}$	SUM(simultaneous effect)
0.733	0.5079	0.0778	-0.0899	0.4641	0.4519
0.03	0.1346	1.6145	-0.0387	5.7152	7.2910
0.003	0.0452	17.474	-0.0389	44.791	62.227

It should be noted that the longitudinal conduction  $\partial^2 T / \partial x^2$  is a dominant factor in deviation from the boundary layer theory and that longitudinal shear  $\partial^2 u / \partial x^2$  has negative effect, even though it is small. In addition, the calculation reveals that the effects are largely accentuated, when the Prandtl number

decreases. Considering the simultaneous effect, the value of the Grashof number for the Prandtl number of 0.03 was calculated as  $2.1 \times 10^4$  so as to give 5% positive deviation. Conclusively, the smaller Prandtl number and Grashof number the system has, the larger deviation it has from the boundary layer theory.

Even though the previous calculations were concerned with the case of isothermal vertical plate, and they can not be applied directly to the case of constant heat-flux plate, some qualitative and theoretical knowledge may be obtained for the latter case.

## APPARATUS

The experimental equipment was essentially the same as that used by Julian [67], with the exception that an additional X-Y Plotter was used. The equipment consisted of a container large enough for the fluid to be considered as infinite, an electrically-heated vertical plate to give a constant heat flux, a probe positioning mechanism to move a thermocouple horizontally and vertically, and the temperature versus position recording device.

The container, seven inches wide by nine inches long by thirteen inches deep, was made of type 410 stainless steel. The plate was made of type 302 stainless steel and was two inches high, four inches long, and 0.004 inch thick (Figure 8). The plate was electrically heated using a d.c. power supply in order to generate constant heat flux. The plate was coated with Datacoat (a plasticized acrylic resin of high solid content) to electrically insulate it from the mercury. The probe positioning mechanism consisted of a 7/16-inch thick, eight by thirteen inch base plate with a slot and slide for moving the thermocouple horizontally (to and from the plate). The slide was connected to a 2-rpm synchronous motor by a 1/2-inch, 32 precision pitch screw in order to obtain continuous horizontal motion. Thus, the linear speed of the thermocouple was 1/16 inches per minute. Attached to the motor shaft was a ten-turn, 50 K ohm potentiometer and a battery which gave voltages corresponding to the thermocouple position from the plate. The thermocouple could be moved

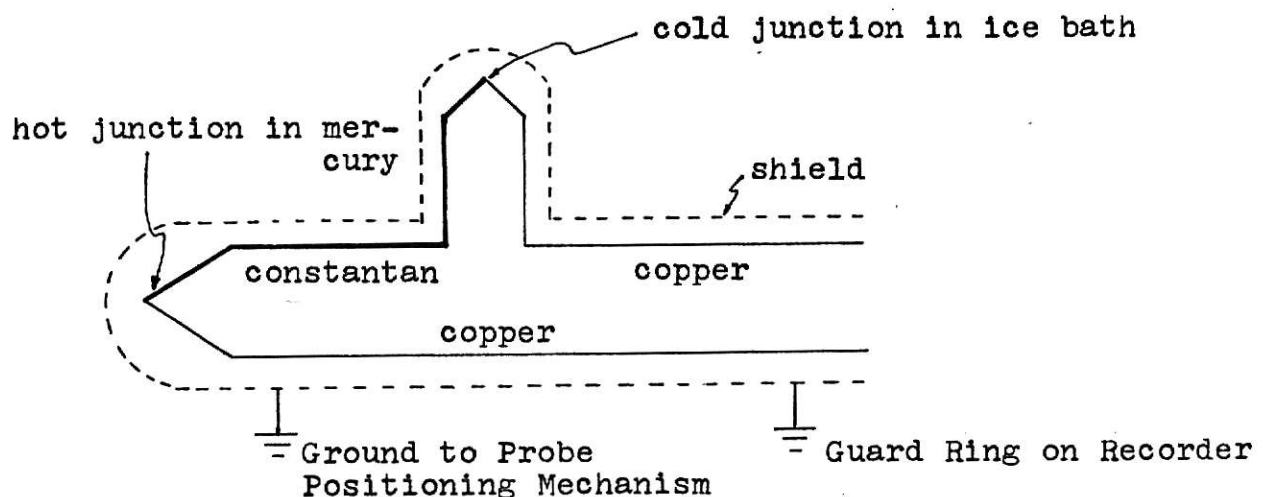




Figure 8. Vertical plate and thermocouple probe

manually to a desired position up the plate by a similar screw arrangement. Figure 9 shows a view of the entire mechanism.

Temperature profiles were measured with a BLH Electronics, HT Micro miniature thermocouple, model TCC-FS-200. The copper-constantan wires were enclosed in a two inch long, 0.014-inch diameter, type 302 stainless steel sheath. The end of the sheath was flattened onto the junction of the thermocouple to increase the response time (0.008-inch by 0.021-inch wide). The time constant was approximately fifty milliseconds. Any disturbances in the flow that were caused by the thermocouple were minimized by having thermocouple pointing upstream (downward). The tip of the thermocouple was bent parallel to the flow to minimize the conduction error. Figure 10 is an enlarged photograph of the thermocouple. The wiring of the thermocouples to the recorder is shown below.



Thermocouple Wiring Diagram

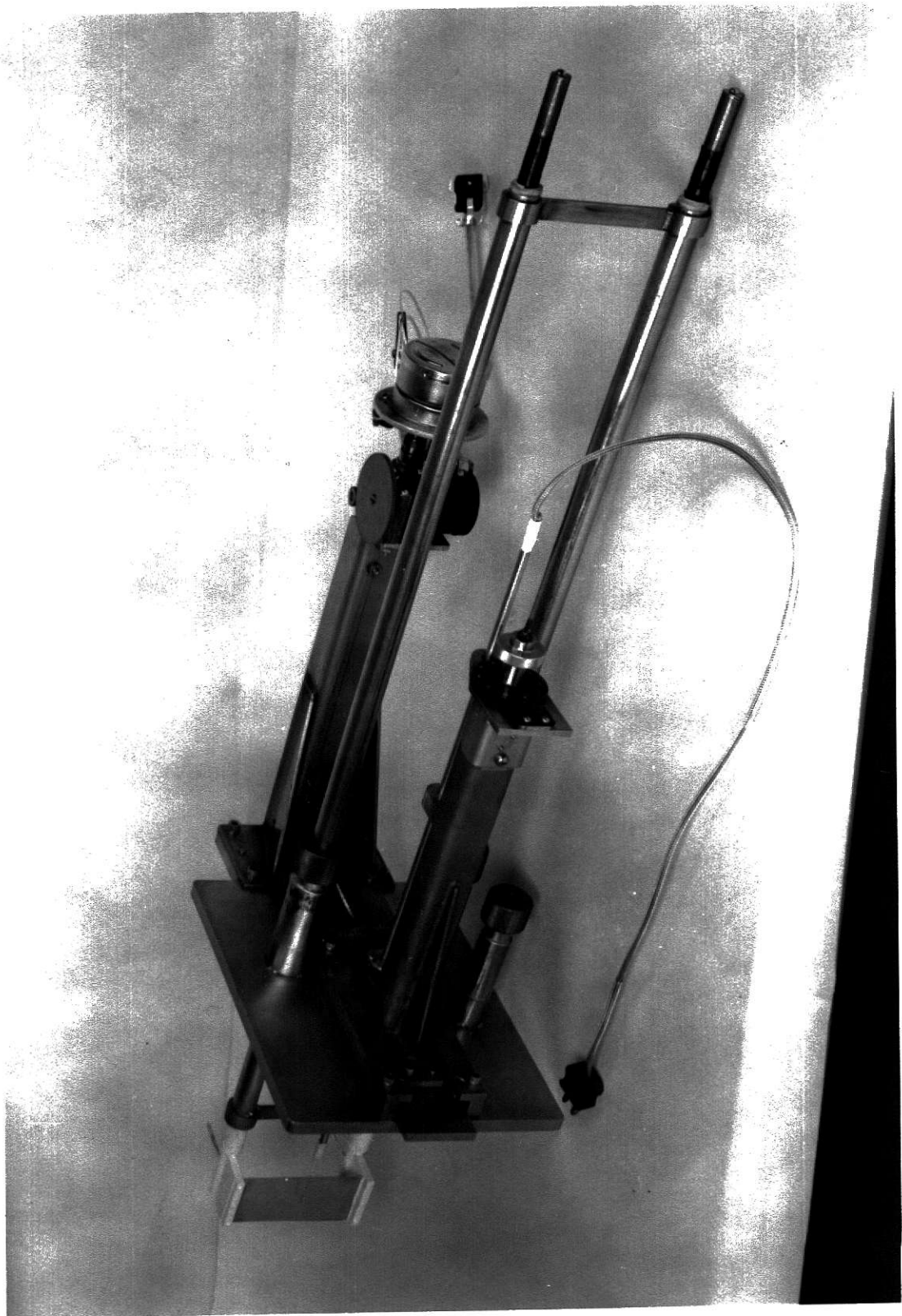


Figure 9. Probe Positioning Mechanism

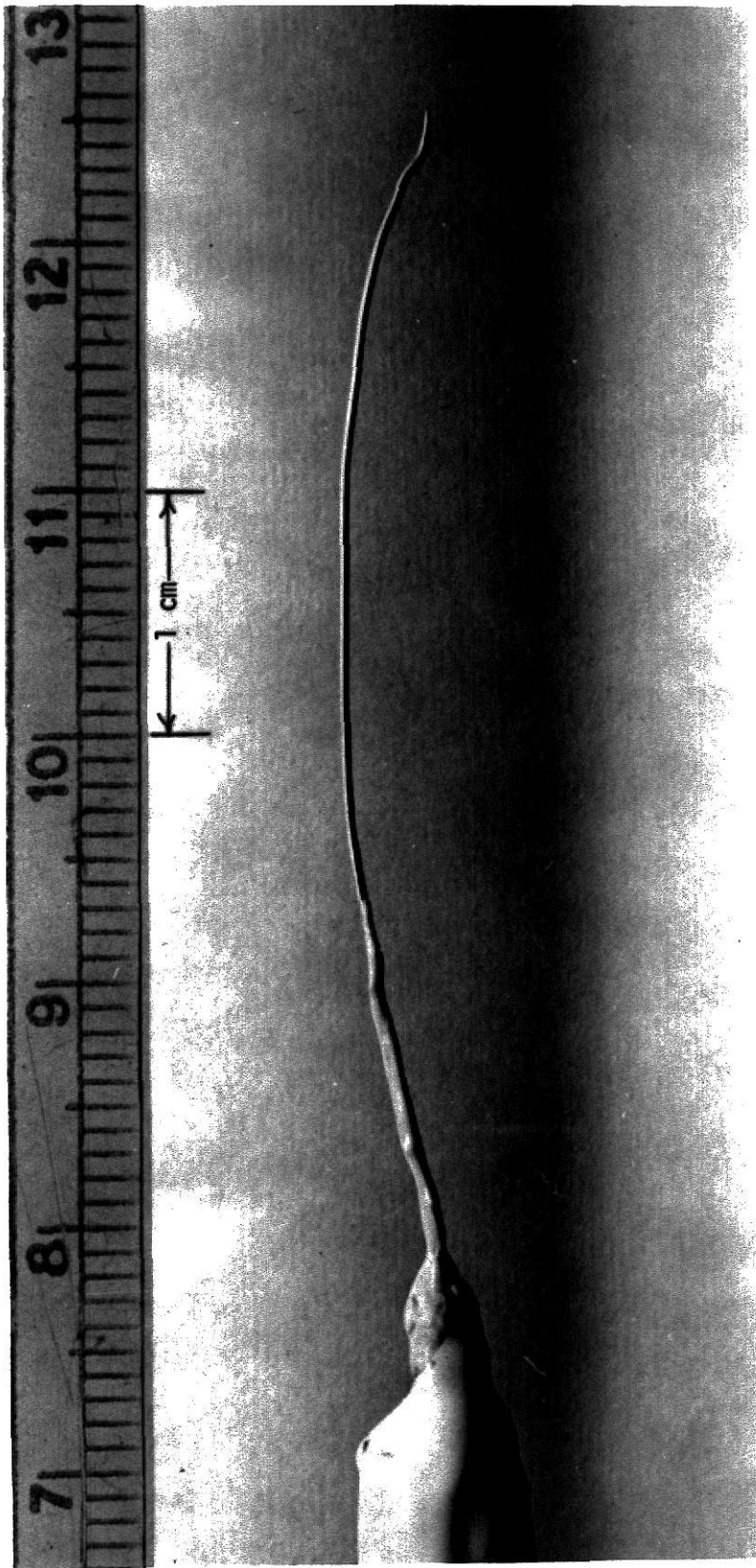


Figure 10. Copper Constantan Micro Miniature Thermocouple.

Stainless Steel Sheath: 0.014 inch diameter

Tip of Thermocouple: 0.008 inch thick

A constant temperature bath was used to keep the whole container at the desired temperature. It controlled the temperature to within one degree centigrade using cooling coil and immersed electrical heaters. This temperature varied too much for measurement of small temperature differences, and therefore the water bath without the cooling coils and heaters was used, and then it was found that temperature change in the mercury was negligible.

The small voltage generated between the thermocouple in the mercury and the thermocouple in the ice-bath (reference temperature) was first amplified in a Sanborn, Model 350-1500, low-level preamplifier and 350 Amplifier, and then plotted on a EAI, Model 1130, Variplotter (X-Y Plotter). The Sanborn recorder has two channels with preamplifiers and an attempt was made to use one channel for amplification and the other for additional amplification and recording. But this failed to produce a uniform amplifying factor and the recording was not stable.

The sensitivity of the Sanborn recorder was two microvolts per millimeter, thus allowing temperature difference measurements to within  $0.03^{\circ}\text{C}$  ( $\frac{1}{2}$  mm of chart width). In order to measure and record even smaller temperature differences, the output of the Sanborn (0 - 5 volts full scale) was plotted on the X-Y Plotter. The maximum amplifying factor of the Sanborn was about 50,000 times, which would give an output of 92.15 mv/mm without any attenuation.

In the Sanborn preamplifier, the maximum error was  $\pm 2\%$

and the response time was twenty-five milliseconds for 99.9% response to a step input. The X-Y plotter had eighteen scale factors. At the minimum scale factor of 1.0 mv/in, a temperature difference of 0.0005 °C could be measured, which was equivalent to one inch of plotting width. The static accuracy was  $\pm 0.1\%$  and scale factor accuracy (range to range) was also  $\pm 0.1\%$ . The eighteen scale factors covered the range from 1 mv/in to 20 v/in each for the X and Y coordinate. In addition, there was six time base ranges in seconds per inch in X axis, therefore temperature versus distance from the plate and temperature versus time at a fixed position could be plotted by choosing proper scale factors.

Input voltage to the Y axis came from the thermocouple in the mercury with the reference thermocouple in the ice-bath through the Sanborn recorder, and the input voltage to the X-axis came from the potentiometer which was attached to the shaft of the synchronous motor used to move the thermocouple horizontally.

The power generated in the plate was determined by measuring the voltage drop across the two copper rods which were connected to the plate. The current was determined by measuring the voltage drop across a 1,500 ampere, fifty millivolt shunt with a Leeds and Northrup millivolt potentiometer.



## PROCEDURE

As preliminary experiments, water was used as a working fluid and it was contained in a glass vessel (the same size as the metal one) for observation of the thermocouple and plate. The plate was adjusted to be flat and vertical. Some experimental data were obtained to check for consistency and to find the minimum possible temperature difference that could be measured by the amplifier and the plotter.

For the primary experiments, the container was placed on a stainless steel support inside the constant temperature bath and was leveled carefully. Mercury, which was previously purified by oxidation and filtering, was poured into the container. The probe positioning mechanism was prepared by locating the thermocouple at the leading edge (bottom) of the plate and adjusting the plate so that it was perpendicular to the top of assembly. The mechanism was carefully set and the clamped on top of the container inside the constant temperature bath. Distilled water was added through an entry tube to bring the level to the top. Mercury had been filled to a level two inches from the top of the container.

The power cables and all other leads were connected and plate supports were checked to see if they were still perpendicular to the top of the mechanism. Enough water was added to the constant temperature bath to a level approximately two inches above the top of the slide on the probe positioning mechanism. Immersion heaters in conjunction with a copper cooling coil inside

the constant temperature bath failed to maintain the temperature sufficiently constant, the variation being about  $1^{\circ}\text{C}$ . Since temperature differences of the order of  $0.01^{\circ}\text{C}$  were to be measured in the container, the bath temperature fluctuations had a great effect on the temperature profiles. It was found that simply allowing the bath to remain at room temperature provided the most constant temperature, and that the bulk heating of the mercury was negligible at the power levels used. After the power to the system was turned on, at least twenty-four hours were allowed for steady state to be reached. A similar period of time was also allowed after the power level to the plate was changed.

Before each set of measurements were made, the Sanborn recorder was calibrated by adjusting the response of the recorder to a known standard cell voltage. The zero position was set twenty-one millimeters from the right hand edge of the chart (corresponding to zero output voltage). This manipulation was made for easy positioning of the plotting pen at any point in the plotting paper by setting X and Y zero positions properly.

The thermocouple was located at the point of interest up the plate by turning the micrometer dial manually. All the profiles were recorded starting from the plate and moving to the bulk, and then from the bulk to the plate by reversing the motor. Starting at the plate, the temperature would remain constant initially, and then start to decrease, indicating that the thermocouple had left the plate. As the probe moved from the



plate to the bulk, the temperature would drop rapidly at first, then would approach a constant value (the "bulk" temperature). At this point, the motor was reversed, and the probe was driven back to the plate. In this manner, two almost identical profiles were obtained, making it possible to check for the steady state and for the effect of probe movement on the profile.

The two profiles were not identical in all cases, the difference being less than  $2 \times 10^{-3} \text{ }^{\circ}\text{C}$ . The temperature at the plate surface varied about the same amount. The position (on the recorded chart) where the thermocouple first left the plate was not identical to the position where it met the plate on returning. The distance from the plate to a given position in the bulk was always shorter when moving from the plate than it was when moving toward the plate. This was thought to be due to the thermocouple probe sticking slightly to the plate requiring a slight pressure to firmly contact the plate. The difference in the apparent plate location was never more than  $1/2 \%$  of the total profile distance. The profiles toward and away from the plate were averaged to produce the profile used for data. It should be noted that it took about twenty minutes for the probe to travel to and from the plate.

After profiles were obtained at several positions up the plate at the same power level, the power was changed and the system was allowed to attain the steady state for approximately one day. For each profile, the voltage drop across the copper rods and shunt, position up the plate, attenuation and zero

suppression on the Sanborn, and X and Y scale factors on the Plotter were recorded.

## DATA ANALYSIS

Some typical X-Y plotter outputs are depicted in Figure 11. Temperatures were plotted versus distance from the plate. Each solid line in Figure 11 represents an average of two profiles: one plotted when the thermocouple started from the plate and moved to the bulk, and the other from the bulk to the plate under same conditions. The dashed lines at an either side of the solid lines show the region of noise contained in the profiles. The fluctuation frequency was so high (60 cycle mostly) that each profile looked like a curved band rather than a single line. From the point of view of the noise, it could be anticipated that the fluctuation was caused primarily by 60 cycle pickup in the recorder or from the thermocouple. Since the voltage generated in the thermocouple was amplified about 50,000 times, any small accompanying noise would be amplified accordingly.

In the first profile, Profile 1, in Figure 11, which was obtained at higher power levels (16.6 watts), the fluctuation range was  $\pm 1\%$ . The ranges for the Profiles 2 and 3 at medium (7.5 watts) and lower (3.9 watts) power levels, respectively, were  $\pm 2\%$  and  $\pm 4\%$ . At the lower power levels where higher amplification was needed, the fluctuation was accentuated, causing an increased error.

Fifteen to twenty-five data points were selected from each profile, each data point representing a temperature and a distance. Each point was transformed into dimensionless variables and all

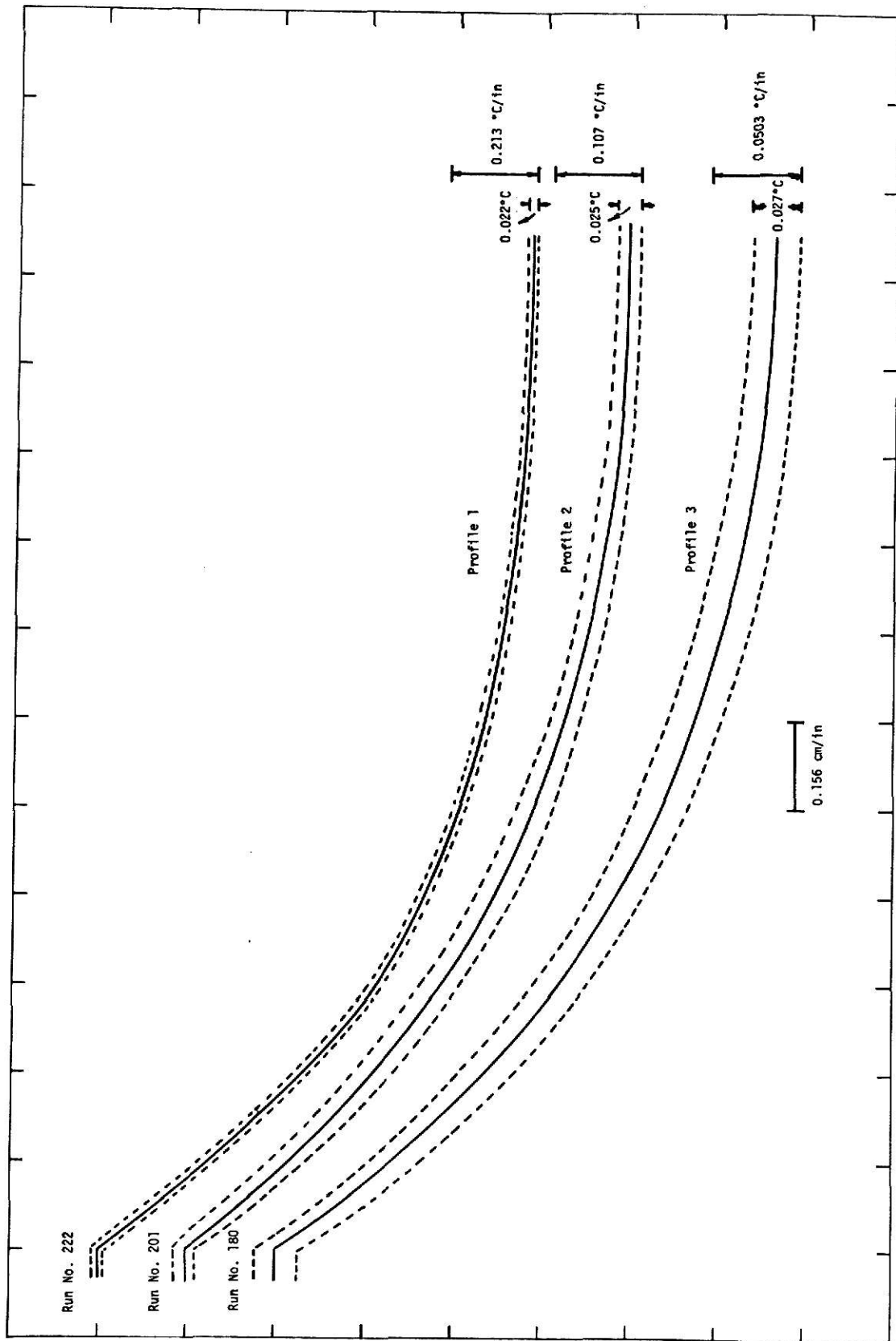


Figure 11. Typical X-Y plotter outputs.

the data were processed by IBM 360/50 digital computer. The computer program is presented in Appendix A. The following paragraphs describe the data reduction.

First, the temperature at the wall and in the bulk were computed with the known recorder characteristics and setting factors. The resulting temperatures in millivolts were converted into degrees centigrade using a fourth-order least square polynomial fit of the copper-constantan thermocouple calibration. The reference temperature for the evaluation of physical properties was calculated from the wall and bulk temperatures as Sparrow [128] recommended, i.e., a weighted average of 70% of wall temperature and 30% of the bulk temperature. Physical properties such as density, viscosity, thermal conductivity, thermal expansion coefficient and Prandtl number were then computed at the reference temperature from corresponding fourth-order least square polynomial equations.

The heat flux was calculated from the power consumed in the plate, which was determined from the total power multiplied by the ratio of the plate resistance to the overall resistance. The plate resistance was computed at the wall temperature from a second-order polynomial equations and the overall resistance from the experimentally measured voltage and current. The local Nusselt number and the modified Grashof number were computed with the physical properties, heat flux, and the vertical position on the plate.

The position of the probe horizontally from the plate was

calculated from the plotter position, X-scale factor, potentiometer output, and the speed of the probe. Finally, temperatures in degrees centigrade and distance in centimeters were converted to dimensionless temperatures and distance, respectively. For the detailed calculation on the data analysis, the reader is referred to the Sample Calculations in Appendix B.

Even though the data had been taken from the averaged curve, the dimensionless data points did not constitute the good smooth curve. The dimensionless data points were fitted by a first to six-order polynomial to obtain the final dimensionless plot. The polynomial fit which had the smallest standard deviation for each set of data was chosen. Careful attention has been paid to see if the polynomial fitting procedure affected any trends or conclusions seriously.

## DISCUSSION OF RESULTS

Boundary layer theory for the free convection from a constant heat flux, vertical plate immersed in mercury was experimentally verified by Julian [67] in 1967. He carried out experiments in moderate range of local modified Grashof number. There has not been an experimental investigation of natural convection in liquid metal at low Grashof numbers, where appreciable deviation from the boundary layer theory were theoretically predicted. The present work presents the experimental results for the free convection from a constant heat flux, vertical plate in mercury at low Grashof numbers. This work is essentially an extension of Julian's work to the much lower range of Grashof numbers. First, overall dimensionless temperature profile is presented to see the general tendency. Next, dimensionless temperature profiles at constant power levels, at fixed vertical positions, and at constant local Grashof numbers are presented in order to see the possible dependence of the profiles.

### OVERALL DIMENSIONLESS TEMPERATURE PROFILE

Results of many experimental runs at various power levels and several positions up the plate are presented in one figure, Figure 12, to investigate general trend. Figure 12 includes the data obtained at five different power levels ranging from 26 to 1150 Btu/hr-ft<sup>2</sup> and at seven different positions from

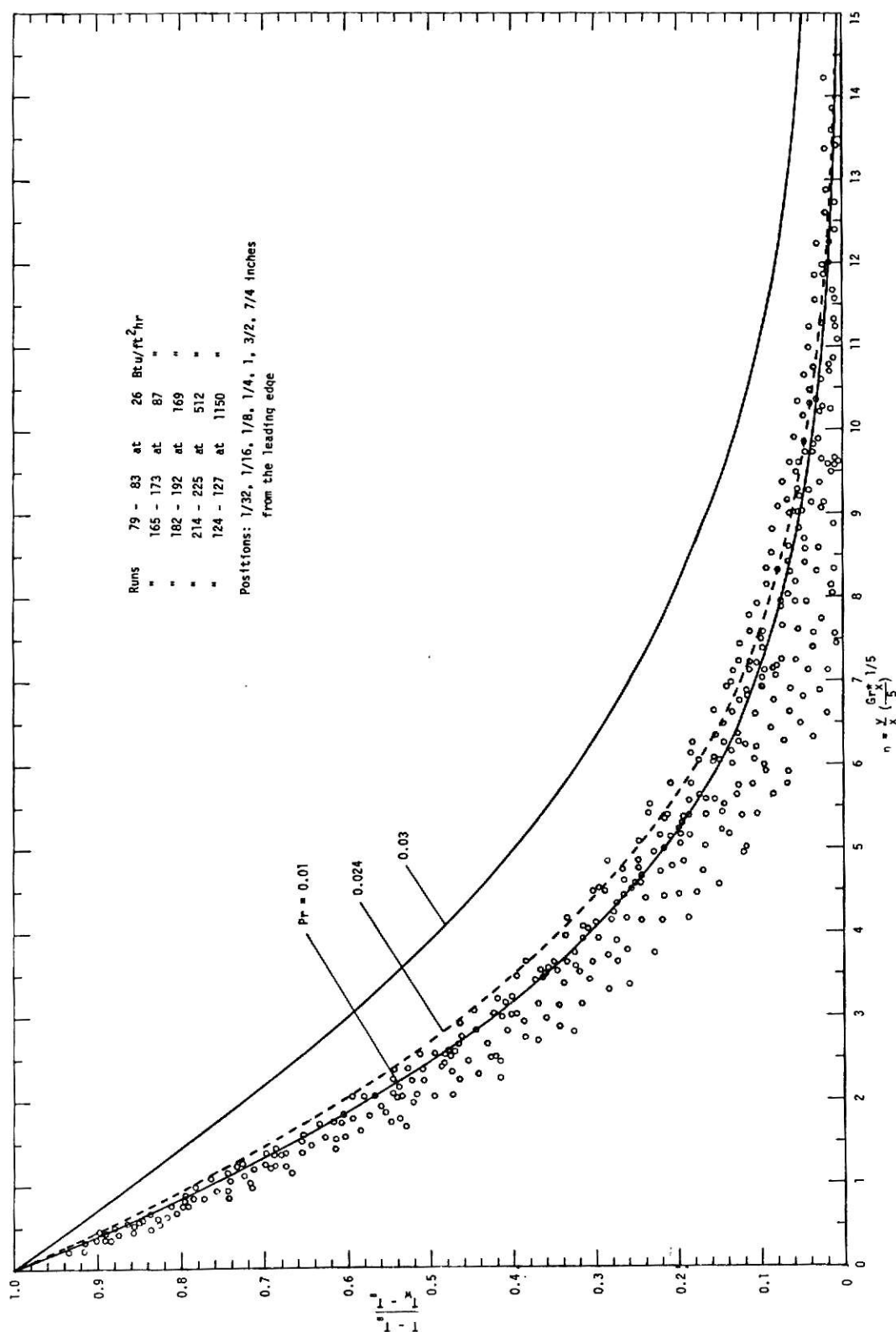


Figure 12. Overall dimensionless temperature distribution -- Present work.



1/64 to 7/8 of the plate height. Two solid lines in the Figure 12 represent the boundary layer solution for the Prandtl number of 0.01 and 0.03, where were obtained by Chang, et. al [15]. A dashed line also represents the boundary layer solution for the Prandtl number of 0.024 which is the case of the present work. Since there had been no published solution for the Prandtl number of 0.024, boundary layer equations for this Prandtl number were solved numerically using a digital computer IBM 360/50. As mentioned previously in the Theoretical Analysis, unknown boundary conditions,  $\theta(0)$  and  $F''(0)$ , were to be guessed for the solution to satisfy all other boundary conditions. These two unknown boundary conditions were found by simulating on an analog computer. It should be noted that even if the Prandtl number is slightly varied with temperatures, the Prandtl number of 0.024 is exact enough for the temperature range used in this experiment.

Most of data are located below the dashed line and also spread widely. As shown in Figures 4 and 5 in the Theoretical Analysis, the perturbation theory predicted the downward shift of profiles from the dashed line in the smaller range of dimensionless distance  $\eta$ , but not in the relatively larger  $\eta$ , and also predicted that the lower position up the plate and/or the lower heat flux would cause the more deviation. In other words, the larger  $x$  and the higher heat flux would make the situation approach to the boundary layer theory. This deviation can be explained to be due to the physical situation which would

not follow the boundary layer assumptions. Since the Grashof numbers used in the present experiment ranged from 1 to  $10^8$  and the temperature difference between the heated plate and bulk ranged from  $0.05^\circ\text{C}$  to  $2.2^\circ\text{C}$ . It is surely obvious that boundary layer theory can not be applicable to the overall range uniformly. In the region where boundary layer assumptions are no longer valid, the neglected terms in the simplified boundary layer equations such as transverse pressure, streamwise conduction, and shear stress should be taken into account. In 1968, Sparrow and Guinle [135] (see Theoretical Analysis) analyzed the effect of those neglected terms for the case of isothermal plate. Since there has not been such an analysis for the case of constant heat-flux plate, direct comparison can not be made quantitatively.

Julian's experimental data are presented in Figure 13 for comparison with the present work. His data along with Saunder's [107] are only existing experimental data in mercury. Most of Julian's data are located near the boundary layer solution for the Prandtl number of 0.03, whereas the Prandtl number he used was 0.022. It was explained that the downward shift of data would be due to the probe thickness, and pointed that the temperature response of thermocouple was not from a single point but from the two points across the probe, and that the effect of the finite thickness of the probe on the downward shift of the data was estimated to be about 18%. Thus, it can be anticipated that the shift of present data would be accentuated

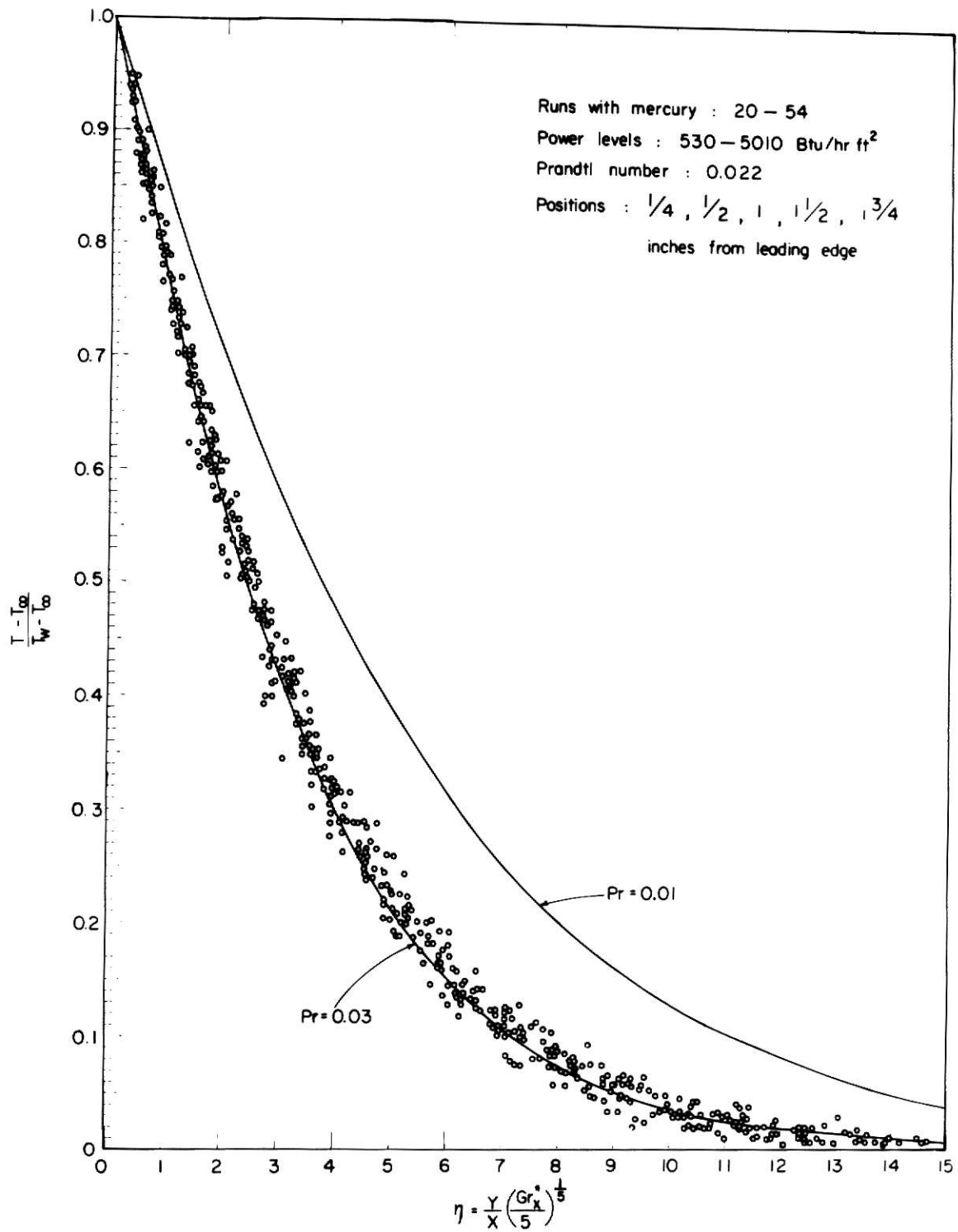


Figure 13. Dimensionless temperature distribution for mercury.  
 Julian's work

by the probe thickness effect. Following table shows the difference in physical situation between the present work and Julian's.

Table 2. Comparison of experimental results with those of Julian

	<u>Present</u>	<u>Julian's</u>
Prandtl No.	0.024	0.022
Heat flux	26 - 1150 Btu/hr-ft <sup>2</sup>	530 - 5010 Btu/hr-ft <sup>2</sup>
$Gr_x^*$	$1 - 10^8$	$10^5 - 10^{10}$
Temperature difference	0.05 - 2.2 °C	1 - 8 °C
Positions up the plate where data were taken	1/32, 1/16, 1/8, 1/4, 1, 3/2, 7/4 inches from leading edge	1/4, 1/2, 1, 3/2, 7/4 inches from leading edge

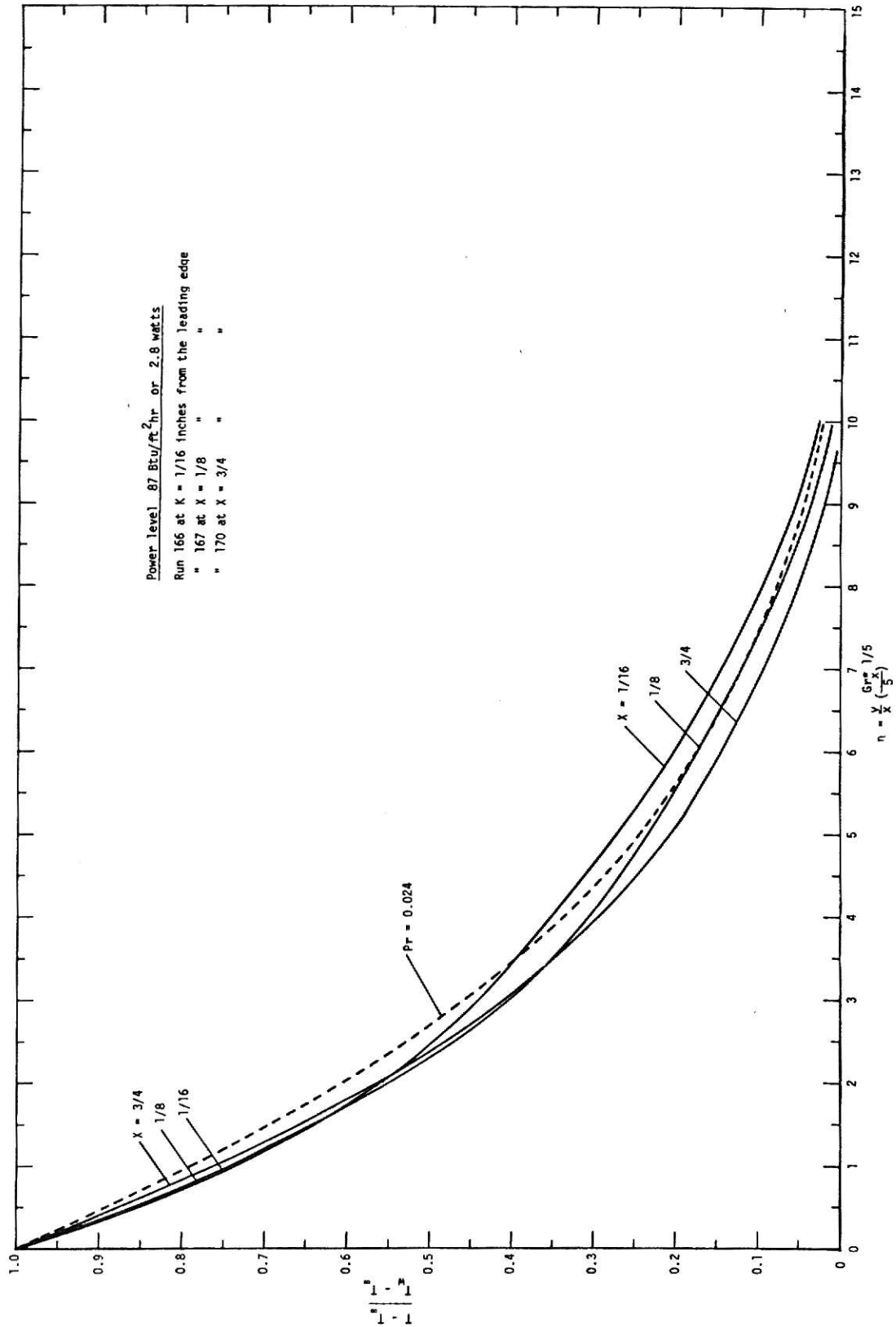
As can be seen in the above table, the present data were obtained at much lower heat flux and lower positions, which resulted the smaller Grashof numbers. Therefore, present data are more widely spread than the Julian's.

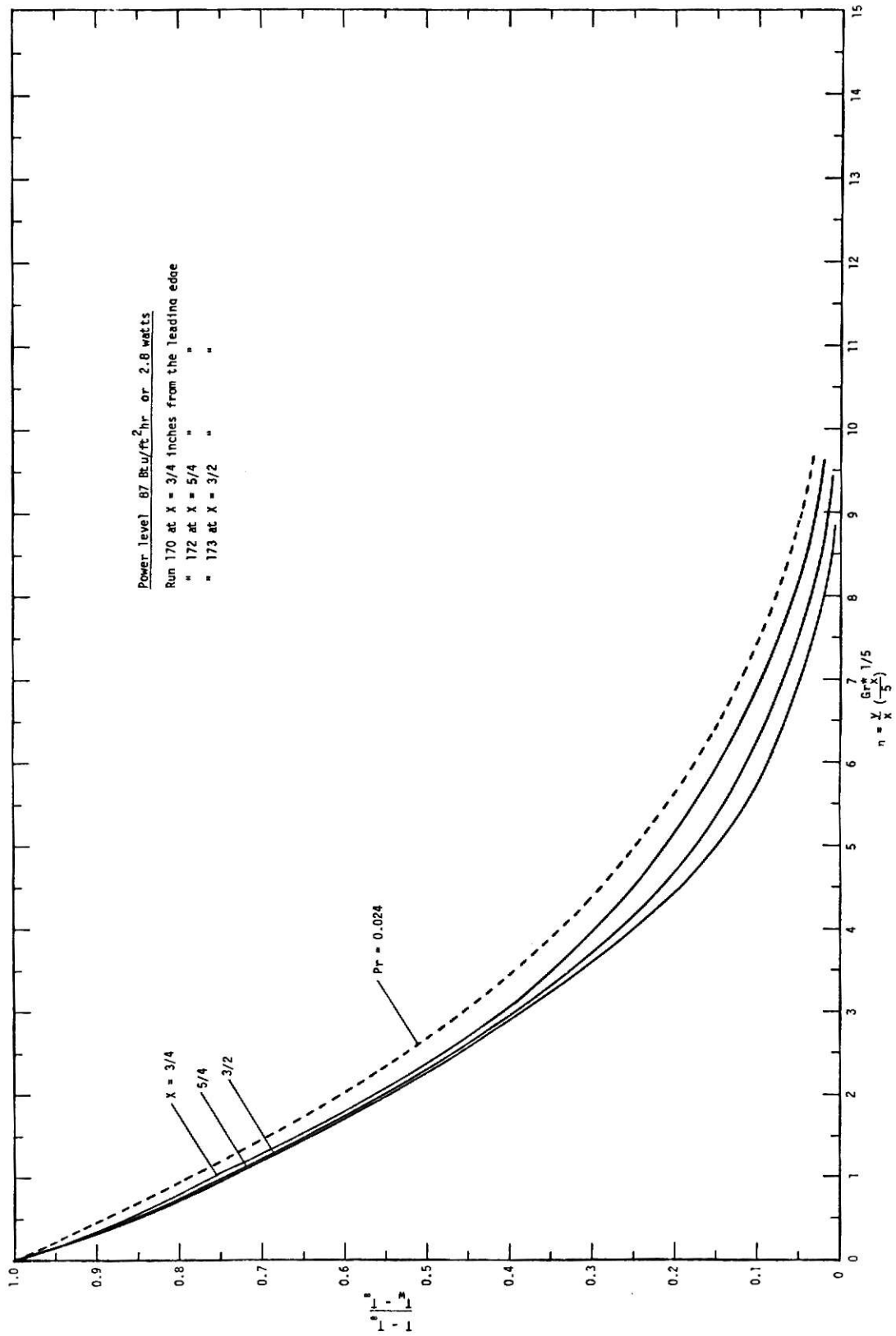
DEPENDENCE OF DIMENSIONLESS PROFILES ON THE DISTANCE UP THE PLATE: AT CONSTANT HEAT FLUX

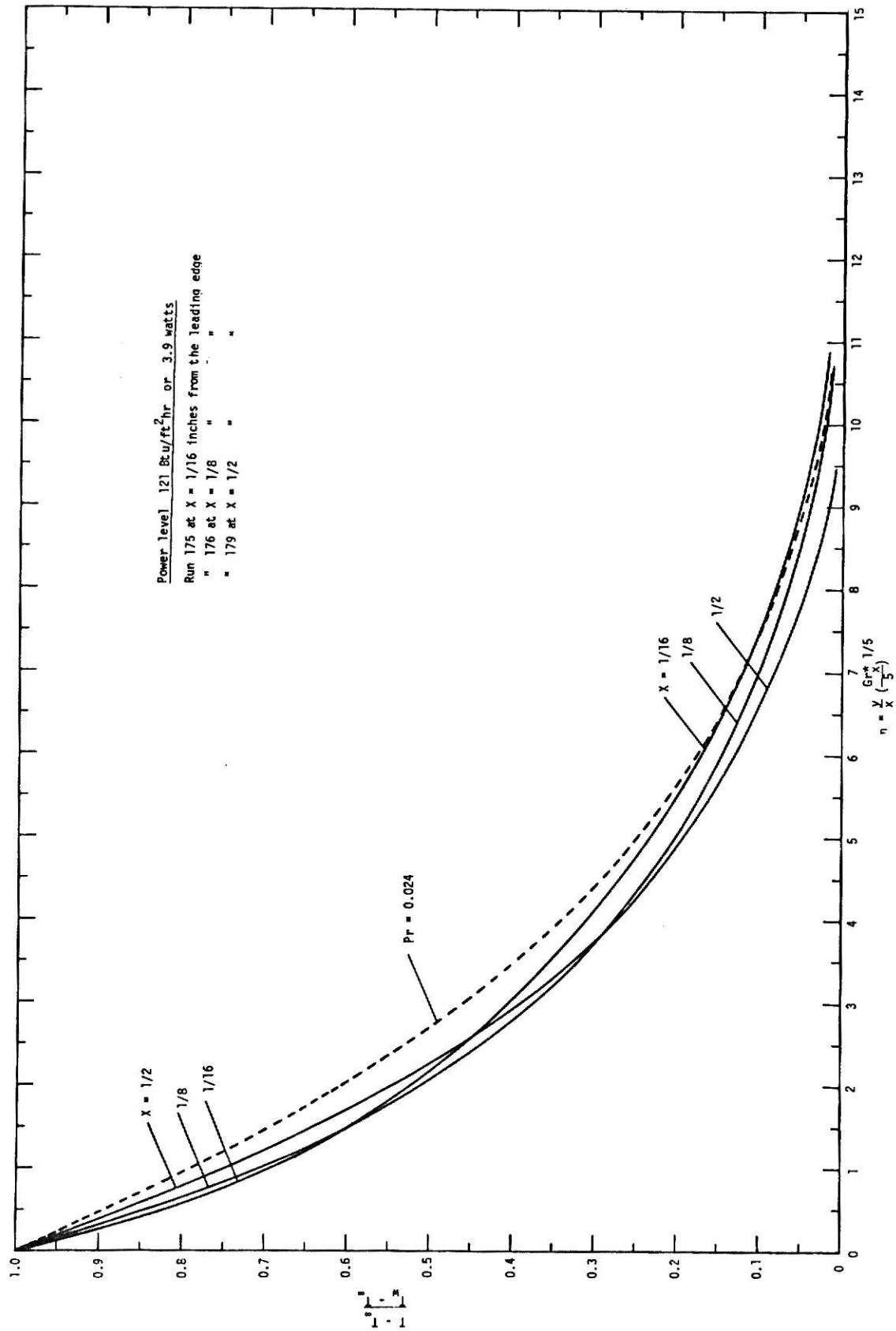
At a certain power level (constant heat flux or constant  $Gr_L^*$ ), several sets of data were obtained with various positions

up the plate. Eleven groups of dimensionless temperature profiles are presented in Figures 14 through 24 at six different power levels: 87, 121, 354, 512, 735 and 1168 Btu/hr-ft<sup>2</sup>. There are two group of profiles each for the first five power levels and one group for the last level, showing the dependence of the profiles on the position up the plate. Because the profiles do not depend on the positions uniformly in one direction, the sets of data at various x at one power level were grouped into two. All the solid lines in these figures and following figures, unless noted specially, represent the best polynomial fit of each experimental data set and dashed lines represent the boundary layer solution for the Prandtl number of 0.024.

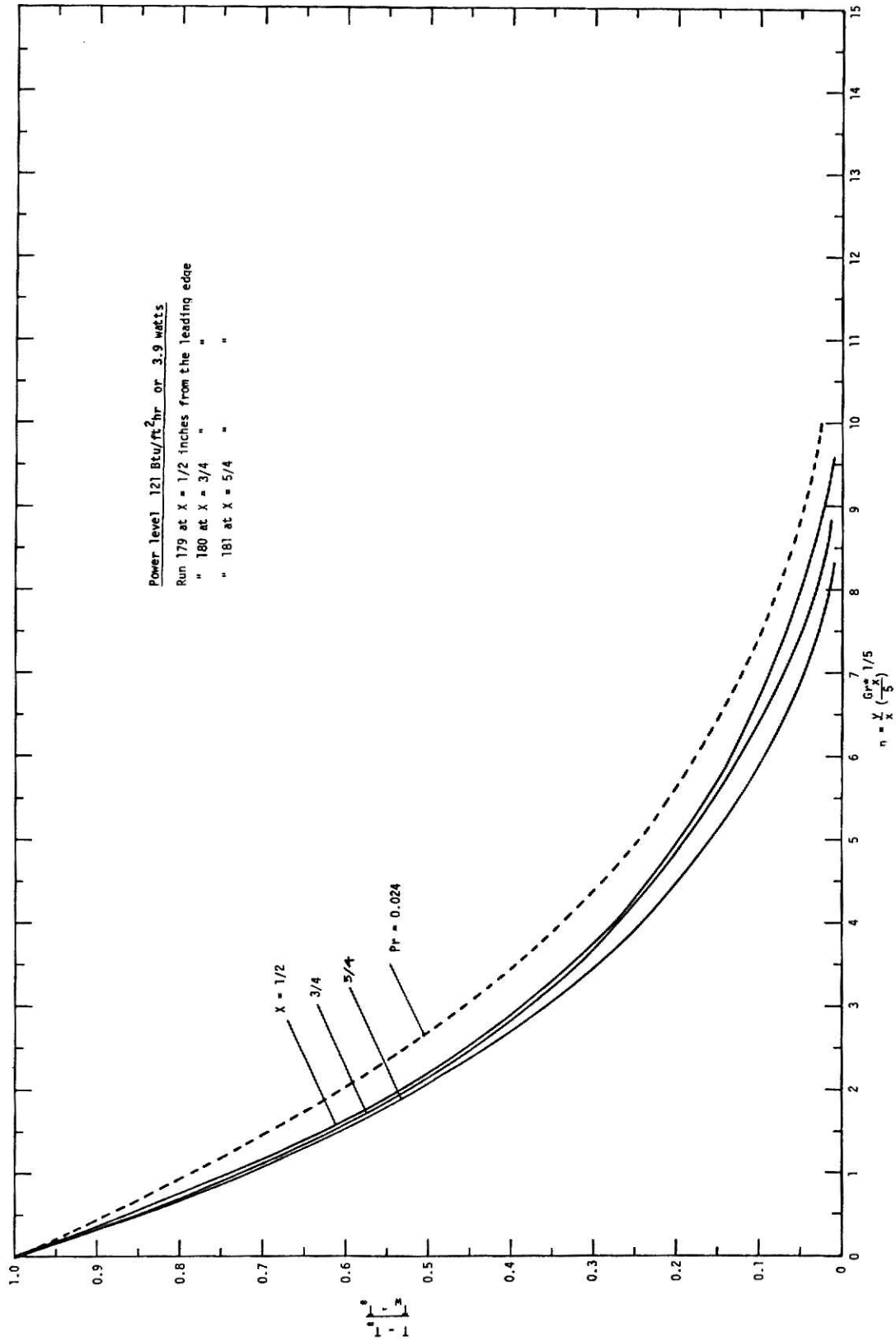
First group of profiles in Figures 14, 16, 18, 20, 22, and 24 are compared with the Figures 4 and 5 which were plotted with the first order perturbation solution. They are in agreement with each other in general shape except the crossing of present profiles. At small dimensionless distance, all the data are located below the boundary layer solution, but at large distance, the data are located on both sides of dashed line. At small region of dimensionless distance, the dependence of profiles on x is the same as that predicted by perturbation theory: the smaller x gives the more deviation, causing the profile to shift downward farther from the dashed line. But experimental data show the reverse dependence in the region of larger dimensionless distance. Thus, the crossing of profiles each other resulted. The crossing of profiles occurred

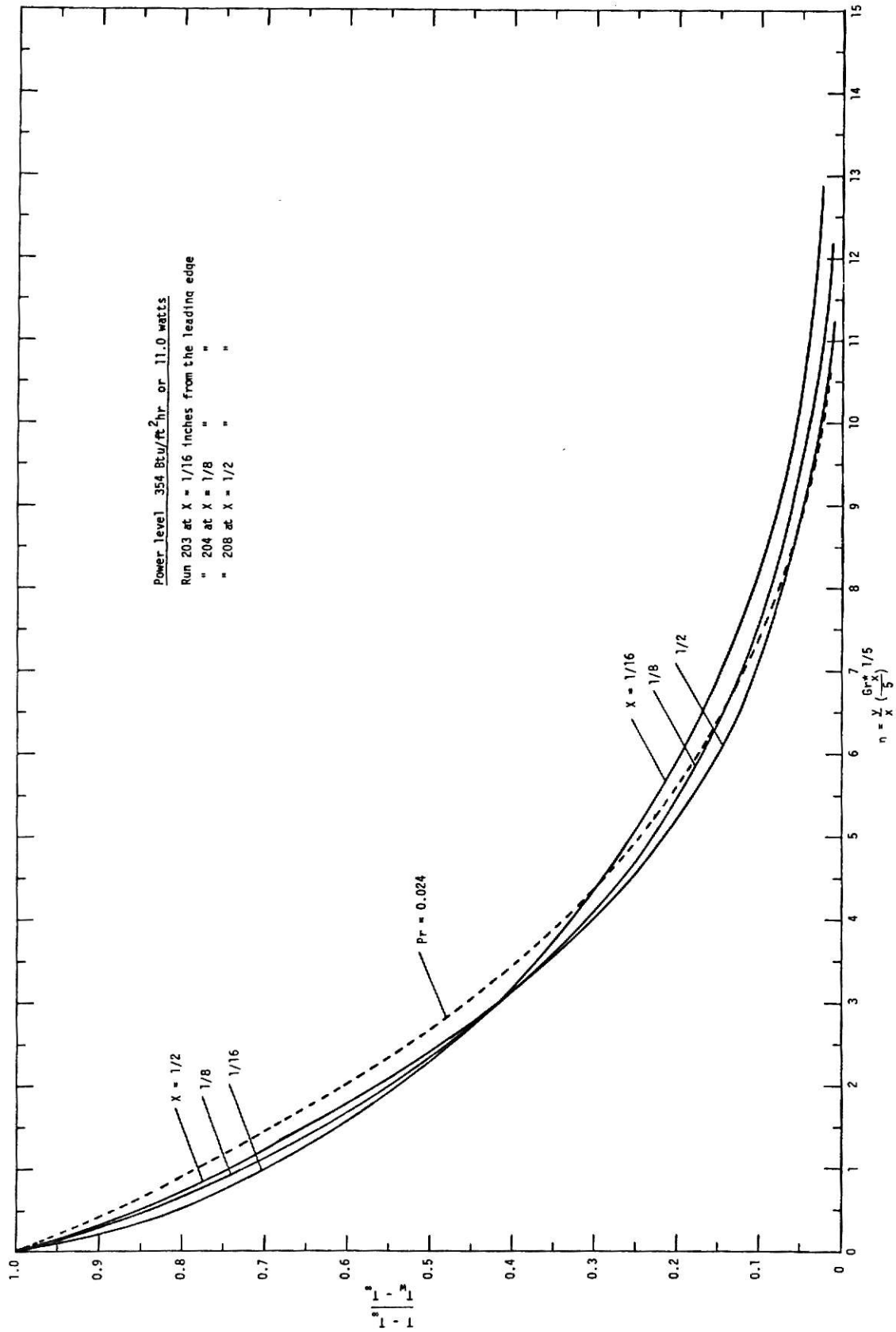
Figure 14. Dimensionless temperature profiles at 87 Btu/ft<sup>2</sup>hr.

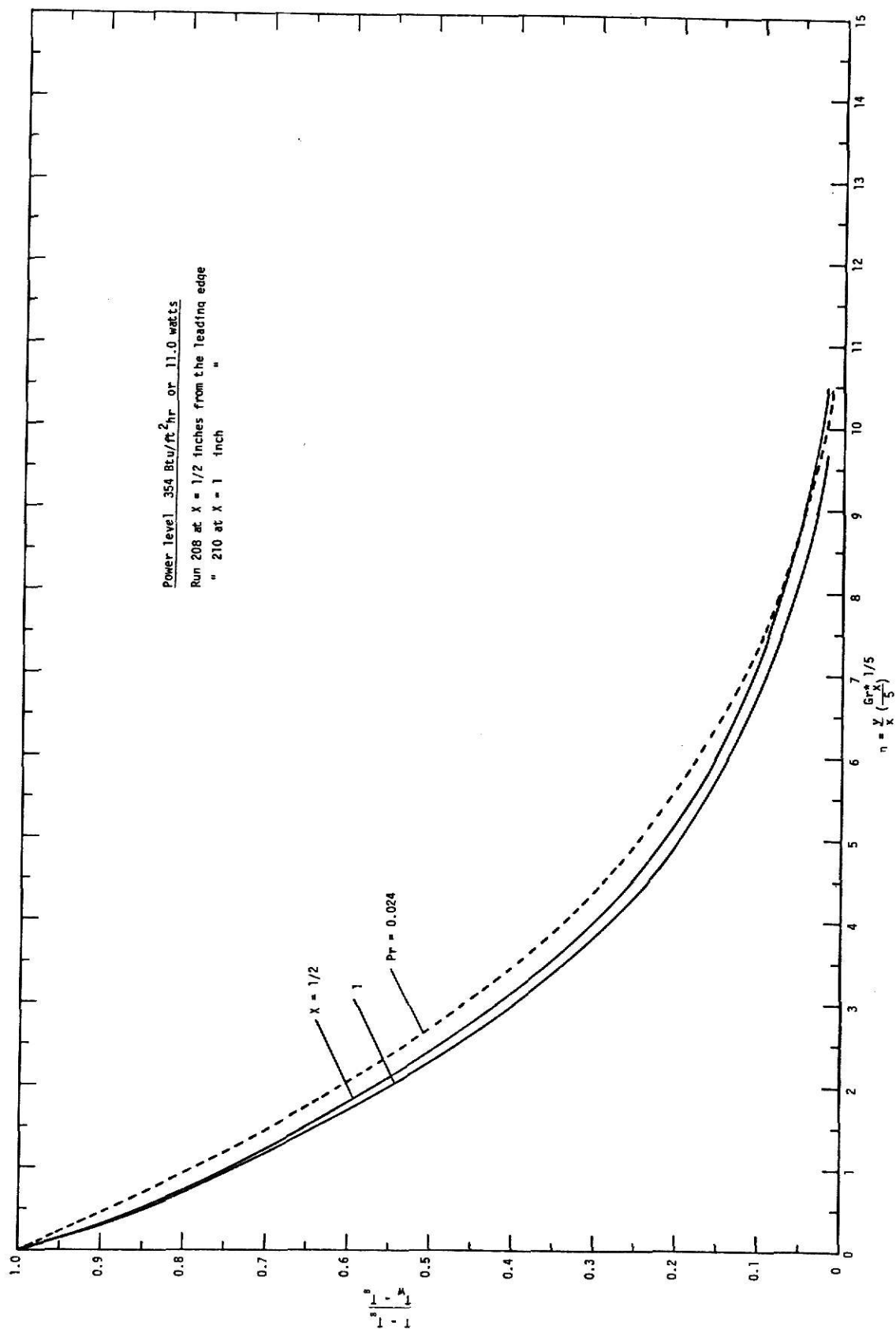
Figure 15. Dimensionless temperature profiles at 87 Btu/ft<sup>2</sup>/hr.

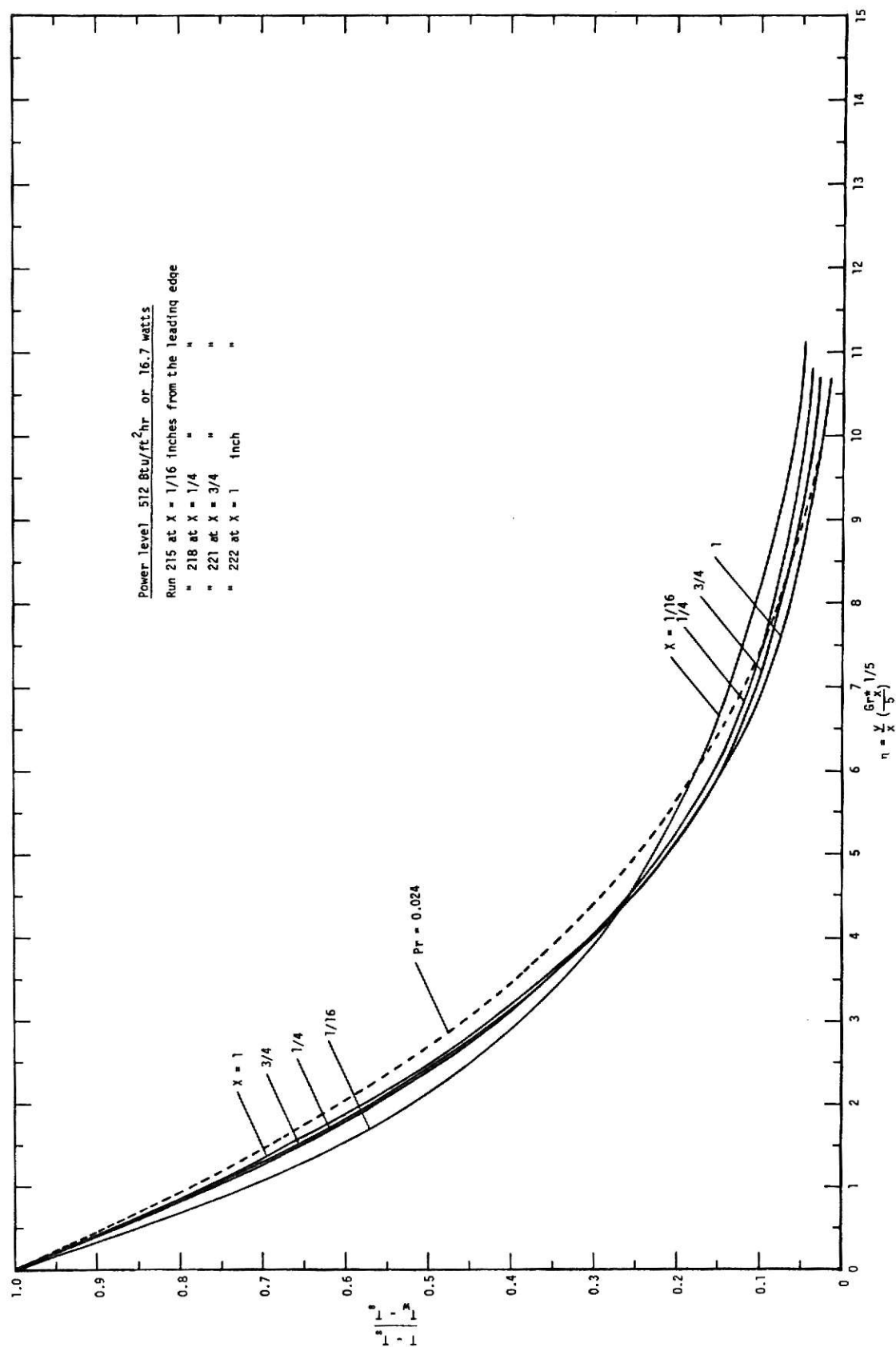
Figure 16. Dimensionless temperature profiles at 121 Btu/ft<sup>2</sup>-hr.

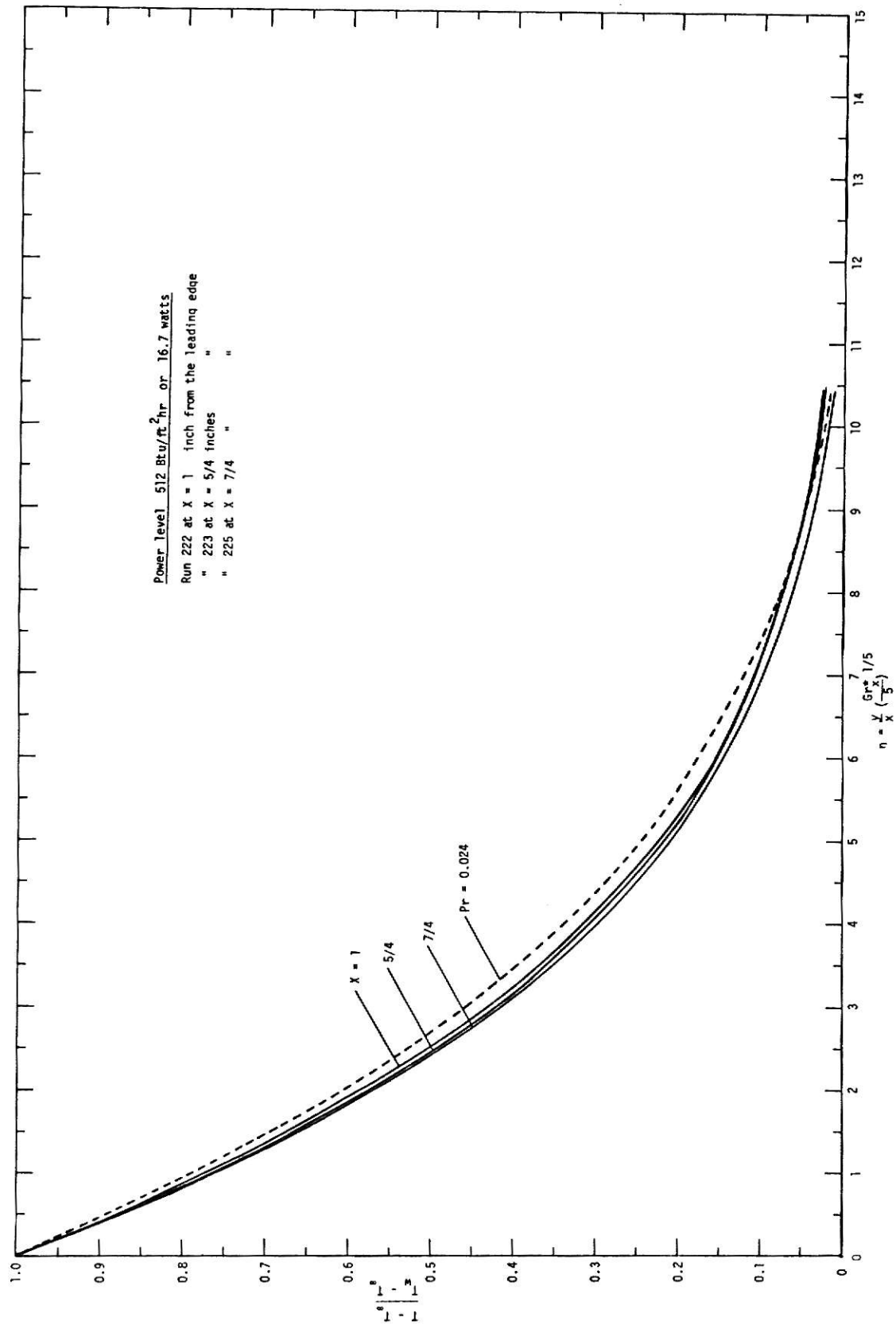


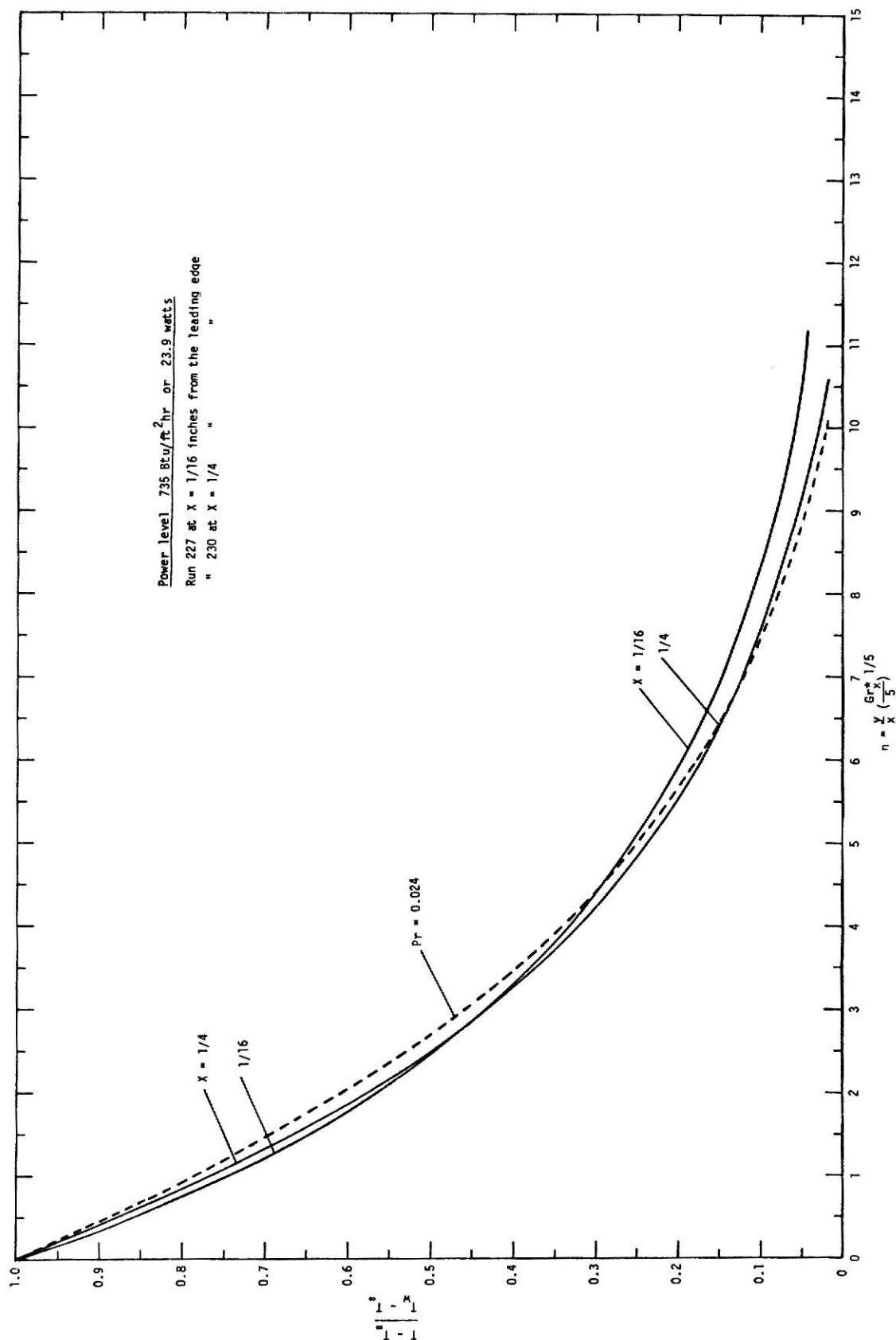
Figure 17. Dimensionless temperature profiles at 121 Btu/ft<sup>2</sup>/hr.

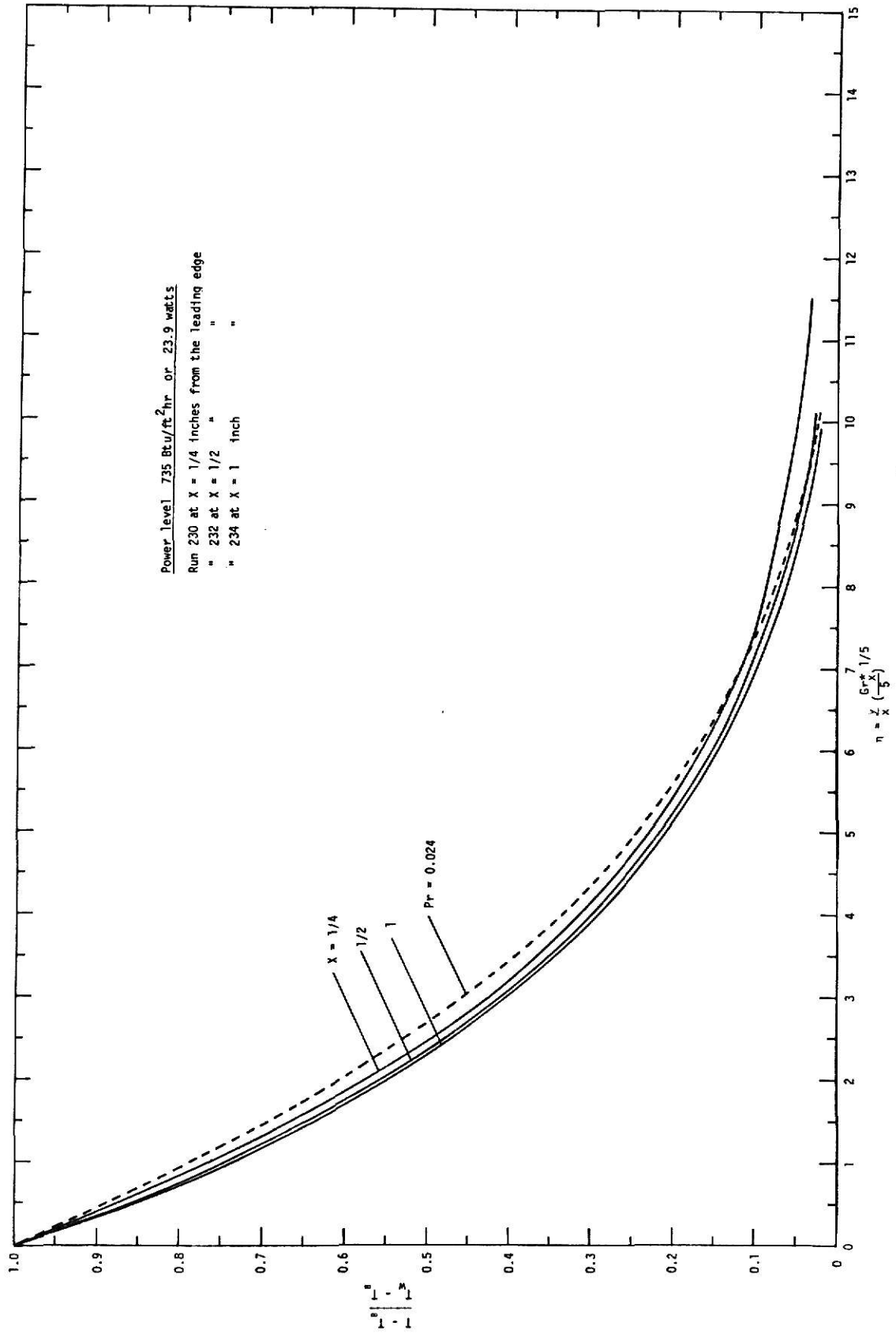
Figure 18. Dimensionless temperature profiles at 354 Btu/ft<sup>2</sup>/hr.

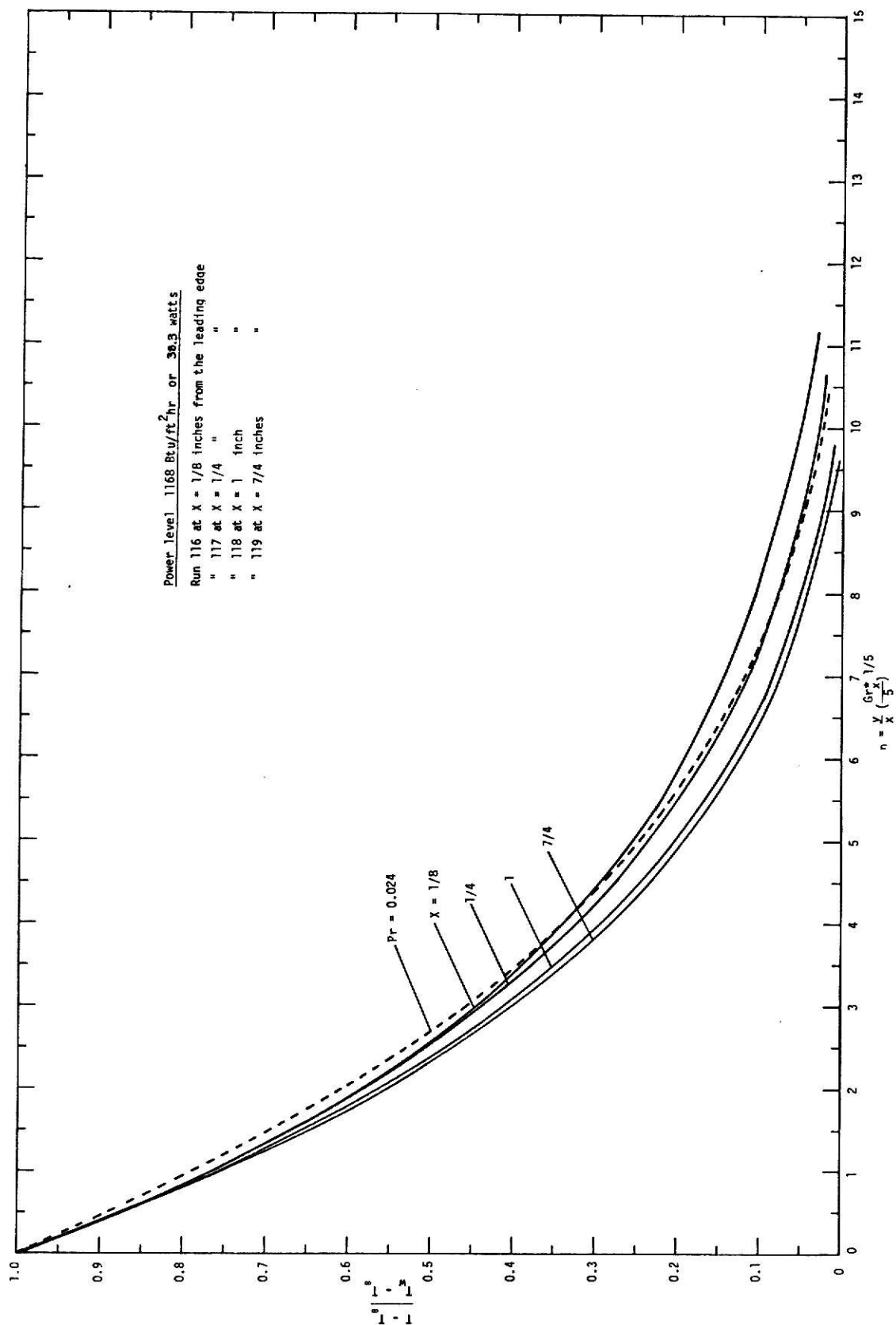
Figure 19. Dimensionless temperature profiles at 354 Btu/ft<sup>2</sup>hr.

Figure 20. Dimensionless temperature profiles at 512 Btu/ft<sup>2</sup>·hr.

Figure 21. Dimensionless temperature profiles at 512 Btu/ft<sup>2</sup>hr.

Figure 22. Dimensionless temperature profiles at 735 Btu/ft<sup>2</sup> hr.

Figure 23. Dimensionless temperature profiles at 735 Btu/ft<sup>2</sup>-hr.

Figure 24. Dimensionless temperature profiles at 1168 Btu/ft<sup>2</sup>·hr.



only in the lower part of the plate. In the upper part of the plate, there is no such crossing of profiles but the dependence on  $x$  is contrary to the perturbation theory. Dimensionless temperature profiles in the upper part of plate are presented in the Figures 15, 17, 19, 21, and 23. Thus, the dependence on  $x$  agreed with perturbation theory only in the small  $\eta$  and in the lower part of the plate, but not in the larger  $\eta$  or in the upper part of the plate. It can be also seen that as the power levels go up, the dependence of profiles on  $x$  is less distinct as compared in the profiles in Figures 4 and 5. The detailed dependence of profiles on the power level will be presented in the following section.

At one power level, increase in  $x$  up to a certain point shifts the profiles upward, but further increase in  $x$  above this point shifts the profiles downward. Close examination of figures indicates that the reverse point depends on the power level: the reverse point tends to go down as the power levels go up. From the Figures 14 through 23, it is found that the reverse points are  $3/8$ ,  $1/4$ ,  $1/4$  and  $1/8$  of the plate height for the power levels of 87, 121, 354 and 735 Btu/hr-ft<sup>2</sup>, respectively. It should be noted that since the data were obtained at several fixed positions in  $x$ , exact reverse points for each power level could not be figured out, however, the general trend is obvious.

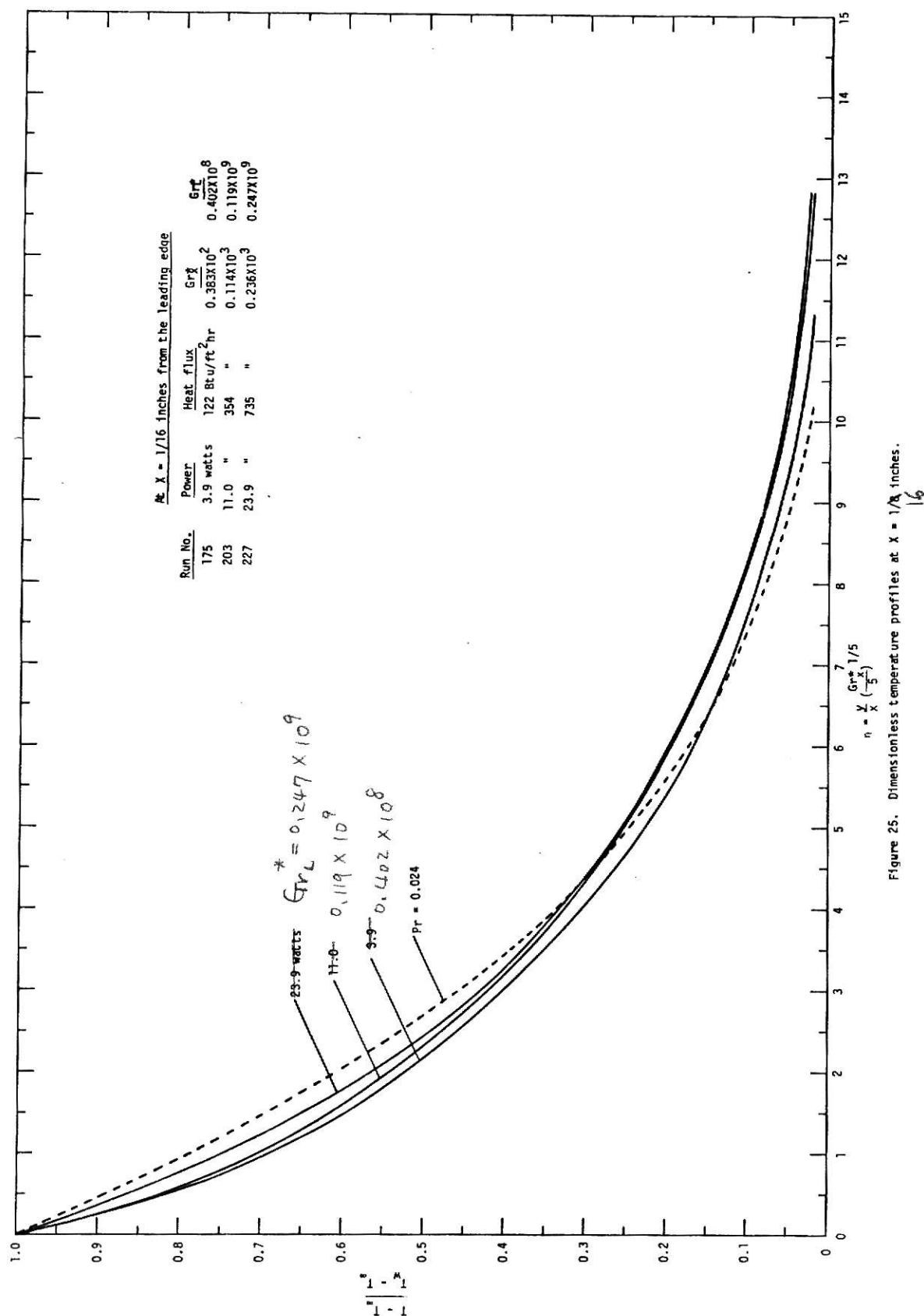
Present dimensionless temperature profiles in the lower part of the plate were found to have the same trend as the

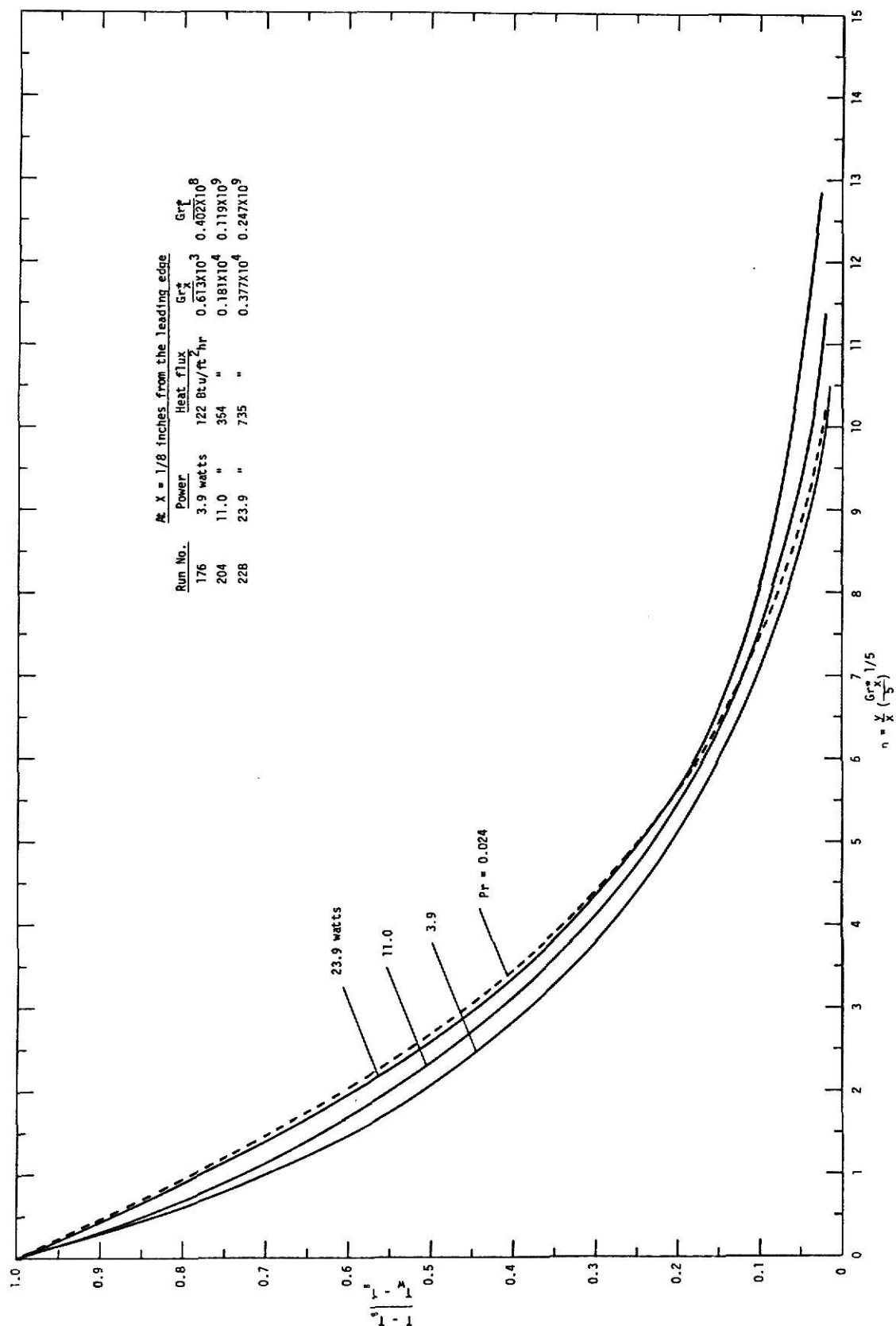
velocity profiles shown in the Figures 6 and 7 in the Theoretical Analysis: In the smaller  $\eta$ , a profile at lower  $x$  locates below a profile at upper  $x$ , and in the larger  $\eta$ , the dependence on  $x$  is reversed. Therefore crossing of profiles seems to occur at the point a little farther than the points where maximum velocity can be observed. From the figures shown, this tendency can be seen.

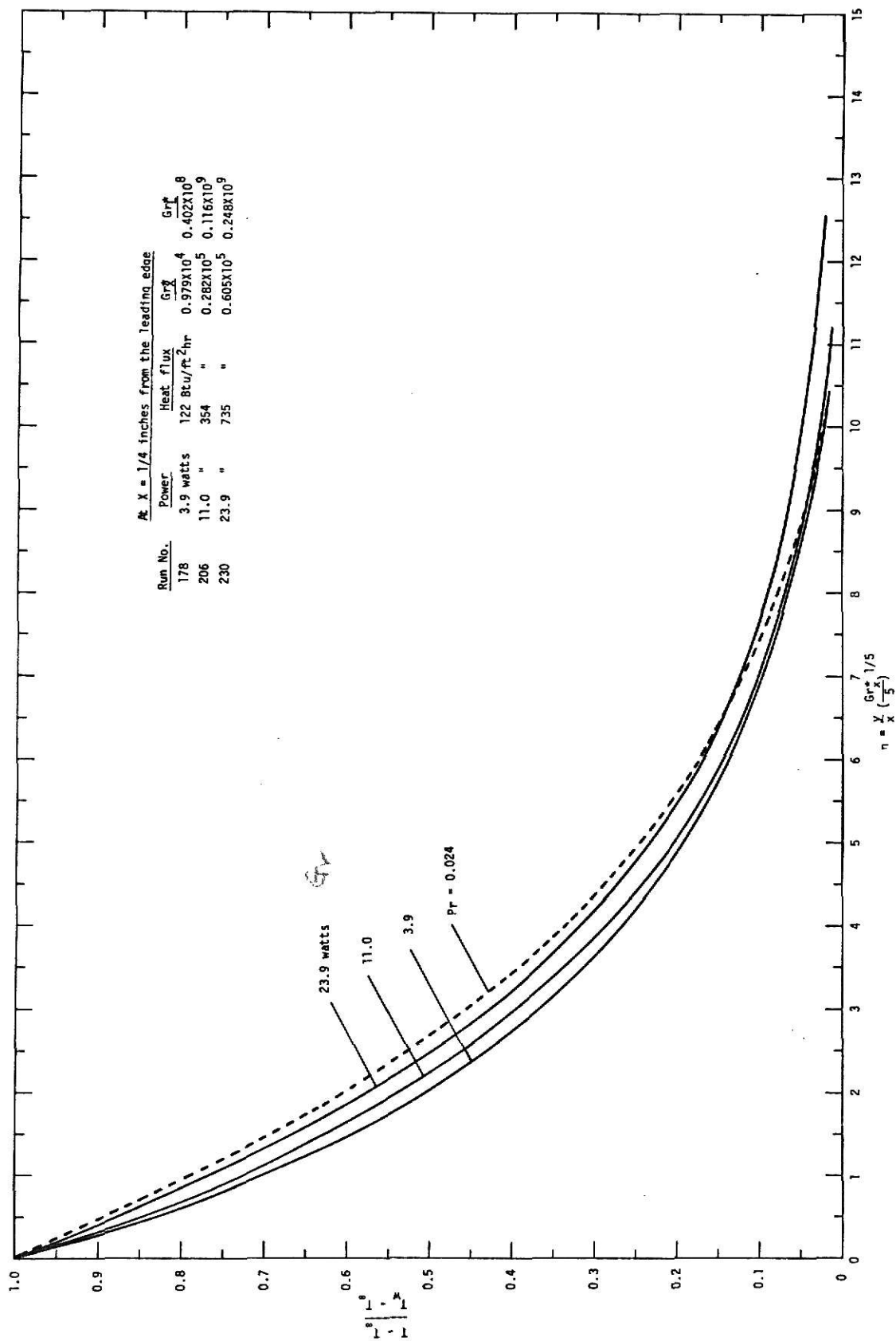
#### DEPENDENCE OF DIMENSIONLESS PROFILES ON THE POWER LEVEL: AT FIXED POSITION UP THE PLATE

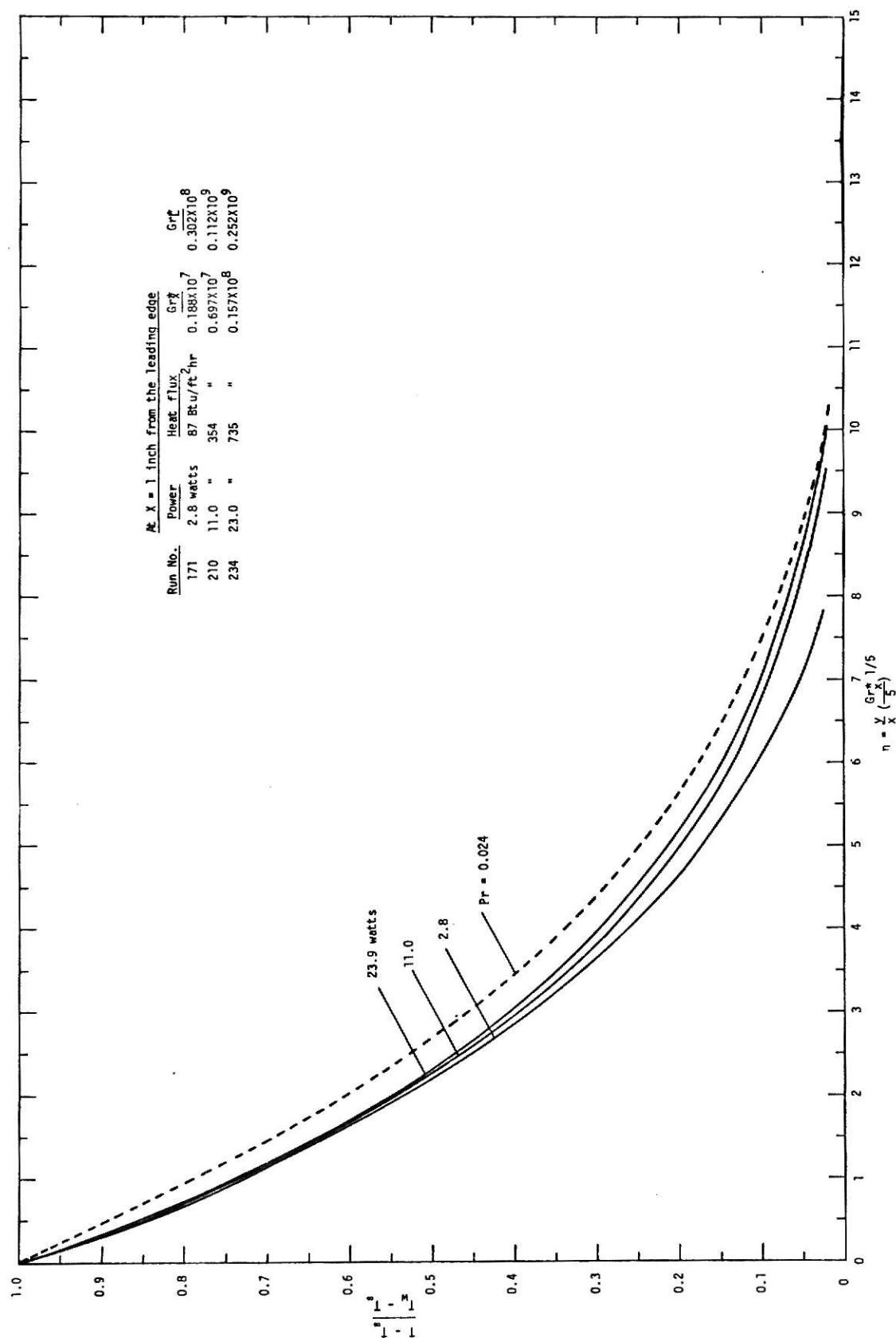
At a fixed position up the plate, dimensionless profiles were plotted in the Figures 25 through 29 with power level as a parameter. Because  $x$  is fixed, power levels (heat flux) are directly related with the  $Gr_L^*$  and  $Gr_x^*$ . Five group of profiles at the positions of  $1/32$ ,  $1/16$ ,  $1/4$ ,  $1/2$  and  $5/8$  of the plate height are presented with the parameter of three power levels which represent the higher, medium, and lower range.

In the Figures 25, 26, and 27 for the lower part of plate, shape of profiles, compared with the dashed line, is exactly the same as that of the Figure 4. At the higher part of plate, shape of profiles shown in the Figures 28 and 29 are slightly different especially in the larger dimensionless distance. In the Figures 25 through 29, the profiles do not cross each other and the dependence of profiles on the power level are uniform such that smaller power level causes larger deviation from the boundary layer theory. Thus profiles at smaller heat

Figure 25. Dimensionless temperature profiles at  $X = 1/16$  inches.

Figure 26. Dimensionless temperature profiles at  $X = 1/8$  inches.

Figure 27. Dimensionless temperature profiles at  $X = 1/4$  inches.

Figure 28. Dimensionless temperature profiles at  $X = 1$  inch.

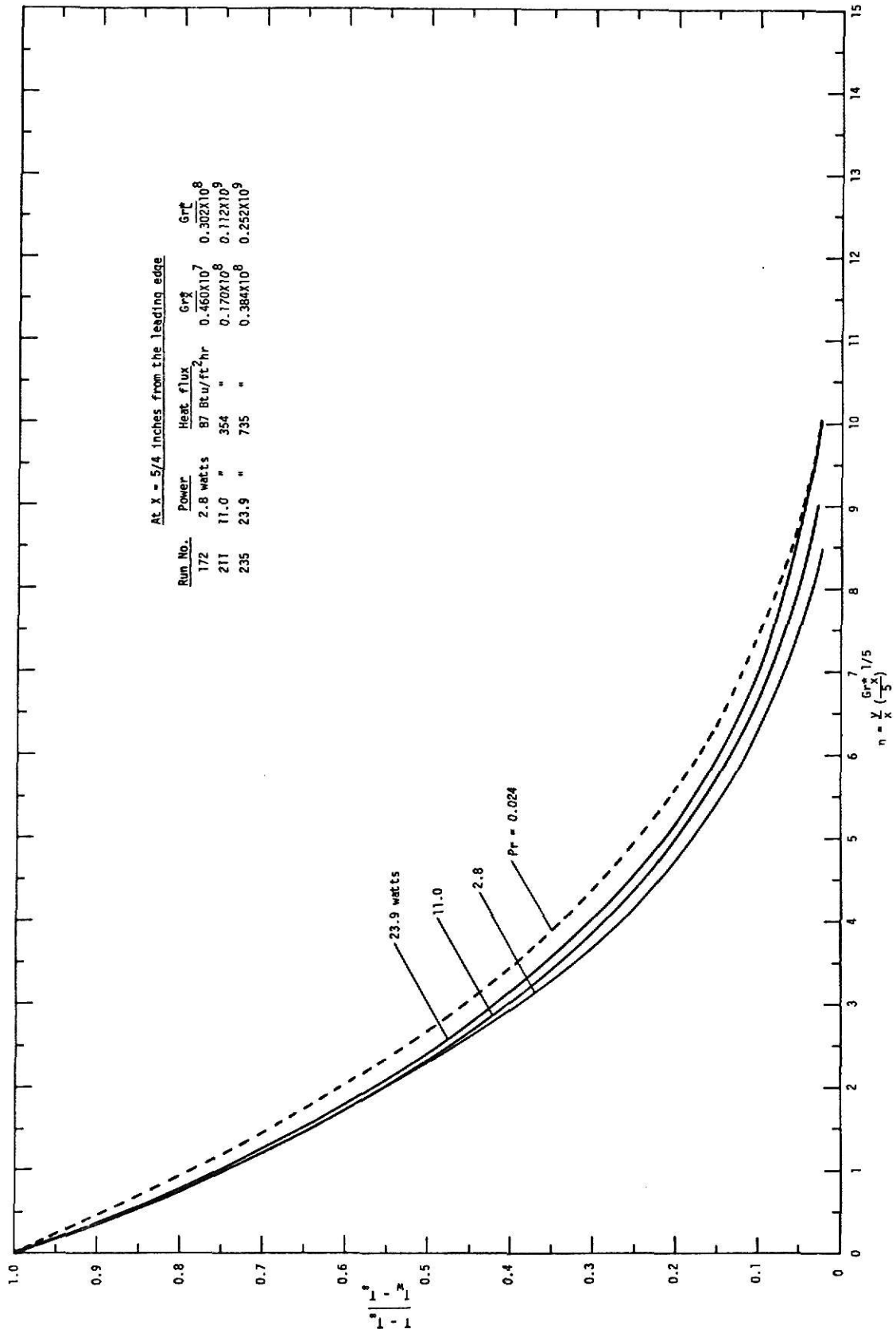


Figure 29. Dimensionless temperature profiles at  $x = 5/4$  inches.

flux are located farther below from the dashed line than the profiles at larger heat flux are. In other words, profiles tend to approach to dashed line by increasing the power level.

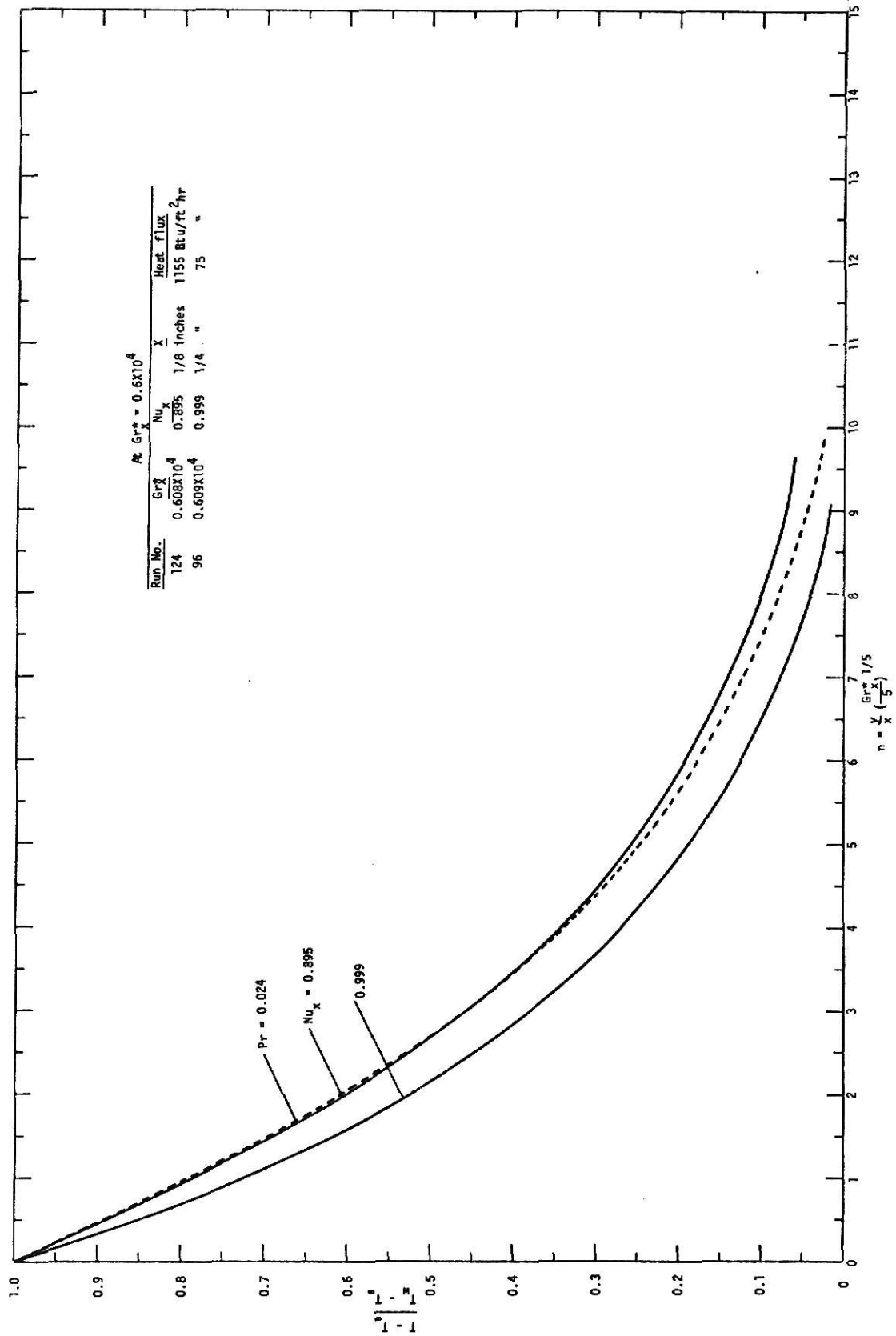
It can be also seen that the distinction of profiles depending on the heat flux are clearer in lower part of plate, but it diminishes in the upper part of plate. This is similar to the fact that the boundary layer thickness is more sensitive to power level in the lower part of plate than in the upper part of the plate.

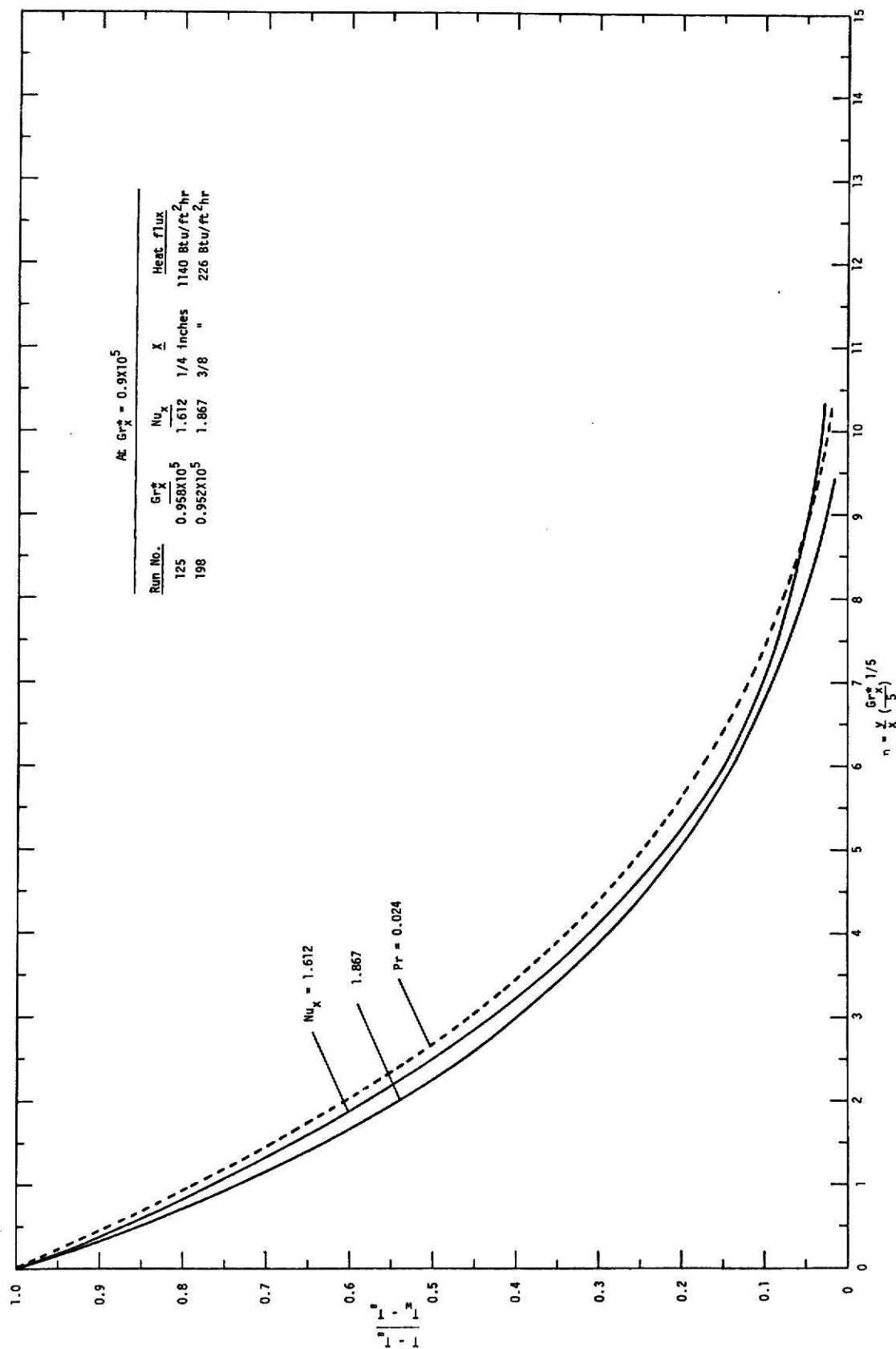
#### DEPENDENCE OF DIMENSIONLESS PROFILES ON NUSSOLT NUMBER: AT CONSTANT $Gr_x^*$

Constant  $Gr_x^*$  could be obtained by changing distance up the plate and power level properly. Because of the experimental procedure, it was not easy to find exactly the same values of  $Gr_x^*$  with various  $x$ 's and  $q$ 's, and constancy of  $Gr_x^*$  here implies fairly close values to each other. Dimensionless profiles are presented in Figures 30 through 34 at values of  $Gr_x^*$  of approximate  $10^4$ ,  $10^5$ ,  $10^6$ ,  $10^7$  and  $10^8$  with a parameter of the local Nusselt number.

At constant  $Gr_x^*$ , dependence of profiles on power level is found to be the same as the dependence at fixed position  $x$ : lower power level causes more departure from the dashed line, but the dependence on  $x$  at constant  $Gr_x^*$  is contrary to the perturbation theory. Therefore a certain mixed parameter should be found rather than separate parameter of  $x$  and  $q$  for the case.



Figure 30. Dimensionless temperature profiles at  $Gr_x^* = 0.6 \times 10^4$ .

Figure 31. Dimensionless temperature profiles at  $Gr_x^* = 0.9 \times 10^5$ .

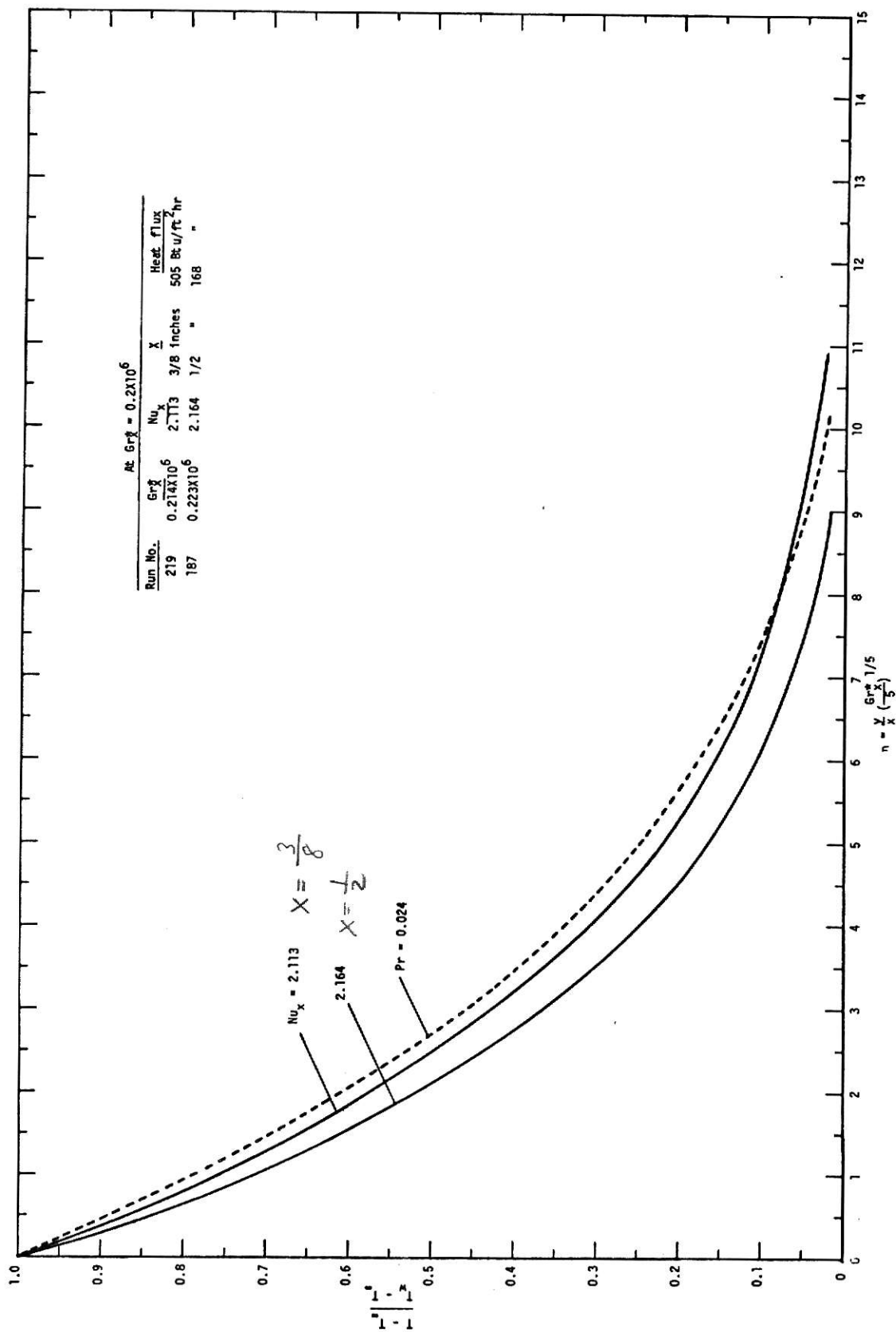
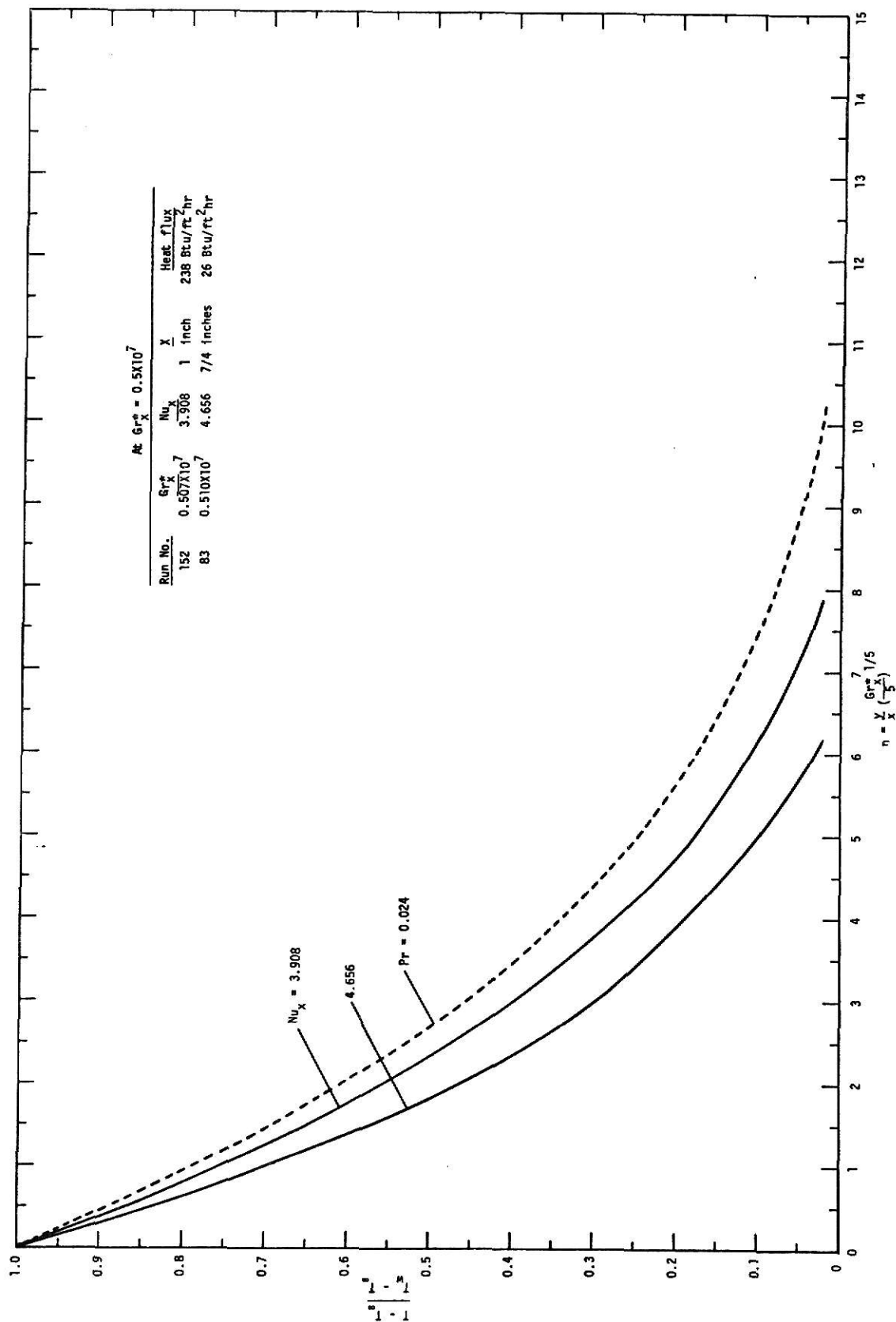


Figure 32. Dimensionless temperature profiles at  $Gr_x = 0.2 \times 10^6$ .



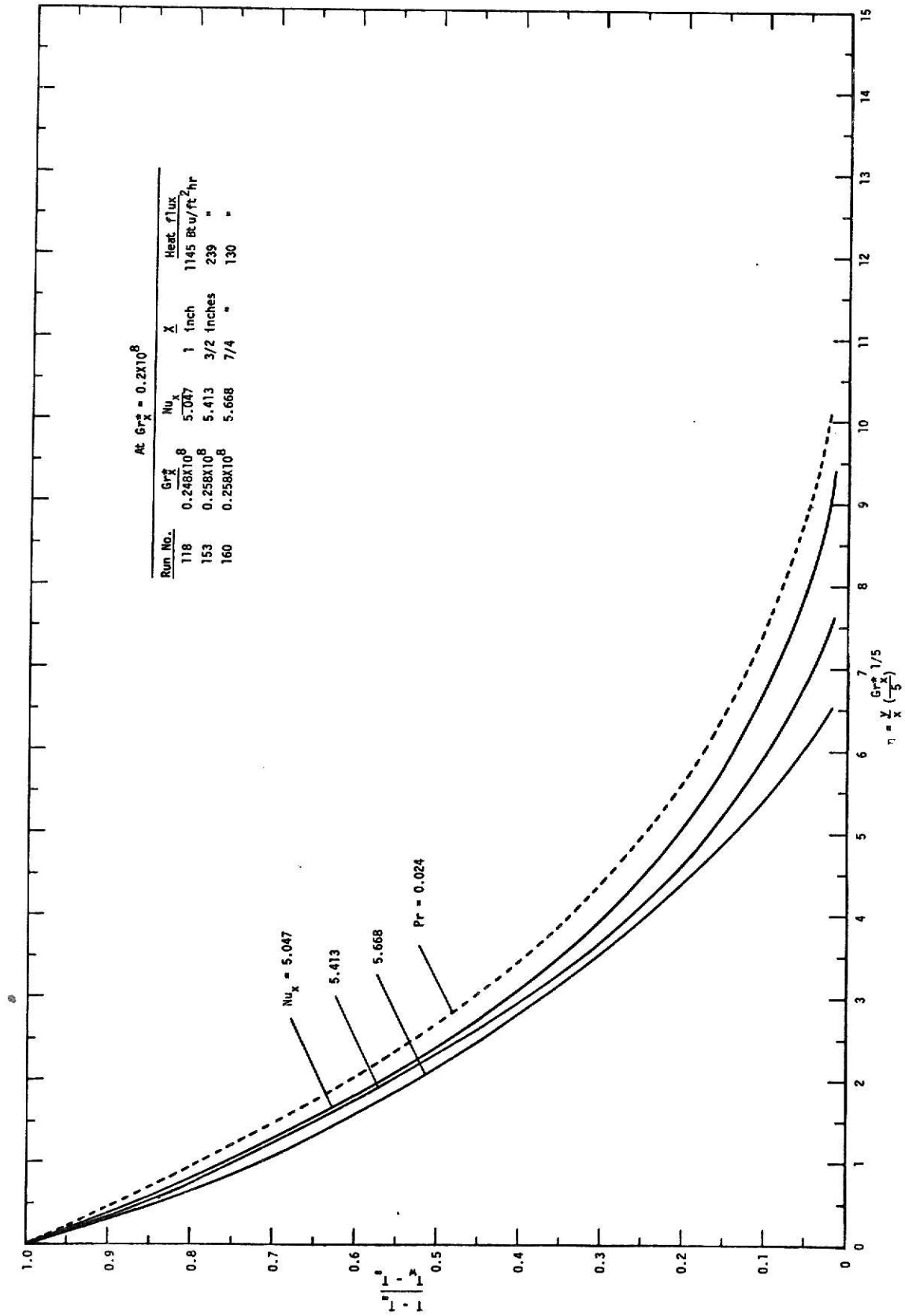


Figure 34. Dimensionless temperature profiles at  $Gr_X^* = 0.2 \times 10^8$ .

of constant  $Gr_x^*$ . The local Nusselt number is found to be good parameter. Since the Nusselt number is expressed as:

$$Nu_x = \frac{h_x x}{k} = \frac{q x}{(T_w - T_\infty)k}$$

it is surely a mixed variable. From the Figures 30 through 34 the dependence of profiles on  $Nu_x$  are distinct. At constant  $Gr_x^*$ , increase in  $Nu_x$  gives more deviation from the boundary layer theory. This result is in agreement with the Sparrow and Guinle's analysis [135]: actual heat transfer would be greater than the heat transfer predicted by the boundary layer theory, and greater heat transfer implies more deviation from the theory. Detailed heat transfer data versus  $Gr_x^*$  will be shown in the following section, and the deviation will be seen clearly.

#### LOCAL NUSSULT NUMBER VERSUS $Gr_x^*$

Figure 35 presents the local Nusselt numbers versus the modified local Grashof numbers. The dashed line shows Sparrow and Gregg's theoretical correlation [131]:

$$\frac{Gr_x^{*1/5}}{Nu_x} = 5^{1/5} \theta(0) \quad (\text{Equation 36 on page 30}).$$

For the Prandtl number of 0.024, it is found that

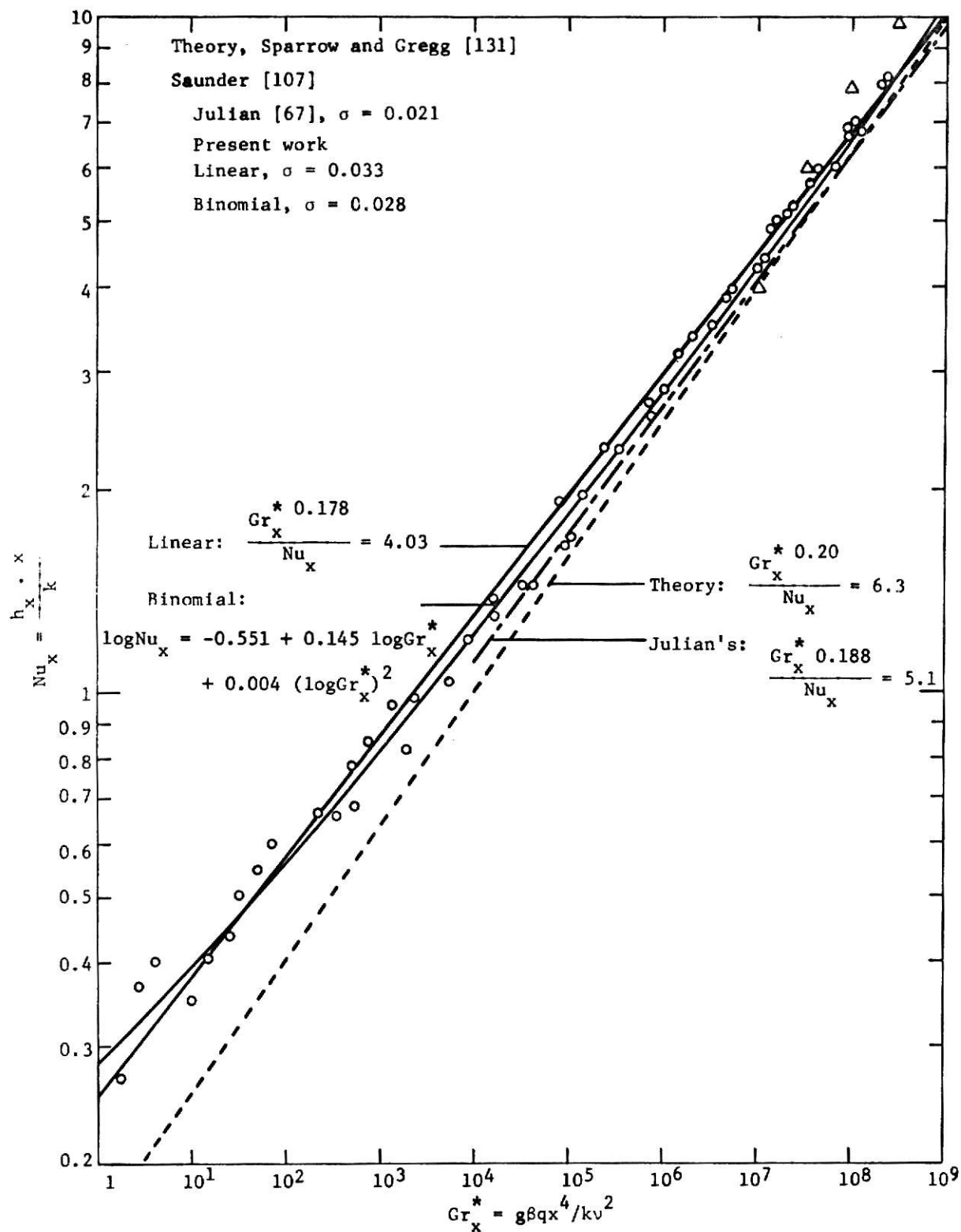


Figure 35. Nusselt number - Grashof number correlations.

$$\frac{Gr_x^{*1/5}}{Nu_x} = 6.3$$

Julian's heat transfer data [67] are included in the Figure 35 and his correlation was

$$\frac{Gr_x^{*0.188}}{Nu_x} = 5.1$$

with the standard deviation of 0.021. His heat flux range was from 530 to 5010 Btu/ft<sup>2</sup>-hr. Also included are Saunder's data [107] which are the only available heat transfer data in mercury, along with the Julian's data.

For the present work, sixty data points were correlated for the overall relationship between  $Gr_x^*$  and  $Nu_x$ . The correlations are:

Linear correlation:

$$\begin{aligned} \log Nu_x &= -0.605 + 0.178 \log Gr_x^* \\ \text{or } \frac{Gr_x^{*0.178}}{Nu_x} &= 4.03 \quad (\sigma = 0.033) \end{aligned}$$

Binomial correlation:

$$\begin{aligned} \log Nu_x &= -0.551 + 0.145 \log Gr_x^* + 0.004(\log Gr_x^*)^2 \\ (\sigma &= 0.028) \end{aligned}$$



The linear correlation can be directly compared with the Sparrow and Gregg's theoretical correlation [131] and the Julian's experimental correlation [67].

Examination of the binomial correlation indicates that Nusselt numbers are generally are greater than their theoretical values, and that as  $Gr_x^*$  decreases, the deviation is accentuated and as  $Gr_x^*$  increases,  $Nu_x$  approaches gradually to the theoretical prediction. Sparrow and Guinle [135] estimated the deviation as  $q/q^o$  where  $q^o$  is theoretical heat transfer rate. At the  $Gr_x^* = 2.1 \times 10^4$  and  $Pr = 0.03$ , the ratio was estimated to be 1.05 (5% positive deviation) for the case of isothermal plate. From the present binomial correlation,  $Nu_x/Nu_x^o$  is estimated to be 1.20 (20% positive deviation) at the same value of  $Gr_x^*$  and the Prandtl number of 0.024. As mentioned previously, since  $Nu_x$  is a function of heat transfer rate, distance up the plate, and temperature difference, a direct quantitative comparison failed. Qualitatively, the data surely deviated from the theory.

## CONCLUSIONS

The first-order perturbation solution to the problem of two dimensional free convection in a liquid metal (mercury) at rest from a uniformly heated vertical plate with both leading and trailing edges has been experimentally examined especially in the low range of modified Grashof numbers.

The classical boundary layer assumptions used to simplify the coupled equations of motion, energy, and continuity have been experimentally shown to be invalid in the case where the modified Grashof number is small in the mercury.

General deviations from the boundary layer theory due to the low Grashof numbers have been shown in the dimensionless temperature profile plotted with overall experimental data by comparing both with the boundary layer solution and with Julian's work [67] which experimentally verified the boundary layer theory in the moderate range of Grashof numbers in the mercury.

Dependence of the deviation on the distance up the plate at constant heat flux were in good agreement with the first-order perturbation theory only at small values of dimensionless distance; the data taken at the lower regions of the plate had larger deviation than the data in the upper portion of the plate. The dependence did not followed the perturbation prediction when the dimensionless distance  $\eta$  was large or in the upper part of the plate. The dimensionless temperature profiles plotted for the lower part of the plate crossed each other just

like the velocity profiles predicted by the perturbation theory. The crossing points were observed to be a little farther from the plate than where the maximum velocity occurred.

Dependence of the deviation on the heat flux ( $Gr_L^*$  or  $Gr_x^*$ ) at a fixed vertical position agreed well with perturbation solution; the data at lower heat flux have larger deviations than the data at higher heat flux.

Dependence of the deviation on the Nusselt number at constant  $Gr_x^*$  were in excellent agreement with the Sparrow and Guinle's prediction [135]; the actual heat transfer was greater than that predicted by the boundary layer theory at lower values of  $Gr_x^*$ .

The experimental data were correlated for the relation between the Grashof number ( $Gr_x^*$ ) and the Nusselt number ( $Nu_x$ ) as following:

Linear correlation:

$$\log Nu_x = -0.605 + 0.178 \log Gr_x^*$$

$$\text{or } \frac{Gr_x^{*0.178}}{Nu_x} = 4.03 \quad (\sigma = 0.033)$$

Binomial correlation:

$$\log Nu_x = -0.551 + 0.145(\log Gr_x^*) + 0.004 (\log Gr_x^*)^2$$

$$(\sigma = 0.028)$$

From the binomial correlation, the positive deviation of Nusselt number from the boundary layer theory was calculated to be 20% at  $Gr_x^* = 2.1 \times 10^4$  and  $Pr = 0.024$ . As  $Gr_x^*$  increased, heat transfer data ( $Nu_x$ ) were less deviated from the theoretical values and as  $Gr_x^*$  decreased,  $Nu_x$ 's were gradually more deviated. At the higher range of  $Gr_x^*(10^4 - 10^9)$ , the data were in fairly good agreement with the only existing experimental data (Julian's [67] and Saunder's [107]). In the lower range of  $Gr_x^*(1 - 10^4)$ , there have been no available data to compare with.

Even though the boundary layer assumptions do not predict the correct profiles or heat transfer rates in the low Grashof number range, the predictions are precise enough for almost any practical use.

## NOMENCLATURE

$C_p$	heat capacity at constant pressure, Btu/lb °F
$C_v$	heat capacity at constant volume, Btu/lb °F
$F(\eta)$	zeroth-order velocity function, dimensionless
$\bar{F}(\eta)$	dimensionless function defined by equation (86)
$f_{00}(\eta), f_n(\eta)$	first-order velocity functions, dimensionless
$\bar{f}_0(\eta), \bar{f}_n(\eta)$	zeroth-and first-order velocity functions for isothermal plate case defined by equation (82)
$G$	dimensionless gravitational acceleration defined by equation (54)
$\bar{G}$	dimensionless temperature function defined by equation (87)
$Gr_x$	Grashof number based on $x$ , $\frac{g\beta(T_w-T)x^3}{\nu^2}$ , dimensionless
$Gr_x^*$	modified Grashof number based on $x$ , $\frac{g\beta x^4 q}{k\nu^2}$ , dimensionless
$Gr_L^*$	modified Grashof number based on $L$ , $\frac{g\beta L^4 q}{k\nu^2}$ , dimensionless
$g$	acceleration gravity, ft/sec <sup>2</sup>
$\bar{g}$	gravity force vector, ft/sec <sup>2</sup>
$g_x$	gravity force in $x$ direction, ft/sec <sup>2</sup>
$h_x$	local heat transfer coefficient, Btu/hr ft <sup>2</sup> °F
$k$	thermal conductivity, Btu-ft/hr ft <sup>2</sup> °F
$L$	vertical length of plate, ft
$Nu_x$	local Nusselt number, $\frac{h_x x}{k}$ or $\frac{qx}{k(T_w-T_\infty)}$ , dimensionless

$Nu_x^0$	local Nusselt number evaluated from the boundary layer theory
$p$	pressure, lb f/ft <sup>2</sup>
$P$	dimensionless pressure defined by equation (54)
$Pr$	Prandtl number, $\nu/\alpha$ or $C_p \mu/k$ , dimensionless
$q$	heat flux, Btu/hr ft <sup>2</sup>
$q_0$	constant heat flux Btu/hr ft <sup>2</sup>
$q^0$	heat transfer rate evaluated from the boundary layer theory
$S$	0.864806 .....
$T$	temperature, °F
$T_w$	wall temperature, °F
$T_\infty$	bulk temperature, °F
$T_R$	reference temperature, °F
$t$	time, hr
$u$	velocity component in x direction, ft/sec
$\bar{u}$	dimensionless velocity component in x direction
$v$	velocity component in y direction, ft/sec
$\bar{v}$	dimensionless velocity component in y direction
$\bar{V}$	velocity vector, ft/sec
$\hat{V}$	volume per unit mass, ft <sup>3</sup> /lbm
$w(x)$	velocity function, ft/sec
$x$	vertical coordinate
$\bar{x}$	dimensionless vertical coordinate, $x/L$
$X$	transformed dimensionless vertical coordinate defined by equation (56)

$y$	horizontal coordinate,
$\bar{y}$	dimensionless horizontal coordinate, $y/L$
$Y$	transformed dimensionless horizontal coordinate defined by equation (56)
$\alpha$	thermal diffusivity, $k/C_p \rho$ , $\text{ft}^2/\text{sec}$
$\beta$	coefficient of thermal expansion, $1/^\circ\text{F}$
$\delta(x)$	boundary layer thickness, $\text{ft}$
$\epsilon$	small constant parameter in series expansion, $\text{Gr}_L^{*-1/5}$ , dimensionless
$\mathcal{E}$	small constant parameter in series expansion, $\text{Gr}_x^{-1/2}$ , dimensionless
$\eta$	similarity variable, $\frac{y}{x} \left( \frac{\text{Gr}_x^*}{5} \right)^{1/5}$ , dimensionless
$\bar{\eta}$	similarity variable, $\frac{y}{x} \left( \frac{\text{Gr}_x^*}{4} \right)^{1/4}$ , dimensionless
$\theta(\eta)$	temperature variable, $\left( \frac{\text{Gr}_x^*}{5} \right)^{1/5} \frac{k}{q x} (T - T_\infty)$
$\bar{\theta}(\eta)$	dimensionless temperature, $(T - T_\infty)/(T_w - T_\infty)$
$\theta_{00}(\eta), \theta_n(\eta)$	first-order temperature functions, dimensionless
$\textcircled{H}$	dimensionless temperature defined by equation (54)
$\textcircled{H}^{(0)}, \textcircled{H}^{(1)}$	zeroth- and first-order temperature of $H$ , dimensionless
$\mu$	viscosity, $\text{lbm}/\text{ft sec}$
$\nu$	kinematic viscosity, $u/\rho$ , $\text{ft}^2/\text{sec}$
$\pi$	3.14159 .....
$\rho$	density $\text{lbm}/\text{ft}^3$
$\sigma$	standard deviation
$\bar{\tau}$	stress tensor, $\text{lbm}/\text{ft sec}^2$
$\psi$	stream function

- $\psi_1$  dimensionless velocity function defined by equation (82)
- $\bar{\psi}$  dimensionless stream function defined by equation (54)
- $\Psi$  transformed dimensionless stream function defined by equation (56)
- $\Psi^{(0)}, \Psi^{(1)}$  zeroth- and first-order  $\Psi$ , dimensionless



## BIBLIOGRAPHY

1. Acrivos, A., "A Theoretical Analysis of Laminar Natural Convection Heat Transfer to Non-Newtonian Fluids", A.I.Ch.E. Journal, 6, 4, p. 584 (1960).
2. Acrivos, A., "On the Solution of the Convection Equation in Laminar Boundary Layer Flows", Chemical Engineering Science, 17, pp. 457-465 (1962).
3. Amato, W. S., and C. Tien, "Free Convection Heat Transfer from Isothermal Spheres in Water", A.I.Ch.E. 62nd Annual Meeting, Symposium, Fundamentals in Transport Processes, Part II (1969).
4. Asire, D. H., "Application of the Integral Method to Steady State Laminar Mixed Convection Heat Transfer", Ph.D. Thesis (6603968), Oklahoma State University (1965).
5. Azer, A. Z., and B. T. Chao, "A Mechanism of Turbulent heat Transfer in Liquid Metals", Int. J. Heat Mass Transfer, 1, pp. 121-138 (1960).
6. Babso, R. P., "A Closed-Form Solution for Laminar Free Convection on a Vertical Plate with Prescribed, Nonuniform, Wall Heat Flux", J. Aerospace Sci., 26, 12, pp. 846-7 (1959).
7. Bayley, F. J., "An Analysis of Turbulent Free Convection Heat Transfer", Proceedings of the Institution of Mechanical Engineers, 169, 20, p. 361 (1955).
8. Bird, R. B., W. E. Stewart, and E. N. Lightfoot, "Transport Phenomena", pp. 297-300 and 330-333, John Wiley, New York (1962).
9. Braun, W. H., and J. E. Heighway, "Integral Method for Natural-Convection Flows at High and Low Prandtl numbers", NASA, TN D-292 (1960).
10. Buhr, H. O., "Heat Transfer to Liquid Metals", Ph.D. Thesis, University of Cape Town (1967).
11. Buhr, H. O., A. D. Carr, and R. E. Balzhiser, "Temperature Profiles in Liquid Metals and the Effect of Superimposed Free convection in Turbulent Flow", Int. J. Heat Mass Transfer, 11, 4, p. 641 (1968).
12. Buyco, E. H., "Heat and Momentum Transfer in Liquid Metals", Ph.D. Thesis, Purdue University (1961).

13. Buznik, V. M., and K. A. Bezlomtsey, "A Generalized Equation for the Heat Exchange of Natural and Forced Convection During External Flow about Bodies", Izv. Uyssh. Ucheb. Zaved., 2, pp. 68-74 (1960).
14. Carr, A. D., and R. E. Balzhiser, "Temperature Profiles and Eddy Diffusivities in Liquid Metals", Br. Chem. Engng., 12, pp. 53-57 (1967).
15. Chang, K. C., R. G. Akins, L. Burris, and S. G. Bankoff, "Free Convection of a Low Prandtl Number Fluid in Contact with a Uniformly Heated Vertical Plate", Argonne National Laboratory ANL-6835 (1964).
16. Chang, K. S., R. G. Akins, and S. G. Bankoff, "Free Convection of a Liquid Metal from a Uniformly Heated Vertical Plate", I & EC Fundamentals, 5, 1, pp. 26-37 (1966).
17. Cheesewright, R., "Natural Convection from a Plane, Vertical Surface in Non-isothermal Surroundings", Int. J. Heat Mass Transfer, 10, 12, p. 1847 (1967).
18. Cheesewright, R., "Turbulent Natural Convection From A Vertical Plane Surface", J. Heat Transfer, 90, 1, p. 1 (1968).
19. Cheng, K. C., "Laminar Forced Convection in Regular Polygonal Ducts with Uniform Peripheral Heat Flux", J. Heat Transfer, 2, pp. 156-157 (1969).
20. Cheng, K. C., and G. J. Hwang, "Numerical Solution for Combined Free and Forced Laminar Convection in Horizontal Rectangular Channels", J. Heat Transfer, 2, pp. 59-66 (1969).
21. Chung, P. M., and A. D. Anderson, "Unsteady Laminar Free Convection", J. Heat Transfer, Trans. ASME, C83, pp. 473-8 (1961).
22. Cygan, D. A., and P. D. Richardson, "A Transcendental Approximation For a Natural Convection at Small Prandtl Numbers", Can. J. Chem. Engng., 46, 5, p. 321 (1968).
23. Dotson, J. P., "Heat Transfer from a Vertical Plate by Free Convection", M. S. Thesis, Purdue University (1954).
24. Dring, R. P., and B. Gebhart, "A Theoretical Investigation of Disturbance Amplification in External Laminar Natural Convection", J. Fluid Mech., 34, part 3, pp. 551-564 (1968).

13. Buznik, V. M., and K. A. Bezlomtsey, "A Generalized Equation for the Heat Exchange of Natural and Forced Convection During External Flow about Bodies", Izv. Uyssh. Ucheb. Zaved., 2, pp. 68-74 (1960).
14. Carr, A. D., and R. E. Balzhiser, "Temperature Profiles and Eddy Diffusivities in Liquid Metals", Br. Chem. Engng., 12, pp. 53-57 (1967).
15. Chang, K. C., R. G. Akins, L. Burris, and S. G. Bankoff, "Free Convection of a Low Prandtl Number Fluid in Contact with a Uniformly Heated Vertical Plate", Argonne National Laboratory ANL-6835 (1964).
16. Chang, K. S., R. G. Akins, and S. G. Bankoff, "Free Convection of a Liquid Metal from a Uniformly Heated Vertical Plate", I & EC Fundamentals, 5, 1, pp. 26-37 (1966).
17. Cheesewright, R., "Natural Convection from a Plane, Vertical Surface in Non-isothermal Surroundings", Int. J. Heat Mass Transfer, 10, 12, p. 1847 (1967).
18. Cheesewright, R., "Turbulent Natural Convection From A Vertical Plane Surface", J. Heat Transfer, 90, 1, p. 1 (1968).
19. Cheng, K. C., "Laminar Forced Convection in Regular Polygonal Ducts with Uniform Peripheral Heat Flux", J. Heat Transfer, 2, pp. 156-157 (1969).
20. Cheng, K. C., and G. J. Hwang, "Numerical Solution for Combined Free and Forced Laminar Convection in Horizontal Rectangular Channels", J. Heat Transfer, 2, pp. 59-66 (1969).
21. Chung, P. M., and A. D. Anderson, "Unsteady Laminar Free Convection", J. Heat Transfer, Trans. ASME, C83, pp. 473-8 (1961).
22. Cygan, D. A., and P. D. Richardson, "A Transcendental Approximation For a Natural Convection at Small Prandtl Numbers", Can. J. Chem. Engng., 46, 5, p. 321 (1968).
23. Dotson, J. P., "Heat Transfer from a Vertical Plate by Free Convection", M. S. Thesis, Purdue University (1954).
24. Dring, R. P., and B. Gebhart, "A Theoretical Investigation of Disturbance Amplification in External Laminar Natural Convection", J. Fluid Mech., 34, part 3, pp. 551-564 (1968).

25. Dropkin, D., and E. Somerscales, "Heat Transfer by Natural Convection by Two Parallel Plates which are Inclined at Various Angles with Respect to the Horizontal", J. Heat Transfer, Trans. ASME, C87, 1, pp. 77-84 (1965).
26. Eckert, E. R. G., and R. M. Drake, "Heat and Mass Transfer", McGraw-Hill, New York, Second edition, pp. 311-333 (1959).
27. Eckert, E. R., J. P. Hartnett, and T. F. Irvine, "Flow Visualization Studies of Transition to Turbulence in Free Convection Flow", ASME Paper No. 60-WA-250.
28. Eckert, E. R. G., and T. W. Jackson, "Analysis of Turbulent Free-Convection Boundary Layer on Flat Plate", NACA Report 1015, 37 (1951).
29. Eckert, E. R. G., and E. Soehngnen, "Interferometric Studies on the Stability and Transition to Turbulence of a Free Convection Boundary Layer", Inst. Mech. Eng. and ASME, Proc. General Disc. on Heat Trans., 321, London (1951).
30. Eckert, E. R. G., and E. Soehngnen, "Studies on Heat Transfer in Laminar Free Convection with the Zehnder-Mach interferometer", USAF Report 5747 (1948).
31. Eichhorn, R., "Flow Visualization and Velocity Measurement in Natural Convection with the Tellurium Dye Method", J. Heat Transfer, Trans. ASME, C83, 3, pp. 379-81 (1961).
32. Eichhorn, R., "Measurement of Low Speed Gas Flows by Particle Trajectories: A New Determination of Free Convection Velocity Profiles", Int. J. Heat Mass Transfer, 5, p. 915 (1962).
33. Emery, A. F., "The Effect of a Magnetic Field upon the Free Convection of a Conducting Fluid", J. Heat Transfer, Trans. ASME, C85, 2, pp. 119-24 (1963).
34. Emery, A. F., and D. A. Bailey, "Heat Transfer to Fully-developed Liquid Metal Flow in Tubes", J. Heat Transfer, 89, 3, p. 272 (1967).
35. Emery, A. F., and N. C. Chu, "Heat Transfer across Vertical Layers", J. Heat Transfer, Trans. ASME, C87, 1, pp. 110-16
36. Faris, G. N., and R. Viskanta, "An Analysis of Laminar Combined Forced and Free Convection Heat Transfer in a Horizontal Tube", Int. J. Heat Mass Transfer, 12, pp. 1295-1309 (1969).

37. Fedorovich, Ye. D., and B. L. Paskar, "Correlation of Experimental Data on Convective Heat Transfer in Channels with Partially Heated Perimeters", Heat Transfer-Soviet Research, 1, 5, p. 73 (1969).
38. Finston, M., "Free Convection past a Vertical Plate", ZAMP, 7, pp. 527-9 (1956).
39. Foote, J. R., "An Asymptotic Method for Free Convection past a Vertical Plate", ZAMP, 9, pp. 64-7 (1958).
40. Fujii, T., "An Analysis of Turbulent Free Convection Heat Transfer from a Vertical Surface", Bul. of Japan Soc. of Mech. Eng., JSME, 2, 8, pp. 539-63 (1959).
41. Fujii, T., "Mathematical Analysis of Heat Transfer from a Vertical Flat Surface by Laminar Free Convection", Bul. of Japan Soc. of Mech. Eng., JSME, 2, 7, pp. 365-9 (1959).
42. Gebhart, B., "Effects of Viscous Dissipation in Natural Convection", J. Fluid Mech., 14, pp. 225-32 (1962).
43. Gebhart, B., "Heat Transfer", McGraw-Hill, New York, pp. 251-73 (1961).
44. Gebhart, B., "On Boundary Conditions for Natural Convection Transients", J. Heat Transfer, Trans. ASME, C85, p. 184 (1963).
45. Gebhart, B., "On Inflexion Points in Natural Convection Profiles", J. Aerospace Sci., 29, pp. 485-6 (1962).
46. Gebhart, B., "Transient Natural Convection from Vertical Element", J. Heat Transfer, Trans. ASME, C83, 1, pp. 61-70 (1961).
47. Gebhart, B., "Natural Convection Flow, Instability, and Transition", J. Heat Transfer, 91, Paper No. 69-HT-29 (1969).
48. Gebhart, B., and D. E. Adams, "Measurement of Transient Natural Convection on Flat Vertical Surfaces", J. Heat Transfer, Trans. ASME, C85, p. 25 (1963).
49. Gebhart, B., And R. P. Dring, "The leading edge Effect in Transient Natural Convection from A Vertical Plate", J. of Heat Transfer, 89, 8, pp. 274-275 (1967).
50. Gebhart, B., R. P. Dring, and C. E. Polymeropoulos, "Natural Convection from Vertical Surface, the Convection Transient Regime", J. Heat Transfer, Trans. ASME, C89, 1, pp. 53-9 (1967).



51. Gelman, L. I., and I. Z. Kopp, "Film Boiling Heat Transfer to Mercury in a Vertical Tube", Heat Transfer-Soviet Research, 1, 5, (1969).
52. Genin, L. G., V. G. Zhilin, and B. S. Petukhov, "Experimental Investigation of Turbulent Flow of Mercury in a Circular Tube in a Longitudinal Magnetic Field", High Temperature, 5, 2, p. 266 (1967).
53. Goldstein, S., "Modern Developments in Fluid Dynamics", Oxford University Press, London, pp. 638-45 (1938).
54. Goldstein, S., "Modern Developments in Fluid Dynamics II", Oxford University Press, London, p. 641 (1957).
55. Goldstein, R. J., and E. R. G. Eckert, "The Steady and Transient Free Convection Boundary Layer on a Uniformly Heated Vertical Plate", Int. J. Heat Mass Transfer, 1, 2/3, pp. 208-18 (1960).
56. Goren, S. L., "On Free Convection in Water at 4° C", Chem. Eng. Science, 21, pp. 515-18 (1966).
57. Griffiths, E., and A. H. Davis, "The Transmission of Heat by Radiation and Convection", Dept. of Scientific and Industrial Research, Food Investigation Board, Special Report, No. 9, His Majesty's Stationery Office, London (1922).
58. Gupta, A. S., "Laminar Free Convection Flow of an Electrically Conducting Fluid from a Vertical Plate with Uniform Surface Heat Field", ZAMP, 13, 4, p. 324 (1962).
59. Hausen, H., "Neue Gleichungen Für die Wärmeüber bei Freier oder erzwungener Stömung", Allg. Wärmetech., 9, p. 75 (1959).
60. Hayday, A. A., D. A. Bowlus, and R. A. McGraw, "Free Convection from a Vertical Flat Plate with Step Discontinuities in Surface Temperature", J. Heat Transfer, 89, 8, pp. 244-250 (1967).
61. Hellums, J. D., and S. W. Churchill, "Dimensional Analysis and Natural Circulation", Chem. Eng. Prog. Symposium Series, 57, 32, pp. 75-80 (1961).
62. Hellums, J. D., and S. W. Churchill, "Transient and Steady State, Free and Natural Convection, Numerical Solution; Part I, The Isothermal, Vertical Plate, Part II, the Region Inside a Horizontal Cylinder", A.I.Ch.E. Journal, 8, pp. 690-5 and 719 (1962).

63. Hill, J. C., and C. A. Sleicher, "Convective Heat Transfer from Small Cylinders to Mercury", Int. J. Heat Mass Transfer, 12, pp. 1595-1604 (1969).
64. Hill, R. C., "An Experimental Investigation of Free Convection Heat Transfer from a Non-Isothermal Vertical Flat Plate", Master's Thesis, University of California (1961).
65. Jakob, Max., "Heat Transfer", John Wiley and Sons, New York, Vol. 1, pp. 522-87 (1949).
66. University of California, Institute of Engineering Research Report: Contract AT-11-Gen, Project 5, Phase II, (1953).
67. Julian, D. V., "An Experimental Study of Natural Convection Heat Transfer from a Uniformly Heated Vertical Plate Immersed in Mercury", Ph.D. Thesis, Kansas State University (1967).
68. Julian, D. V., and R. G. Akins, "Experimental Investigation of Natural Convection Heat Transfer to Mercury", I & EC Fundamentals, 8, 4, pp. 641-646 (1969).
69. Kaplum, S., "Fluid Mechanics and Singular Perturbations", Academic Press, New York (1967).
70. Kato, H., N. Nishwaki, and M. Hirata, "On the Turbulent Heat Transfer by Free Convection from a Vertical Plate", Int. H. Heat Mass Transfer, 11, 7, p. 1117 (1968).
71. Kennard, R. B., "An Optical Method for Measuring Temperature Distribution and Convective Heat Transfer", J. Res. Natl. Bur. Standards, 8, pp. 787-805 (1932).
72. Knowles, C. P., and B. Gebhart, "The Stability of the Natural Convection Boundary Layer", J. Fluid Mech., 34, 4, p. 657 (1968).
73. Kuiken, H. K., "Axisymmetric free Convection Boundary Layer Flow Past Slender Bodies", Int. J. Heat Mass Transfer, 11, 7, p. 1141 (1968).
74. Kuiken, H. K., "Free Convection at low Prandtl numbers", J. Fluid Mech., 37, 4, pp. 785-789 (1969).
75. Kuiken, H. K., "General Series Solution for Free Convection Past a Nonisothermal Vertical Flat Plate", Appl. Scient. Res., 20, 2-3, p. 205 (1969).

76. Kuo, Y. H., "On the Flow of an Incompressible Viscous Fluid past a Flat Plate at Moderate Reynolds Numbers", J. Math. Phys., 32, pp. 83-101 (1953).
77. Landis, F., and H. Yanowitz, "Transient Natural Convection in a Narrow Vertical Cell", Proc. of 3rd International Heat Transfer Conference, 2, 56, p. 139-51 (1966).
78. Lauber, T. S., and A. U. Welch, "Natural Convection Heat Transfer between Vertical Flat Plates with Uniform Heat Flux", Proc. of 3rd International Heat Transfer Conf., 2, 54, pp. 126-31 (1966).
79. Lefevre, E. J., Ninth Intern. Congr. Appl. Mech. Paper I p. 168 (1956).
80. Lemlich, R., and J. Vardi, "Steady Free Convection to a Flat Plate with Uniform Surface Heat Flux and Nonuniform Acceleration", J. Heat Transfer, Trans. ASME, C86, 4, pp. 562-3 (1964).
81. Lightfoot, E. N., "Free Convection Heat and Mass Transfer: The Limiting Case of  $Gr^{AB}/Gr \rightarrow 0$  and  $Pr/Sc \rightarrow 0$ ", Chem. Engng. Sci., 33, 8, p. 931 (1968).
82. Lock, G. S. H., and F. J. deB. Trotter, "Observations on the Structure of a Turbulent Free Convection Boundary Layer", Int. J. Heat Mass Transfer, 11, pp. 1225-1232 (1968).
83. Lorenz, L., "Ueber das leitungsvermogen der metalle fur Wärme und Electricitat", Wiedemanns Annalen, 13, p. 582 (1881).
84. Lorenz, H., "Die Wärmeübertragung an einer ebenen Senkrechten Platte an Öl bei natürlicher Konvektion", Z. techn. Physik, 9, pp. 362-366 (1934).
85. Lykoudis, P. S., "Natural Convection of an Electrically Conducting Fluid in the Presence of a Magnetic Field", Int. J. Heat Mass Transfer, 5, pp. 23-34 (1962).
86. Lyon, R. N., Editor, "Liquid Metals Handbook", Atomic Energy Commission, Second Edition (1952).
87. MacGregor, R. K., and P. S. Lykoudis, "Natural Convection Experiment with Mercury in a Transverse Magnetic Field", NSF GP-927; A & ES-64-9, Purdue University, Lafayette, Inc. (1964).
88. MacGregor, R. K., and A. F. Emery, "Free Convection through Vertical Plane Layers, Moderate and High Prandtl Number Fields", J. Heat Transfer, 91, 8, pp. 391-403 (1969).



89. Marco, S. M., and H. R. Velkoff, "Effect of Electrostatic Fields on Free Convection Heat Transfer from Flat Plates", ASME paper 63-HT-9 (1963).
90. Malcolm, D. G., "Some Aspects of Turbulence Measurement in Liquid Mercury using Cylindrical Quartz-insulated Hot-film Sensors", J. Fluid Mech., 37, 4, pp. 701-713 (1969).
91. McAdams, W. H., "Heat Transmission", McGraw-Hill, New York, Third Edition, pp. 165-83 (1954).
92. Merkin, J. H., "The Effect of Buoyancy Forces on the Boundary Layer Flow Over a Semi-infinite Vertical Flat Plate in a Uniform Free Stream", J. Fluid Mech., 35, 3, pp. 439-450 (1969).
93. Merriam, R. L., R. P. Stein, and B. L. Richardson, "A Liquid Metal Heat Transfer Experiment and Its Relation to Recent Theory", Int. J. Heat Mass Transfer, 11, 4, p. 769 (1968).
94. Niuman, F., and K. Pohlhausen, Remarks on the paper by M. Finston: "Free Convection Past a Vertical Plate", ZAMP, 9, pp. 67-9 (1958).
95. Nishikawa, K., and Ito, R., "An Analysis of Free Convective Heat Transfer from an Isothermal Vertical Plate to Supercritical Fluids", Int. J. Heat Mass Transfer, 12, pp. 1449-1463 (1969).
96. Nusselt, W., and W. Jürges, VDI-Zeitschr., 72, p. 597 (1928).
97. O'Brien, R. J., and A. J. Shine, "Some Effects of an Electric Field on Heat Transfer from a Vertical Plate in Free Convection", J. Heat Transfer, Trans. ASME, C89, pp. 114-6 (1967).
98. Ostrach, S., "An Analysis of Laminar Free-Convection Flow and Heat Transfer about a Flat Plate Parallel to the Direction of the Generating Body Force", National Advisory Committee for Aeronautics, Report 1111, pp. 63-79 (1953).
99. Ostrach, S., and D. Pnueli, "The Thermal Instability of Completely Confined Fluids inside Some Particular Configurations", J. Heat Transfer, 85, pp. 346-354 (1963).
100. Papaïliou, D. D., and P. S. Lykoudis, "Magneto-fluid-Mechanic laminar Natural Convection -An Experiment", Int. J. Heat Mass Transfer, 11, pp. 1385-1391 (1968).

101. Pohlhausen, E., "Der Wärmeaustausch Zwischen festen Korpen und Flüssigkeiten mit kleiner Reibung und kleiner Wärmeleitung", ZAMM, 1, 115-21 (1921).
102. Polymeropoulos, C. E., and B. Gebhart, "Incipient Instability in Free Convection Laminar Boundary Layers", J. Fluid Mech., 30, 2, pp. 225-239 (1967).
103. Prandtl, L., "Über Flüssigkeitsbewegung bei sehr kleiner Reibung", Proceedings of the Third Intern. Math. Kongr., Heidelberg (1904), Reprinted in Vier Abhdl. Zur Hydro-Aerodynamik, Göttingen (1927), also translated in NACA TM-452 (1928).
104. Reeves, B. L., and C. J. Kippenhan, "On a Particular Class of Similar Solutions of the Equations of Motion and Energy of a Viscous Fluid", J. Aerospace Sci., 20, pp. 38-47 (1962).
105. Reilly, I. G., C. Tien, and M. Adelman, "Experimental Studies of Natural Convective Heat Transfer from a Vertical Plate in a Non-Newtonian Fluid", Can. J. Chem. Eng., 65, 4, pp. 157-60 (1965).
106. Riley, N., "Magnetohydrodynamic Free Convection", J. Fluid Mech., 18, 4, p. 577 (1964).
107. Saunders, O. A., "Natural Convection in Liquids", Proc. Roy. Society (London), A172, pp. 55-71 (1939).
108. Saunders, O. A., "The Effect of Pressure upon Natural Convection in Air", Proc. Roy. Society (London), A157, pp. 278-91 (1936).
109. Saville, D. A., and S. W. Churchill, "Simultaneous Heat and Mass Transfer in Free Convection Boundary Layers", A.I.Ch.E.J., 16, 2, pp. 268-273 (1970).
110. Schardin, H., Z. Instrumentenk., 53, pp. 396-402 and 424-36 (1933).
111. Schechter, R. S., and H. S. Isbin, "Natural-Convection Heat Transfer in Regions of Maximum Fluid Density", A.I.Ch.E. Journal, 4, pp. 81-9 (1958).
112. Scherberg, M. G., "Natural Convection at a Thermal Leading Edge on a Vertical Wall", Int. J. Heat Mass Transfer, 8, 10, pp. 1319-1331 (1965).
113. Scherberg, M. G., "Natural Convection from Wall Sections of Arbitrary Distribution by an Integral Method", Int. J. Heat Mass Transfer, 7, pp. 501-16 (1964).

114. Scherberg, M. G., "Natural Convection near and above Thermal Leading Edges on Vertical Walls", Int. J. Heat Mass Transfer, 5, pp. 1001-10 (1962).
115. Sherman, M., and S. Ostrach, "Lower Bounds to the Critical Rayleigh Number in Completely Confined Regions", J. Appl. Mech., 34, 2, p. 308 (1967).
116. Schetz, J. A., "Natural Convection in the Vicinity of a Vertical Plate with a Step-Change in Wall Temperature", Mechanical Eng. Dept. Report #HT-4, Princeton University (1961).
117. Schetz, J. A., and R. Eichhorn, "Natural Convection with Discontinuous Wall Temperature Variations", J. Fluid Mech., 18, p. 167 (1964).
118. Schlichting, H., "Boundary Layer Theory", McGraw-Hill, New York, Fourth edition, pp. 243-60 (1960).
119. Schmidt, E., "Schlierenaufnahmen der Temperaturefelder in der Nahe warmeabgebender Korper", Forsch. Ing.-Wes., 3, p. 181 (1932).
120. Schmidt, E., and W. Beckmann, "Das Temperatur und Geschwindigkeitfeld vor einer Wärme Abgebenden Senkrechten Platte bei Natürlicher Konvektion", Tech. Mech. Thermodynamik, Bd. 1, No. 10, pp. 341-9 (1930), continued Bd. 1, 11, pp. 391-406 (1930).
121. Schrock, S. L., "Eddy Diffusivity Ratios in Liquid Metals", Ph.D. Thesis, Purdue University (1964).
122. Schuh, H., "Einige Probleme bei freier Stromung zäher Flüssigkeiten", Göttinger Monographien, Bd. B, Grenzschichten (1946).
123. Shevchuk, Ye. N., "Study of Free Convection Heat Transfer to Boiling Alkali Metals", Heat Transfer-Soviet Research, 2, 1, p. 44 (1970).
124. Shevchuk, Ye. N., "Free Convection Heat Transfer to Boiling Potassium", Heat Transfer-Soviet Research, 2, 1, p. 84 (1970).
125. Simon, H. A., and E. R. G. Eckert, "Laminar Free Convection in Carbon Dioxide near its Critical Point", Int. J. Heat Mass Transfer, 6, 8, pp. 681-90 (1963).

126. Sinaha, P. C., "Fully developed Laminar Free Convection Flow between Vertical Parallel Plates", Chem. Engng. Sci. 24, 1, p. 33 (1969).
127. Soliman, M., and P. L. Chambre, "On the Time-dependent Convective Heat Transfer in Fluids with Vanishing Prandtl Number", Int. J. Heat Mass Transfer, 12, pp. 1221-1230 (1969).
128. Sparrow, E. M., "Free Convection with Variable Properties and Variable Wall Temperatures", Ph.D. Thesis, Harvard University (1956).
129. Sparrow, E. M., "Laminar Free Convection on a Vertical Plate with Prescribed Nonuniform Wall Heat Flux or Prescribed Nonuniform Wall Temperature", NACA TN 3508 (1955).
130. Sparrow E. M., and R. D. Cess, "The Effect of a Magnetic Field on Free Convection Heat Transfer", Int. J. Heat Mass Transfer, 3, 4, pp. 267-274 (1961).
131. Sparrow, E. M., and J. L. Gregg, "Laminar Free Convection from a Vertical Plate with Uniform Surface Heat Flux", Trans. ASME, 78, pp. 435-440 (1956).
132. Sparrow, E. M., and J. L. Gregg, "Similar Solutions for Free Convection from a Nonisothermal Vertical Plate", Trans. ASME, 80, pp. 379-86 (1958).
133. Sparrow, E. M., and J. L. Gregg, "The Variable Fluid-Property Problem in Free Convection", Trans. ASME, 80, pp. 879-86 (1958).
134. Sparrow, E. M., F. K. Tsou, and E. F. Kurtz, Jr., "Stability of Laminar Free-Convection Flow on a Vertical Plate", Physics Fluids, 8, 8, p. 1559 (1965).
135. Sparrow, E. M., and L. DeM. F. Guinle, "Deviations from Classical Free Convection Boundary Layer Theory at Low Prandtl Numbers", Int. J. Heat Mass Transfer, 11, 9, p. 1403 (1968).
136. Sparrow, E. M., and R. B. Husar, "Free Convection from a Plane Vertical Surface with a Non-horizontal Leading Edge", Int. J. Heat Mass Transfer, 12, 3, p. 365 (1969).
137. Stein, R. P. "Liquid Metal Heat Transfer", in Advanced Heat Transfer, edited by T. F. Irvine Jr. and J. P. Harnett, Vol. 3, p. 101, Academic Press, New York (1966).

138. Sugawara, S., and I. Michiyoshi, "Effects of Prandtl Number on Heat Transfer by Natural Convection - The Case where Prandtl Number is Comparatively Small", Proc. 3rd Japan National Congress for Applied Mechanics (1953).
139. Suriano, F. J., K. T. Yang, and J. A. Donlon, "Laminar Free Convection along a Vertical Plate at Extremely Small Grashof Numbers", Int. J. Heat Mass Transfer, 8, pp. 815-31 (1965).
140. Suriano, F. J., and K. T. Yang, "Laminar Free Convection about Vertical and Horizontal Plates at Small and Moderate Grashof Numbers", Int. J. Heat Mass Transfer, 11, 3, pp. 473-490 (1968).
141. Takhar, H. S., "Free Convection from a Flat Plate", J. Fluid Mech., 34, 1, p. 81 (1968).
142. Tanaev, A. A., "Heat Interchange under Conditions of Free Laminar Motion of a Gas with Variable Viscosity at a Vertical Wall", Zhurnal Tekhnicheskoi Fiziki, 26, p. 2714 (1956).
143. Tien, C., "Laminar Natural Convection Heat Transfer from Vertical Plate to Power-Law Fluid", Appl. Sci. Res., 17, pp. 233-248 (1967).
144. Tien, C., and H. S. Tsuei, "Laminar Natural Convection Heat Transfer in Ellis Fluids", Appl. Sci. Res., 20, pp. 131-147 (1969).
145. Tsung, Y. N., and A. G. Hansen, "Possible Similarity Solutions of the Laminar Natural Convection Flow of Non-Newtonian Fluids", Int. J. Heat Mass Transfer, 9, pp. 261-2 (1966).
146. Van Dyke, M., "Perturbation Method in Fluid Mechanics", Academic Press, New York (1964).
147. Vanier, C. R., and C. Tien, "Further work on free convection in water at 4° C", Chem. Engng. Sci., 22, 12, p. 1747 (1967).
148. Vest, C. M., and V. S. Arpaci, "Stability of Natural Convection in a Vertical Slot", J. Fluid Mech., 36, 1, pp. 1-15 (1969).
149. Vliet, G. C., "Natural Convection Local Heat Transfer on Constant Heat flux included Surfaces", J. Heat Transfer, 91, 11, pp. 511-516 (1969).



150. Vliet, G. C., and C. K. Liu, "An Experimental Natural Convection Boundary Layers", J. Heat Transfer, 91, 11, pp. 517-531 (1969).
151. Warner, C. Y., and V. S. Arpaci, "An Experimental Investigation of Turbulent Natural Convection in Air at Low Pressure Along a Vertical Heated Plate", Int. J. Heat Mass Transfer, 11, 3, pp. 397-406 (1968).
152. Weise, R., "Wärmeübergang durch freie konvektion an quadratischen Platten", Forschung auf dem Gebiete des Ingenieurwesens, 6, pp. 281-292 (1935).
153. Yang, K. T., "An Improved Integral Procedure for Compressible Laminar Boundary-Layer Analysis", J. Appl. Mech., Trans. ASME, E83, pp. 9-20 (1961).
154. Yang, K. T., "Laminar Free-Convection Wake above a Heated Vertical Plate", J. Appl. Mech., Trans. ASME, E31, 1, pp. 131-8 (1964).
155. Yang, K. T., "On an Improved Karman-Pohlhausen's Integral Procedure and a Related Error Criterion", Proc. of the 4th U. S. National Congress of applied Mechanics, ASME, pp. 1419-29 (1962).
156. Yang, K. T., "Possible Similarity Solutions for Laminar Free Convection on Vertical Plates and Cylinders", J. Appl. Mech., Trans. ASME, E82, pp. 230-6 (1960).
157. Yang, K. T., "Remarks on Transient Laminar Free Convection along a Vertical Plate", Int. J. Heat Mass Transfer, 9, 5, pp. 511-3 (1966).
158. Yang, K. T., and E. W. Jerger, "First-Order Perturbations of Laminar Free-Convection Boundary Layers on a Vertical Plate", J. Heat Transfer, Trans. ASME, C86, 1, pp. 107-15 (1964).
159. Yung, S. C., R. B. Oetting, "Free Convection Heat Transfer from an Inclined Heated Flat Plate in Air", J. Heat Transfer, 91, 2, pp. 192-194 (1969).

## ACKNOWLEDGEMENTS

The author wishes to express his sincere gratitude to his major advisor, Dr. Richard G. Akins for his constant guidance and encouragement. Appreciation is also extended to the advisory committee for reading the manuscript. The author also would like to acknowledge National Science Foundation for the financial support.

**APPENDIX A****COMPUTER PROGRAM**





## APPENDIX B

### SAMPLE CALCULATIONS

## SAMPLE CALCULATIONS

Run with mercury No. 201

February 20, 1970

(Refer to the second profile in Figure 11)

Voltage drop across the copper rods : 0.412 volts

Current :  $0.7661 \times 30 = 22.98$  amperes

Position up the plate : 1 inch = 2.54 cm

potentiometer voltage : 5.5 volts

Zero suppression : 0.9526 mv.

Attenuation : 1

Sensitivity : 0.002 mv/mm in Sanborn chart

Sanborn Output : 92.15 mv/mm in Sanborn chart

X-scale factor : 0.2 v/in in the Plotter

Y-scale factor : 200 mv/in in the Plotter

Temperature at the wall

$$\begin{aligned}
 T_w(\text{mv}) &= (\text{Zero suppression}) - [(\text{Y-scale factor})(\text{\#inch}) \\
 &\quad (\text{attenuation})(\text{sensitivity})/(\text{Sanborn Output factor})] \\
 &= 0.9526 (\text{mv}) - \frac{200(\frac{\text{mv}}{\text{in}}) \times 0 (\text{in}) \times 1.0 \times 0.002(\frac{\text{mv}}{\text{mm}})}{92.15 (\frac{\text{mv}}{\text{mm}})} \\
 &= 0.9526 \text{ mv}
 \end{aligned}$$

$$T_w(^{\circ}\text{C}) = 24.098^{\circ}\text{C}$$

Temperature at bulk

$$\begin{aligned}
 T_{\text{inf}} (\text{mv}) &= 0.9526 (\text{mv}) - \frac{200(\frac{\text{mv}}{\text{in}}) \times 4.95(\text{in}) \times 1.0 \times 0.002(\frac{\text{mv}}{\text{mm}})}{92.15 (\frac{\text{mv}}{\text{mm}})} \\
 &= 0.9311 \text{ mv}
 \end{aligned}$$

$$T_{\text{inf}} (^{\circ}\text{C}) = 23.563^{\circ}\text{C}$$

Reference temperature for physical properties

$$\begin{aligned}
 T_R &= T_w(0.7) + T_{\text{inf}}(0.3) \quad (\text{Reference 128}) \\
 &= (24.098)(0.7) + 23.563 (0.3) \\
 &= 23.937^{\circ}\text{C}
 \end{aligned}$$

Physical Properties

$$\text{Coefficient of thermal expansion, } \beta : 0.1818 \times 10^{-3} /^{\circ}\text{C}$$

Prandtl number,  $Pr$  : 0.02426

Density,  $\rho$  : 13.5362 gm/cm<sup>3</sup>

Viscosity,  $\mu$  : 0.01529 gm/cm-sec

Conductivity,  $k$  : 0.02099 cal/cm-sec-°C

Power dissipated in plate

Total power ( $P_T$ ) = (Volts)(Currents)

$$= (0.412)(22.98)$$

$$= 9.467 \text{ watts}$$

Overall resistance (plate, copper rods, contact, etc.)( $R_T$ )

$$= \frac{\text{Volts}}{\text{current}}$$

$$= \frac{0.412}{22.98}$$

$$= 0.0179 \text{ ohms}$$

Resistance of plate ( $R_p$ ) =  $\frac{(\text{Resistivity})(\text{length})}{(\text{Area})}$

$$\text{resistivity} = 7.315 \times 10^{-5} \text{ ohm-cm}$$

$$\text{length of plate} = 4 \text{ (in)} \times 2.54 \left( \frac{\text{cm}}{\text{in}} \right) = 10.16 \text{ cm}$$

$$\begin{aligned} \text{Cross Sectional Area} &= 2 \text{ (in)} \times 0.004 \text{ (in)} \times 2.54 \left( \frac{\text{cm}}{\text{in}} \right)^2 \\ &= 0.0516 \text{ cm}^2 \end{aligned}$$

$$R_p = \frac{(7.315 \times 10^{-5})(10.16)}{0.0516} = 0.0144 \text{ ohm}$$

$$\begin{aligned}\text{Power dissipated in plate} &= P_T \times \frac{R_P}{R_T} = 9.467 \times \frac{0.0144}{0.0179} \\ &= 7.616 \text{ watts (80.4\%)}\end{aligned}$$

### Heat flux

$$\begin{aligned}\text{Heat flux} &= \frac{\text{Power}}{\text{Surface Area}} = \frac{7.616(\text{watts})}{2 \times 2 \times 4(\text{in}^2)} = 0.4760 \frac{\text{watts}}{\text{in}^2} \\ &= 0.4760 \left( \frac{\text{watts}}{\text{in}^2} \right) \times 492 \left( \frac{\text{Btu/hr-ft}^2}{\text{watts/in}^2} \right) = 234.192 \frac{\text{Btu}}{\text{hr-ft}^2} \\ &= 0.4760 \left( \frac{\text{watts}}{\text{in}^2} \right) \times 0.0371 \left( \frac{\text{Cal/sec-cm}^2}{\text{watts/in}^2} \right) \\ &= 0.0176 \frac{\text{cal}}{\text{sec-cm}^2}\end{aligned}$$

### Modified Grashof numbers

$$\begin{aligned}\text{Based on } x : \quad Gr_x^* &= \frac{g \beta \rho^2 q x^4}{k \mu^2} \\ Gr_x^* &= \frac{980 \left( \frac{\text{cm}}{\text{sec}^2} \right) \times 0.1818 \times 10^{-3} \left( \frac{1}{^\circ\text{C}} \right) \times 13.5314^2 \left( \frac{\text{gm}^2}{\text{cm}^6} \right) \times 0.0176 \left( \frac{\text{cal}}{\text{sec-cm}^2} \right)}{0.0211 \left( \frac{\text{cal}}{\text{cm-sec-}^\circ\text{C}} \right) \times 0.01519^2 \left( \frac{\text{gm}^2}{\text{cm}^2\text{-sec}^2} \right)} \\ &\quad \times 2.54^4 (\text{cm}^4)\end{aligned}$$

$$Gr_x^* = 0.4908 \times 10^7$$

$$\begin{aligned}\text{Based on } L : \quad Gr_L^* &= \frac{g \beta \rho^2 q L^4}{k \mu^2} = 0.7854 \times 10^8\end{aligned}$$

Nusselt number

$$Nu_x = \frac{h_x \cdot x}{k}$$

$$q = h_x(T_w - T_{inf})$$

$$Nu_x = \frac{q \cdot x}{k(T_w - T_{inf})} = \frac{0.0176\left(\frac{\text{cal}}{\text{sec-cm}^2}\right) \times 2.54(\text{cm})}{0.0211\left(\frac{\text{cal}}{\text{cm-sec-}^\circ\text{C}}\right) \times (24.098 - 23.563)(^\circ\text{C})}$$

$$Nu_x = 3.938$$

Dimensionless temperature at sample location

Temperature 2.1 inch at the position 2 inch from the plate

$$T = 0.9526 - \frac{200 \times 2.1 \times 1 \times 0.002}{92.15}$$

$$= 0.9435 \text{ mv}$$

$$T = 23.863 \text{ }^\circ\text{C}$$

$$\theta = \frac{T - T_{inf}}{T_w - T_{inf}} = \frac{23.863 - 23.563}{24.098 - 23.563} = 0.561$$

Dimensionless distance at sample location

Pitch of horizontal screw :  $\frac{1}{32}$  inch per turn of motor

Number of teeth in potentiometer wheel : 120

Number of teeth in motor shaft wheel : 24

$$\frac{120}{24} = 5 \frac{\text{turn of motor}}{\text{turn of potentiometer}}$$

Voltage change in ten-turn potentiometer :

$$\frac{10}{5.5} \frac{\text{turns of potentiometer}}{\text{Voltage change}}$$

X-scale factor      0.2 v/inch of pen

$$\text{Factor} = \frac{1}{32} \left( \frac{\text{inch of probe}}{\text{turn of motor}} \right) \times \frac{120}{24} \left( \frac{\text{turn of motor}}{\text{turn of potentiometer}} \right)$$

$$\times \frac{10}{5.5} \left( \frac{\text{turn of potentiometer}}{\text{voltage change}} \right) \times 0.2 \left( \frac{\text{voltage}}{\text{inch of pen}} \right)$$

$$\times 2.54 \left( \frac{\text{cm}}{\text{in}} \right)$$

$$= 0.1443 \left( \frac{\text{cm of probe}}{\text{in of pen}} \right)$$

$$\begin{aligned} y = \text{distance from plate at sample position} &= 0.1443 \times 2.0(\text{in}) \\ &= 0.2886 \text{ cm} \end{aligned}$$

$$\begin{aligned} \text{dimensionless distance} \cdot \eta &= \frac{y}{x} \left( \frac{Gr_x^*}{5} \right)^{1/5} \\ &= \frac{0.2886}{2.54} \left( \frac{0.4908 \times 10^7}{5} \right)^{1/5} \\ &= 1.7941 \end{aligned}$$

### Measurement Errors

#### 1. Temperature

Temperature fluctuation amplitude was  $\pm 0.15$  inch

$$\frac{200 \left( \frac{\text{mV}}{\text{in}} \right) \times 0.15(\text{in}) \times 1.0 \times (0.002 \frac{\text{mV}}{\text{in}})}{92.15 \left( \frac{\text{mV}}{\text{mm}} \right)} \times 25 \left( \frac{^{\circ}\text{C}}{\text{mV}} \right) = \pm 0.016 ^{\circ}\text{C}$$



$$T = 23.863 \pm 0.016$$

## 2. Position up the plate

The micrometer dial can be set to within  $\frac{1}{50}$  turn

$$\frac{1}{32} \frac{\text{inch}}{\text{rev.}} \times \frac{1}{50} = 0.0006 \text{ inch or } 0.00158 \text{ cm}$$

A more important error would be in not knowing exactly where the thermocouple junction is located inside the sheath.

This error would be about 0.007 inch or 0.02 cm.

$$x = 2.54 \pm 0.02 \text{ cm}$$

## 3. Position away from the plate

distance difference about 0.2 inch

$$0.1443 \left( \frac{\text{cm of probe}}{\text{in or pen}} \right) \times (\pm 0.1)(\text{in of pen}) = \pm 0.01443$$

$$y = 0.2886 \pm 0.01443$$

**APPENDIX C****COPPER-CONSTANTAN THERMOCOUPLE  
CALIBRATION**

C	DEGREES CENTIGRADE				MILLIVOLTS	REFERENCE JUNCTION 0 C.			
	.0	.1	.2	.3		.6	.7	.8	.9
0	.0000	.0038	.0076	.0114	.0152	.0190	.0228	.0266	.0304
1	.0380	.0419	.0458	.0497	.0536	.0575	.0614	.0653	.0692
2	.0770	.0809	.0848	.0887	.0926	.0965	.1004	.1043	.1082
3	.1160	.1199	.1238	.1277	.1316	.1355	.1394	.1433	.1472
4	.1550	.1589	.1628	.1667	.1706	.1745	.1784	.1823	.1862
5	.1940	.1979	.2018	.2057	.2096	.2135	.2174	.2213	.2252
6	.2330	.2369	.2408	.2447	.2486	.2525	.2564	.2603	.2642
7	.2720	.2759	.2798	.2837	.2876	.2915	.2954	.2993	.3032
8	.3110	.3149	.3188	.3227	.3266	.3305	.3344	.3383	.3422
9	.3500	.3539	.3578	.3617	.3656	.3695	.3734	.3773	.3812
10	.3890	.3930	.3970	.4010	.4050	.4090	.4130	.4170	.4210
11	.4290	.4329	.4368	.4407	.4446	.4485	.4524	.4563	.4602
12	.4680	.4719	.4758	.4797	.4836	.4875	.4914	.4953	.5000
13	.5080	.5119	.5158	.5197	.5236	.5275	.5314	.5353	.5392
14	.5470	.5509	.5548	.5587	.5626	.5665	.5704	.5743	.5782
15	.5860	.5899	.5938	.5977	.6016	.6055	.6094	.6133	.6172
16	.6250	.6289	.6328	.6367	.6406	.6445	.6484	.6523	.6562
17	.6640	.6679	.6718	.6757	.6796	.6835	.6874	.6913	.6952
18	.7030	.7069	.7108	.7147	.7186	.7225	.7264	.7303	.7342
19	.7420	.7459	.7498	.7537	.7576	.7615	.7654	.7693	.7732
20	.7810	.7849	.7888	.7927	.7966	.8005	.8044	.8083	.8122
21	.8200	.8239	.8278	.8317	.8356	.8395	.8434	.8473	.8512
22	.8590	.8629	.8668	.8707	.8746	.8785	.8824	.8863	.8902
23	.8980	.9019	.9058	.9097	.9136	.9175	.9214	.9253	.9292
24	.9370	.9409	.9448	.9487	.9526	.9565	.9604	.9643	.9682
25	.9760	.9799	.9838	.9877	.9916	.9955	.9994	.0033	.0072
26	.0150	.0189	.0228	.0267	.0306	.0345	.0384	.0423	.0462
27	.0540	.0579	.0618	.0657	.0696	.0735	.0774	.0813	.0852
28	.0930	.0969	.1008	.1047	.1086	.1125	.1164	.1203	.1242
29	.1320	.1359	.1398	.1437	.1476	.1515	.1554	.1593	.1632
30	.1710	.1749	.1788	.1827	.1866	.1905	.1944	.1983	.2022
31	.2100	.2139	.2178	.2217	.2256	.2295	.2334	.2373	.2412
32	.2490	.2529	.2568	.2607	.2646	.2685	.2724	.2763	.2802
33	.2880	.2919	.2958	.2997	.3036	.3075	.3114	.3153	.3192
34	.3270	.3309	.3348	.3387	.3426	.3465	.3504	.3543	.3582
35	.3660	.3699	.3738	.3777	.3816	.3855	.3894	.3933	.3972
36	.4050	.4089	.4128	.4167	.4206	.4245	.4284	.4323	.4362
37	.4440	.4479	.4518	.4557	.4596	.4635	.4674	.4713	.4752
38	.4830	.4869	.4908	.4947	.4986	.5025	.5064	.5103	.5142
39	.5220	.5259	.5298	.5337	.5376	.5415	.5454	.5493	.5532
40	.5610	.5649	.5688	.5727	.5766	.5805	.5844	.5883	.5922
41	.6000	.6039	.6078	.6117	.6156	.6195	.6234	.6273	.6312
42	.6390	.6429	.6468	.6507	.6546	.6585	.6624	.6663	.6702
43	.6780	.6819	.6858	.6897	.6936	.6975	.7014	.7053	.7092
44	.7170	.7209	.7248	.7287	.7326	.7365	.7404	.7443	.7482
45	.7560	.7599	.7638	.7677	.7716	.7755	.7794	.7833	.7872
46	.7950	.7989	.8028	.8067	.8106	.8145	.8184	.8223	.8262
47	.8340	.8379	.8418	.8457	.8496	.8535	.8574	.8613	.8652
48	.8730	.8769	.8808	.8847	.8886	.8925	.8964	.9003	.9042
49	.9120	.9159	.9198	.9237	.9276	.9315	.9354	.9393	.9432
50	.9510	.9549	.9588	.9627	.9666	.9705	.9744	.9783	.9822
51	.9900	.9939	.9978	.0017	.0056	.0095	.0134	.0173	.0212
52	.0290	.0329	.0368	.0407	.0446	.0485	.0524	.0563	.0602
53	.0680	.0719	.0758	.0797	.0836	.0875	.0914	.0953	.0992
54	.1070	.1109	.1148	.1187	.1226	.1265	.1304	.1343	.1382
55	.1460	.1499	.1538	.1577	.1616	.1655	.1694	.1733	.1772
56	.1850	.1889	.1928	.1967	.2006	.2045	.2084	.2123	.2162
57	.2240	.2279	.2318	.2357	.2396	.2435	.2474	.2513	.2552
58	.2630	.2669	.2708	.2747	.2786	.2825	.2864	.2903	.2942
59	.3020	.3059	.3098	.3137	.3176	.3215	.3254	.3293	.3332
60	.3410	.3449	.3488	.3527	.3566	.3605	.3644	.3683	.3722
61	.3800	.3839	.3878	.3917	.3956	.3995	.4034	.4073	.4112
62	.4190	.4229	.4268	.4307	.4346	.4385	.4424	.4463	.4502
63	.4580	.4619	.4658	.4697	.4736	.4775	.4814	.4853	.4892
64	.4970	.5009	.5048	.5087	.5126	.5165	.5204	.5243	.5282
65	.5360	.5399	.5438	.5477	.5516	.5555	.5594	.5633	.5672
66	.5750	.5789	.5828	.5867	.5906	.5945	.5984	.6023	.6062
67	.6140	.6179	.6218	.6257	.6296	.6335	.6374	.6413	.6452
68	.6530	.6569	.6608	.6647	.6686	.6725	.6764	.6803	.6842
69	.6920	.6959	.6998	.7037	.7076	.7115	.7154	.7193	.7232
70	.7310	.7349	.7388	.7427	.7466	.7505	.7544	.7583	.7622
71	.7700	.7739	.7778	.7817	.7856	.7895	.7934	.7973	.8012
72	.8090	.8129	.8168	.8207	.8246	.8285	.8324	.8363	.8402
73	.8480	.8519	.8558	.8597	.8636	.8675	.8714	.8753	.8792
74	.8870	.8909	.8948	.8987	.9026	.9065	.9104	.9143	.9182
75	.9260	.9299	.9338	.9377	.9416	.9455	.9494	.9533	.9572
76	.9650	.9689	.9728	.9767	.9806	.9845	.9884	.9923	.9962
77	.0040	.0079	.0118	.0157	.0196	.0235	.0274	.0313	.0352
78	.0430	.0469	.0508	.0547	.0586	.0625	.0664	.0703	.0742
79	.0820	.0859	.0898	.0937	.0976	.1015	.1054	.1093	.1132
80	.1210	.1249	.1288	.1327	.1366	.1405	.1444	.1483	.1522
81	.1600	.1639	.1678	.1717	.1756	.1795	.1834	.1873	.1912
82	.2090	.2129	.2168	.2207	.2246	.2285	.2324	.2363	.2402
83	.2480	.2519	.2558	.2597	.2636	.2675	.2714	.2753	.2792
84	.2870	.2909	.2948	.2987	.3026	.3065	.3104	.3143	.3182
85	.3260	.3299	.3338	.3377	.3416	.3455	.3494	.3533	.3572
86	.3650	.3689	.3728	.3767	.3806	.3845	.3884	.3923	.3962
87	.4040	.4079	.4118	.4157	.4196	.4235	.4274	.4313	.4352
88	.4430	.4469	.4508	.4547	.4586	.4625	.4664	.4703	.4742
89	.4820	.4859	.4898	.4937	.4976	.5015	.5054	.5093	.5132
90	.5210	.5249	.5288	.5327	.5366	.5405	.5444	.5483	.5522
91	.5600	.5639	.5678	.5717	.5756	.5795	.5834	.5873	.5912
92	.6090	.6129	.6168	.6207	.6246	.6285	.6324	.6363	.6402
93	.6480	.6519	.6558	.6597	.6636	.6675	.6714	.6753	.6792
94	.6870	.6909	.6948	.6987	.7026	.7065	.7104	.7143	.7182
95	.7260	.7299	.7338	.7377	.7416	.7455	.7494	.7533	.7572
96	.7650	.7689	.7728	.7767	.7806	.7845	.7884	.7923	.7962
97	.8040	.8079	.8118	.8157	.8196	.8235	.8274	.8313	.8352
98	.8430	.8469	.8508	.8547	.8586	.8625	.8664	.8703	.8742
99	.8820	.8859	.8898	.8937	.8976	.9015	.9054	.9093	.9132
100	.9210	.9249	.9288	.9327	.9366	.9405	.9444	.9483	.9522

AN EXPERIMENTAL INVESTIGATION OF NATURAL  
CONVECTION IN MERCURY AT LOW GRASHOF NUMBERS

by

BONG HYON CHANG

B.E., Yonsei University, 1968

---

AN ABSTRACT OF A MASTER'S THESIS

submitted in partial fulfillment of the

requirements for the degree

MASTER OF SCIENCE

Department of Chemical Engineering

KANSAS STATE UNIVERSITY  
Manhattan, Kansas

1970

## ABSTRACT

This thesis presents the results of an experimental investigation of the two dimensional natural convection in a liquid metal (mercury) at rest from a uniformly heated vertical plate. The purpose of this investigation was experimentally to check the validity of the boundary layer theory and the perturbation analysis for the natural convection in the liquid metals, especially at low Grashof numbers.

The temperature profiles about a 2-inch high by 4-inch long by 0.004-inch thick plate were measured with a copper-constantan thermocouple sheathed in a 0.014-inch diameter stainless steel tube. The results are presented on dimensionless plots and show definite deviations from the similarity solution of the boundary layer equations.

The deviations (of dimensionless temperature profiles) were found to depend on the distance up the plate, the heat flux, and the Nusselt number. The results are compared with those of the perturbation analysis.

Experimental data are correlated for the relationship between the modified Grashof number ( $Gr_x^*$ ) and the Nusselt number ( $Nu_x$ ), and compared with the only two existing experimental data for moderate and large Grashof numbers. They are in good agreement with each other only in the higher range of Grashof numbers. There is no available data for comparison at lower Grashof numbers. The correlations of the present experimental data ( $Gr_x^* 1-10^8$ )

are:

Linear correlation:

$$\log \text{Nu}_x = -0.605 + 0.178 \log \text{Gr}_x^* \quad (\sigma = 0.033)$$

Binomial correlation:

$$\log \text{Nu}_x = -0.551 + 0.145 \log \text{Gr}_x^* + 0.004 (\log \text{Gr}_x^*)^2$$

( $\sigma = 0.028$ )